CTIA 01.73
Supporting Procedures

Version 4.0.4

November 2023

Use Instructions

All testing shall be performed in a CTIA Certification Authorized Test Lab and shall be initiated through one of the following methods:

1. By submitting a PTCRB or IoT Network Certified device certification request at https://certify.ptcrb.com/
2. By submitting an OTA Test Plan use request at https://certify.ctiacertification.org/

CTIA Certification LLC
1400 16th Street, NW
Suite 600
Washington, DC 20036

1.202.785.0081

programs@ctiacertification.org

https://ctiacertification.org/test-plans/

© 2001 - 2023 CTIA Certification. All Rights Reserved.

Table of Contents

Appendix A

List of Figures

CTIA
Certification™

CTIA
Certification™

List of Tables

Section 1   Introduction

1.1   Scope

This document defines normative test procedures to calibrate the signal paths and characterize quiet zone performance within the test zone of the chamber. Additionally, this document provides guidance of power measurement procedures for various technologies.

1.2   Test Overview

Section 2 outlines the minimum measurement distance, measured between the center of the quiet zone and the measurement antenna, required for far-field measurements. In Section 3, the required test frequencies and calibration procedures, described in Section 4, and for the normative test site characterization, described in Section 5, are discussed. The precharacerization procedures used for the reverberation chamber testing is covered in Section 6 while for mm-wave testing, the normative test site characterizations for amplitude are outlined in Section 7 and for phase in Section 8. Various power measurement considerations for different technologies and power measurement equipment is discussed in Section 9.

1.3   Acronyms and Definitions

The following specialized terms and acronyms are used throughout this document.

Table 1.3-1 Acronyms and Definitions

Acronym	Definition
8-PSK	8-Phase Shift Keying
ADC	Analog to Digital Converter
ATL	Authorized Test Lab
AUT	Antenna Under Test
AWS	Advanced Wireless Services
BW	Bandwidth
CATR	Compact Antenna Test Range
CBW	Channel Bandwidth
CDMA	Code Division Multiple Access
CP-OFDM	Cyclic-Prefix OFDM
DFT-s-OFDM	Discrete Fourier Transform-spread-OFDM
DSP	Digital Signal Processing
DUT	Device Under Test
EGPRS	Enhanced GPRS

CTIA
Certification™

Acronym	Definition
EIRP	Effective Isotropic Radiated Power
EIS	Effective Isotropic Sensitivity
EVM	Error Vector Magnitude
FDD	Frequency Division Duplex
GMSK	Gaussian Minimum Shift Keying
GNSS	Global Navigation Satellite System
GPRS	General Packet Radio Service
GPS	Global Positioning System
GPS L1	GPS L1 navigation signal with carrier frequency of 1575.420 MHz
GPS L5	GPS L5 navigation signal with carrier frequency of 1176.450 MHz.
GSM	Global System for Mobile Communications
HD-FDD	Half-duplex FDD
HPBW	Half Power Beamwidth
ICP	Integrated Channel Power
IF	Intermediate Frequency
IFF	Indirect Far Field
IoT	Internet of Things
IQ	In-phase/Quadrature
LFF	Large Form Factor
LTE	Long Term Evolution
MA	Measurement Antenna
MBS	Metropolitan Beacon System
M-LMS	Multilateration Location and Monitoring Service
NB-IoT	Narrowband IoT
NBW	Noise Bandwidth
NR	New Radio
OEM	Original Equipment Manufacturer

Acronym	Definition
OFDM	Orthogonal Frequency Division Multiplexing
OTA	Over The Air
PCS	Personal Communications Services
PUSCH	Physical Uplink Shared Channel
QoQZ	Quality of Quiet Zone
QZ	Quiet Zone
RB	Resource Block
RBW	Resolution Bandwidth
RF	Radio Frequency
RMS	Root Mean Square
RSS	Root-Sum-of-Squares
RX	Receive
SCS	Subcarrier Spacing
SFF	Small Form Factor
SME	Subject Matter Expert
SSD	Surface Standard Deviation
TDD	Time Division Duplex
TD-LTE	Time Domain LTE
TDMA	Time Division Multiple Access
TIS	Total Isotropic Sensitivity
TRP	Total Radiated Power
TX	Transmit
UE	User Equipment
UMTS	Universal Mobile Telecommunications System
VBW	Video Bandwidth
WCDMA	Wideband Code Division Multiple Access

1.4   Document References

The following documents are referenced in this test plan:

Document Number, Document Name
[1]   CTIA 01.70, *Measurement Uncertainty*
[2]   CTIA 01.22, *Test Methodology, SISO, Millimeter Wave*
[3]   CTIA 01.21, *Test Methodology, SISO, Reverberation Chamber*
[4]   *Foegelle, M.D., Antenna Pattern Measurement: Theory and Equations, Compliance Engineering, 2002 Annual Reference Guide, Vol. XIX, No. 3, pp.34-43*
[5]   CTIA 01.90, *Informative Reference Material*
[6]   CTIA 01.71, *Positioning Guidelines*
[7]   CTIA 01.01, *Test Scope, Requirements, and Applicability*
[8]   CTIA 01.20, *Test Methodology, SISO, Anechoic Chamber*
[9]   3GPP TS 36.211, *Evolved Universal Terrestrial Radio Access (E-UTRA); Physical Channels and Modulation*
[10]   3GPP TS 36.508, *Evolved Universal Terrestrial Radio Access (E-UT RA) and Evolved Packet Core (EPC); Common Test Environments for User Equipment (UE) Conformance Testing*
[11]   3GPP TS 38.101-1, *NR; User Equipment (UE) radio transmission and reception; Part 1: Range 1 Standalone*
[12]   Hill, D.A., Boundary Fields in Reverberation Chambers, IEEE Transactions on Electromagnetic Compatibility, May 2005
[13]   Remley, K.A, Pirkl, R.J, Shah, H.A, and Wang, C.-M., Uncertainty From Choice of Mode-Stirring Technique in Reverberation-Chamber Measurements, IEEE Transactions on Electromagnetic Compatibility, December 2013
[14]   Remley, K.A., Wang, C.-M., Pirkl, R. J., Kirk, A. T., Aan Den Toorn, J., Williams, D. F., Holloway, C. L., Jargon, J. A., and Hale, P. D., A Significance Test for Reverberation-Chamber Measurement Uncertainty in Total Radiated Power of Wireless Devices, IEEE Transactions on Electromagnetic Compatibility, vol. 58, no. 1, pp. 207-219, February 2016
[15]   Kildal, P.-S, Chen, X., Orlenius, C., Franzen, M. and Patané, C. Lötbäck,, Characterization of Reverberation Chambers for OTA Measurements of Wireless Devices: Physical Formulations of Channel Matrix and New Uncertainty Formula, IEEE Transactions On Antennas and Propagation, August 2012
[16]   Aan Den Toorn, J., Remley, K. A., Holloway, C. L., Ladbury, J. M., and Wang, C.-M, Proximity-Effect Test for Lossy Wireless-Device Measurements in Reverberation Chambers, IET Science, Measurement and Technology, vol. 9, no. 5, 2015, pp. 540-546, August 2015

Section 2 Minimum Measurement Distance for Radiation Pattern Tests

This section describes the minimum measurement distance, R, which the Far-Field test site shall provide. The measurement distance is defined as the distance from the center of rotation of the DUT to the phase center (alternatively, if not accurately known, the nearest point) of the Measurement Antenna. The minimum measurement distance is specified in Table 2-1 below.

Table 2-1 Minimum Measurement Distance for Handheld DUTs

Band	Lower Frequency (MHz)	Upper Frequency (MHz)	Minimum Measurement Distance R (Meters)
3GPP Band 71	617	698	1.12
3GPP Band 12	699	746	1.01
3GPP Band 17	704	746	1.00
3GPP Band 29	717	728	0.99
3GPP Band 13	746	787	0.95
3GPP Band 14	758	798	0.94
3GPP Band 26	814	894	0.90
Cellular (3GPP Band 5)	824	894	0.90
MBS (M-LMS Band)	919.75	927.25	0.90
GNSS (L5 Band)	1166.22	1186.68	0.90
GNSS (L1, E1 Band)	1574	1606	0.96
3GPP Band 70 TX	1695	1710	0.99
AWS-1 TX (3GPP Band 4 TX)	1710	1755	1.00
3GPP Band 66 TX	1710	1780	1.00
PCS (3GPP Band 2)	1850	1990	1.04
3GPP Band 25	1850	1995	1.05
3GPP Band 70 RX	1995	2020	1.05
AWS-1 RX (3GPP Band 4 RX)	2110	2155	1.07
3GPP Band 66 RX	2110	2200	1.07
3GPP Band 30	2305	2360	1.09
3GPP Band 7	2500	2690	1.11
3GPP Band 41	2496	2690	1.11

Band	Lower Frequency (MHz)	Upper Frequency (MHz)	Minimum Measurement Distance R (Meters)
3GPP Band n78	3300	3800	1.02
3GPP Band 48	3550	3700	1.04
3GPP Band 46	5150	5925	0.90

A test site shall provide at least the specified minimum measurement distance for all tests and validation procedures described in this test plan. A minimum measurement distance of 1.2 m may be used for large (< 42 cm) form factor devices, provided the appropriate uncertainty term is included in the uncertainty budget for the test case. This uncertainty term may be taken from *CTIA 01.70* [1]. It is understood that the uncertainty terms in *CTIA 01.70* [1] are based on the large form factor, and as such, represent the worst case uncertainty expected.

These distances derived in Table 2-1 are the minimum recommended to facilitate measurement in the Far-Field for the purposes of this test plan. They are based on selecting the strictest of the three conventional Far-Field criteria within each band. These criteria express that the measurement distance be greater than the largest of $R_{QZ} + 2D_{rad}{}^2/\lambda$ (the phase uncertainty limit from the edge of the quiet zone), $3D$ (the amplitude uncertainty limit), and $R_{QZ} + 2\lambda$ (the reactive Near-Field limit from the edge of the quiet zone). R_{QZ} is the radius of the cylindrical quiet zone, and D_{QZ} is the diameter of the cylindrical quiet Dzone ($D_{QZ} = 2^*R_{QZ}$) and is defined as 30cm in this test plan. D is the largest dimension of the DUT and phantom that participate significantly in determining the TRP or TIS of the DUT and is chosen as D_{QZ}. λ is the free-space wavelength at the frequency band of interest. D_{rad} is the effective radiating aperture which is assumed to be 30cm below 1 GHz and decreasing linearly from 30 cm to 5 cm from 1 GHz to 7.125 GHz. It is furthermore assumed that antennas integrated in the DUT are not phase coherent. The details of the calculations are given for informational purposes only.

Table 2-2 Derivation of Minimum Measurement Distance for Handheld DUTs (Informative Only)

Band	Lower Frequency (MHz)	Upper Frequency (MHz)	λ_L (m)	λ_U (m)	$R > R_{QZ} + 2 D_{RAD}{}^2 / \lambda_U$ (m)	$R > 3 D$ (m)	$R > R_{QZ} + 2\lambda_L$ (m)	Strictest Criterion (m)
3GPP Band 71	617	698	0.49	0.43	0.57	0.90	1.12	1.12
3GPP Band 12	699	746	0.43	0.40	0.60	0.90	1.01	1.01
3GPP Band 17	704	746	0.43	0.40	0.60	0.90	1.00	1.00
3GPP Band 29	717	728	0.42	0.41	0.59	0.90	0.99	0.99
3GPP Band 13	746	787	0.40	0.38	0.62	0.90	0.95	0.95
3GPP Band 14	758	798	0.40	0.38	0.63	0.90	0.94	0.94
Cellular 3GPP Band 26	814	894	0.37	0.34	0.69	0.90	0.89	0.90
Cellular (3GPP Band 5)	824	894	0.36	0.34	0.69	0.90	0.88	0.90
MBS (M-LMS Band)	919.75	927.25	0.33	0.32	0.71	0.90	0.80	0.90

CTIA
Certification

Band	Lower Frequency (MHz)	Upper Frequency (MHz)	λ_L (m)	λ_U (m)	$R > R_{QZ} + 2 D_{RAD}^2 / \lambda_U$ (m)	$R > 3 D$ (m)	$R > R_{QZ} + 2 \lambda_L$ (m)	Strictest Criterion (m)
GNSS (L5 Band)	1166.22	1186.68	0.26	0.25	0.86	0.9	0.66	0.90
GNSS (L1, E1 Band)	1574	1606	0.19	0.19	0.96	0.90	0.53	0.96
3GPP Band 70 TX	1695	1710	0.18	0.18	0.99	0.90	0.50	0.99
AWS-1 TX (3GPP Band 4 TX)	1710	1755	0.18	0.17	1.00	0.90	0.50	1.00
3GPP Band 66 TX	1710	1780	0.18	0.17	1.00	0.90	0.50	1.00
PCS (3GPP Band 2)	1850	1990	0.16	0.15	1.04	0.90	0.47	1.04
3GPP Band 25	1850	1995	0.16	0.15	1.05	0.90	0.47	1.05
3GPP Band 70 RX	1995	2020	0.15	0.15	1.05	0.90	0.45	1.05
AWS-1 RX (3GPP Band 4 RX)	2110	2155	0.14	0.14	1.07	0.90	0.43	1.07
3GPP Band 66 RX	2110	2200	0.14	0.14	1.07	0.90	0.43	1.07
3GPP Band 30	2305	2360	0.13	0.13	1.09	0.90	0.41	1.09
3GPP Band 7	2500	2690	0.12	0.11	1.11	0.90	0.39	1.11
3GPP Band 41	2496	2690	0.12	0.11	1.11	0.90	0.39	1.11
3GPP Band n78	3300	3800	0.09	0.08	1.02	0.90	0.33	1.02
3GPP Band 48	3550	3700	0.08	0.08	1.04	0.90	0.32	1.04
3GPP Band 46	5150	5925	0.06	0.05	0.54	0.90	0.27	0.90

Future additions of new frequency bands will follow the same far-field criteria derivation. It is understood that near-field measurement techniques can permit an accurate measurement to be performed at distances smaller than those specified here, with proper mathematical manipulation of the raw amplitude and phase data. Such systems may be considered by CTIA Certification for inclusion in this test plan when they have been demonstrated for TRP and TIS measurements for the relevant modulation methods.

CTIA
Certification™

Section 3   Test Frequencies for Test Site Characterization and Range Reference Procedure

The following tables list the frequencies to be used to test for the quality of the quiet zone.

Table 3-1 Frequencies for Test Site Characterization/Ripple Test (below 6GHz)

Band	Test Frequency (MHz)
LTE 600 MHz (3GPP Bands 71)[1]	617 ± 1 MHz
LTE 700 MHz (3GPP Bands 12, 17, 29, 13, 14)[1]	722 ± 1 MHz
Cellular (3GPP Band 5 and 26), and MBS[1]	836.5 ± 1 MHz
GNSS (GPS L5)	1176.45 ± 1 MHz
GNSS (GPS L1, GALILEO E1)[1]	1575.42 ± 1 MHz
AWS-1 TX (3GPP Band 4 TX, 3GPP Band 70 TX, 3GPP Band 66 TX)	1732.5 ± 1 MHz
PCS (3GPP Band 2 and 3GPP Band 25 and 3GPP Band 70 RX)[1]	1880 ± 1 MHz
AWS-1 RX (3GPP Band 4 RX and 3GPP Band 66 RX)	2132.5 ± 1 MHz
Bands in the range 2300-2800 MHz (3GPP Bands 7, 30, 41)[1]	2450 ± 1 MHz
Bands in the range 3300-3800 MHz (3GPP Bands 48, n78)[1]	3600 ± 1 MHz
Bands in the range 5000-6000 MHz (3GPP Band 46)[1]	5500 ± 1 MHz
Note 1: Note that the test frequencies have been chosen to optimize the quiet zone test requirements.	

The FR2 frequency range from 24250 to 52600 MHz is split up into four different ranges, referred to as FR2_1 through FR2_4, as outlined in *CTIA 01.22* [2] limit the number of test frequencies to a manageable number. Defining test frequencies per operating band would likely increase to an impractical number as additional operating bands are defined. The quality of quiet zone (QoQZ) is determined at two test frequencies per frequency range and the maximum quality of quiet zone measurement at either of these two frequencies would be applied to the MU budget for the respective frequency range, e.g., $QoQZ\ (FR2\_1) = max\ (QoQZ(FR2\_1min), QoQZ(FR2\_1max))$.

Table 3-2 FR2 Frequencies for Quality of the Quiet Zone Tests

Designation	Operating Bands Covered	QoQZ Test Frequencies	
		Min [MHz]	Max [MHz]
FR2_1	n258, n261	24250	32000
FR2_2	n260	32000	40000
FR2_3		40000	48000
FR2_4		48000	52600

Table 3-3 provides the minimum list of reference frequencies to be measured for test frequencies below 6 GHz. This assumes that the performance of the test system is relatively flat so that minor variations in frequency around these points will have negligible effect on the reference value. If this is not the case, additional points should be taken to cover each expected DUT test frequency. A swept spectrum reference measurement is recommended to ensure that there are no sharp resonances in the measurement system near a required test frequency.

Table 3-3 Test Frequencies for the Range Reference Measurement and Reverberation Chamber Precharacterization (below 6GHz)

Band	Frequency (MHz)
3GPP Band 71, TX low	663
3GPP Band 71, RX low	617.5
3GPP Band 71, TX mid	680.5
3GPP Band 71, RX mid	634.5
3GPP Band 71, TX high	698
3GPP Band 71, RX high	652
3GPP Band 12, TX low	699
3GPP Band 12, RX low	729
3GPP Band 12, TX mid	707.5
3GPP Band 12, RX mid	737.5
3GPP Band 12, TX high	716
3GPP Band 12, RX high	746
3GPP Band 17, TX low	704
3GPP Band 17, RX low	734
3GPP Band 17, TX mid	710
3GPP Band 17, RX mid	740
3GPP Band 17, TX high	716
3GPP Band 17, RX high	746
3GPP Band 29, RX low	717
3GPP Band 29, RX mid	722.5
3GPP Band 29, RX high	728
3GPP Band 13, TX low	777

Band	Frequency (MHz)
3GPP Band 13, RX low	746
3GPP Band 13, TX mid	782
3GPP Band 13, RX mid	751
3GPP Band 13, TX high	787
3GPP Band 13, RX high	756
3GPP Band 14, TX low	788
3GPP Band 14, RX low	758
3GPP Band 14, TX mid	793
3GPP Band 14, RX mid	763
3GPP Band 14, TX high	798
3GPP Band 14, RX high	768
3GPP Band 26, TX low	814
3GPP Band 26, RX low	859
3GPP Band 26, TX mid	831.5
3GPP Band 26, RX mid	876.5
3GPP Band 26, TX high	849
3GPP Band 26, RX high	894
Cellular (3GPP Band 5), TX low	824
Cellular (3GPP Band 5), RX low	869
Cellular (3GPP Band 5), TX mid	836.5
Cellular (3GPP Band 5), RX mid	881.5
Cellular (3GPP Band 5), TX high	849
Cellular (3GPP Band 5), RX high	894
MBS (M-LMS Band)	925.977
GPS L5	1176.45
GPS L1, GALILEO E1	1575.42
PCS (3GPP Band 2), TX low	1850

Band	Frequency (MHz)
PCS (3GPP Band 2), RX low	1930
PCS (3GPP Band 2), TX mid	1880
PCS (3GPP Band 2), RX mid	1960
PCS (3GPP Band 2), TX high	1910
PCS (3GPP Band 2), RX high	1990
3GPP Band 25, TX low	1850
3GPP Band 25, RX low	1930
3GPP Band 25, TX mid	1882.5
3GPP Band 25, RX mid	1962.5
3GPP Band 25, TX high	1915
3GPP Band 25, RX high	1995
3GPP Band 70, TX low	1695
3GPP Band 70, RX low	1995
3GPP Band 70, TX mid	1702.5
3GPP Band 70, RX mid	2002.5
3GPP Band 70, TX high	1710
3GPP Band 70, RX high	2010
3GPP Band 70, DL only RX high	2020
AWS-1 (3GPP Band 4), TX low	1710
AWS-1 (3GPP Band 4), RX low	2110
AWS-1 (3GPP Band 4), TX mid	1732.5
AWS-1 (3GPP Band 4), RX mid	2132.5
AWS-1 (3GPP Band 4), TX high	1755
AWS-1 (3GPP Band 4), RX high	2155
3GPP Band 66, TX low	1710
3GPP Band 66, RX low	2110
3GPP Band 66, TX mid	1745

Band	Frequency (MHz)
3GPP Band 66, RX mid	2145
3GPP Band 66, TX high	1780
3GPP Band 66, RX high	2180
3GPP Band 66, DL only RX high	2200
3GPP Band 30, TX low	2305
3GPP Band 30, RX low	2350
3GPP Band 30, TX mid	2310
3GPP Band 30, RX mid	2355
3GPP Band 30, TX high	2315
3GPP Band 30, RX high	2360
3GPP Band 7, TX low	2500
3GPP Band 7, RX low	2620
3GPP Band 7, TX mid	2535
3GPP Band 7, RX mid	2655
3GPP Band 7, TX high	2570
3GPP Band 7, RX high	2690
3GPP Band 41, TRX low	2496
3GPP Band 41, TRX mid	2593
3GPP Band 41, TRX high	2690
3GPP Band n78, TRX low	3300
3GPP Band n78, TRX mid	3550
3GPP Band n78, TRX high	3800
3GPP Band 48, TRX low	3550
3GPP Band 48 TRX mid	3625
3GPP Band 48, TRX high	3700
3GPP Band 46 RX low	5150
3GPP Band 46, RX mid	5537.5

Band	Frequency (MHz)
3GPP Band 46, RX high	5925

Table 3-4 provides the minimum coherence bandwidth requirement for each transmission standard for reverberation-chamber precharacterization (see Section 6.1.2). The frequency step shall be selected to give valid results, i.e., significantly smaller than the coherence bandwidth.

Table 3-4 Transmission Standard, Channel Bandwidth (MHz), and Coherence Bandwidth (MHz)

Transmission Standard	Channel Bandwidth (MHz)	Coherence Bandwidth (MHz)
GSM\GRPS\EGPRS	0.2	0.2
UMTS (WCDMA)	3.84	4.0
LTE	No. resource blocks x 180 kHz	4.0[1]
Note 1: The CBW for LTE is based on the upper limit for loading (WCDMA) as opposed to actual channel bandwidth.		

For precharacterization of reverberation-chamber setups, labs shall ensure at least 21 frequency points are acquired by the VNA over the signal bandwidth for each technology to be tested. This VNA frequency step size shall be used for tests including Cable Loss (Section 6.2.1), Proximity Effect (Section 6.2.2), and Reference Power Transfer Function G_{ref} (Section 6.2.3 and Section 2.1 of *CTIA 01.21* [3]). Table 3-5 shows examples that provide 21 frequency points for various signal bandwidths. A smaller frequency step that provides more than 21 frequency points is acceptable. For example, a frequency step size of 240 kHz may be used for both 5 MHz and 10 MHz channels. As well, various frequency step sizes may be used for testing various technologies.

Table 3-5 Examples of VNA Frequency Step Size for Precharacterization When 21 Points Per Channel are Used for Precharacterization of the Reverberation Chamber Set-Up

Channel	Signal Bandwidth (MHz)	Frequency Step Size for 21 Points (kHz)
LTE UL with 8 RBs (e.g., B12 Ch 23035)	5	240
LTE DL with 50 RBs (e.g., B4 Ch 2000)	10	500
W-CDMA (e.g., B2, B5)	4	200
LTE CAT-NB1 with 12 subcarriers	0.18	9
LTE CAT-M1 DL with 4 RBs (e.g., B12, B4)	1.4	70

Table 3-6 provides the minimum list of reference frequencies to be measured for FR2. Additional points should be taken to cover each expected DUT test frequency. A swept spectrum reference measurement is recommended; the exact frequencies in Table 3-3 are not required as long as the frequency resolution is sufficient enough to ensure that there are no sharp resonances in the measurement system near the required test frequencies.

Table 3-6 FR2 Test Frequencies for the Reference Measurement

Band	Range	Frequency [MHz]
3GPP Band n258	UL&DL Low	24300
	UL&DL Mid	25875
	UL&DL High	27450
3GPP Band n260	UL&DL Low	37050
	UL&DL Mid	38499.96
	UL&DL High	39949.92
3GPP Band n261	UL&DL Low	27550.08
	UL&DL Mid	27924.96
	UL&DL High	28299.96

Section 4   Range Reference Procedure

This section describes the required procedure for obtaining the reference measurement used in removing the test system's influence from the Radiated Power and Sensitivity measurements. Before accurate measurements of quantities such as TRP, EIRP, TIS, or EIS can be made, it is necessary to perform a reference measurement to account for the various factors affecting the measurement of these quantities. These factors include components like range length path loss, gain of the receive antenna, cable losses, and so forth. This reference measurement is done using a reference antenna (typically either a dipole or standard gain horn, depending on frequency range) with known gain characteristics. The reference antenna is mounted at the center of the quiet zone to serve as the substitution antenna under test (AUT). The reference measurement is repeated for each variation of the measurement system (i.e., each polarization of the receive antenna, and each possible signal path to the measurement equipment). The reference measurement is combined with the gain of the reference antenna to determine an isotropic reference correction to be applied to DUT measurements performed using the test system. This procedure shall be repeated annually, and any time there is a change in the measurement system that may affect the validity of this reference measurement. For millimeter wave testing, it is recommended to perform this procedure on a monthly or quarterly basis to determine system stability. For non-permanent range installations (those where elements of the test system are disassembled or removed between tests) this procedure shall be repeated each time the range is reconfigured. It is recommended to perform this procedure on a monthly or quarterly basis to determine system stability.

4.1   Theoretical Background

Each individual data point in a radiated power or sensitivity measurement is referred to as the effective isotropic radiated power or effective isotropic sensitivity. That is, the desired information is how the measured quantity relates to the same quantity from an isotropic radiator. Thus, the reference measurement must relate the power received or transmitted at the DUT test equipment (spectrum analyzer or communication tester) back to the power transmitted or received at a theoretical isotropic radiator. The total path loss then, is just the difference in dB between the power transmitted or received at the isotropic radiator and that seen at the test equipment (see Figure 4.1-1).
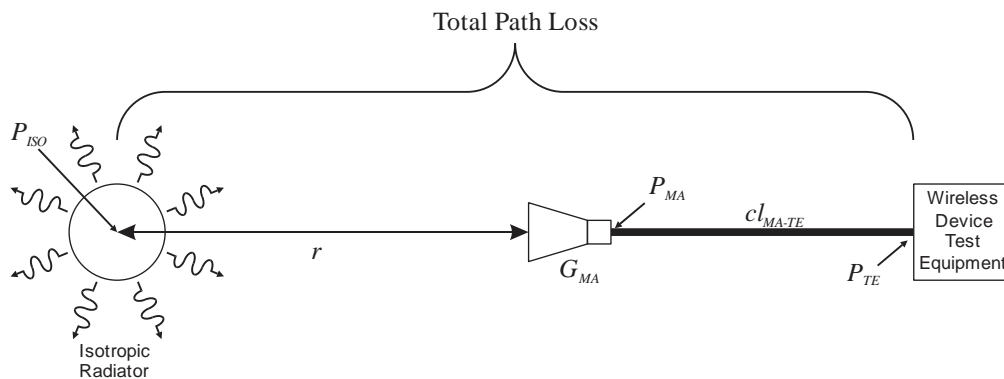
Figure 4.1-1 Theoretical Case for Determining Path Loss

In equation form, this becomes:

Equation 4.1-1

$$PL = P_{ISO} - P_{TE}$$

where PL is the total path loss, P_{ISO} is the power radiated by the theoretical isotropic radiator, and P_{TE} is the power received at the test equipment port. As can be seen in Figure 4.1-2, this quantity includes the range path loss due to the range length r, the gain of the measurement antenna, and any loss terms associated with the cabling, connections, amplifiers, splitters, etc. between the measurement antenna and the test equipment port.

Figure 4.1-2 shows a typical real-world configuration for measuring the path loss. In this case, a reference antenna with known gain is used in place of the theoretical isotropic source. The path loss may then be determined from the power into the reference antenna by adding the gain of the reference antenna. That is:

Equation 4.1-2

$$P_{ISO} = P_{RA} + G_{RA}$$

where P_{RA} is the power radiated by reference antenna, and G_{RA} is the gain of the reference antenna, so that:

Equation 4.1-3

$$PL = P_{RA} + G_{RA} - P_{TE}$$
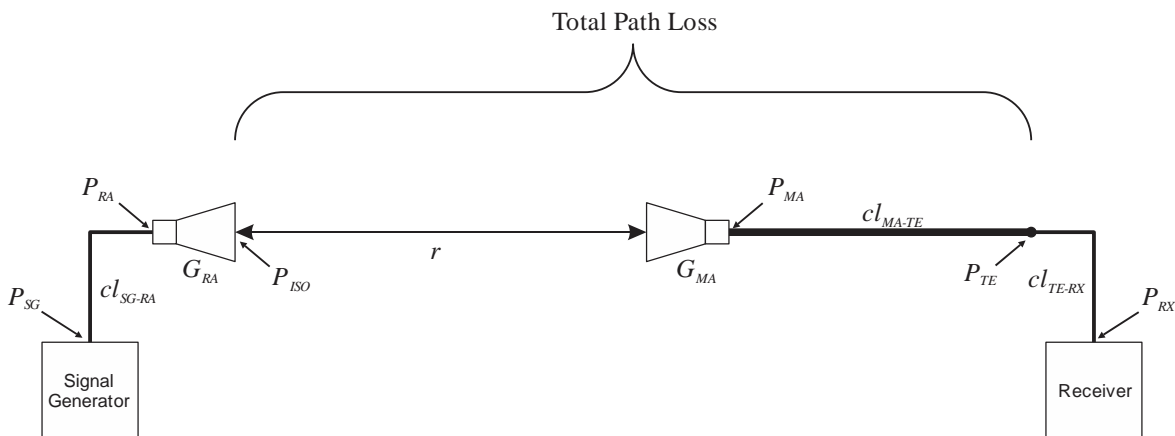
Figure 4.1-2 Typical Configuration for Measuring Path Loss

In order to determine P_{RA}, it is necessary to perform a cable reference measurement to remove the effects of the cable loss between signal generator and reference antenna cl_{SG-RA}, and between the test equipment port and the receiver. This establishes a reference point at the input to the reference antenna. Figure 4.1-3 illustrates the cable reference measurement configuration. Assuming the power level at the signal generator is fixed, it is easy to show that the difference between P_{RA} and P_{TE} in Figure 4.1-2 is given by:

Equation 4.1-4

$$P_{RA} - P_{TE} = P_{RX}{}' - P_{RX}$$

$$P_{RA} = P_{TE}'$$

$$cl_{SG\text{-}RA} \qquad cl_{TE\text{-}RX}$$

$$P_{SG} \qquad\qquad P_{RX}'$$

Signal Generator   Receiver
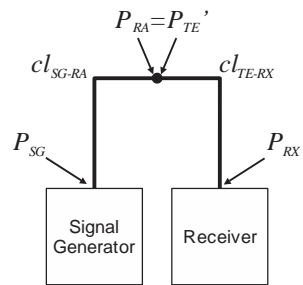
Figure 4.1-3 Cable Reference Calibration Configuration

where P_{RX}' is the power measured at the receiver during the cable reference test, and P_{RX} is the power measured at the receiver during the range path loss measurement in Figure 4.1-2. Note that this formulation assumes that the effects of the reference antenna VSWR are accounted for in the gain of the reference antenna. For more information on this subject, refer to *Antenna Pattern Measurement: Theory and Equations* [4]. Thus, the path loss is then just given by:

Equation 4.1-5

$$PL = G_{RA} + P_{RX}' - P_{RX}$$

4.2   Equipment Required

1. Anechoic chamber and spherical positioning system previously characterized per, and meeting the requirements specified in Section 1.
2. Reference antenna(s) with valid calibrations to cover the required range of test frequencies. Dipoles or horns are typically used, following the system providers guidance on the antenna selection is recommended. Other antennas may be used; however, the uncertainty contribution to the resulting measurements due to calibration and phase center issues may be significant.
   Reference antennas in the mm-wave frequency range are typically directive horn antennas. A single broadband or multiple directive antennas can be used to cover the frequency ranges of interest.

3. Low dielectric constant support structure (e.g., Styrofoam) for positioning the reference antennas.
4. Measurement antenna(s) (e.g. horn or dipole used to perform measurements of the DUT).

   Note: *If multiple measurement antennas are used to cover the required frequency range, the reference measurement must be repeated each time the antennas are repositioned, unless a permanent mounting fixture is used to guarantee repeatable performance. These should be the same antennas used in performing the site characterization in Section 5.*

5. Network analyzer, spectrum analyzer with tracking generator, or stable signal generator and measurement receiver (spectrum analyzer, power meter, etc.) having a wide dynamic range and high linearity, all with current calibration(s).

6. All RF cabling, splitters, combiners, switches, attenuators, etc. required to connect the measurement antenna(s) to the test equipment used for measuring radiated power and sensitivity of the DUT. The connection to the receiver or communication tester used to perform the DUT measurement shall be referred to as the "test port" in this section. These components will be characterized along with the range length and measurement antenna contributions.

7. Additional cabling to reach from the signal source to the reference antenna (the reference port), and from both the reference antenna location and the test port to the receiver input. The source cabling to the reference antenna should be treated with ferrite beads and routed to minimize its influence on the reference measurement. The effects of these cables will be removed from the reference measurement; however, cable lengths should be kept as short as possible to reduce the associated path loss.

8. Low loss cable adapters for performing various interconnects. These should be characterized to determine their influence on the measurements. That influence may be corrected for, if measured, or applied to the measurement uncertainty if estimated.

9. Optional 3 to 10 dB fixed attenuators for reducing standing wave effects in cables.

10. Optional 50 Ω terminations.

4.3   Test Frequencies

The test frequencies for the range reference procedure are defined in Section 3.

4.4   Test Procedure

The range reference measurement is performed in a two-step process whereby the effects of the cables and equipment external to the normal operation of the range are removed from the resulting reference values. By performing the measurement in this manner, the measurement uncertainty is reduced, since the result relies on the linearity of the receiver rather than its absolute value accuracy. Additionally, measuring all components of the signal path at once results in only one measurement uncertainty contribution to the total measurement uncertainty of the path loss measurement; as opposed to measuring the loss of each component and combining them for a total loss, which increases the uncertainty by the square root of the number of measurements required.

4.4.1   Measurement Step 1: Source Reference Test (Cable Calibration)

The first step involves measuring the frequency response of all cabling, connectors, and equipment that are not a part of the test system. This step is normally only done once, provided all required test frequencies can be covered with one set of cables. If different cabling configurations are required for each polarization of the reference antenna, etc., this step must be repeated for each configuration. The two steps should be performed sequentially for each configuration to avoid additional uncertainty contributions due to changes in connections, etc.

For each configuration, perform the following steps:

1. Route the source cable(s) from the signal generator or output port of the network analyzer to the mounting location of the reference antenna. A minimum of 3 dB (preferably 10 dB) pad is recommended at the output (reference antenna side) of the cable to minimize standing waves. This output connection is defined as the reference port.

2. Connect the output of the source cable to the receiver or input port of the network analyzer, either directly (if the receiver can be moved to accommodate this connection) or through another cable (the loopback cable). An additional pad is recommended at the input port of the receiver or at the end of the loopback cable if used.

3. Ensure all equipment has been powered on long enough to have stabilized.

4. Perform a frequency scan or sweep to cover the required test frequencies and record the result. The power level of the signal source must remain fixed for all measurements. Ensure that the received signal is below the compression point of the receiver and any amplifiers or other components in the system (linear region) and sufficiently far above the noise floor of the receiver to account for the expected range path loss. It is recommended that all receivers be set to narrow bandwidth to obtain the lowest possible noise floor. Depending on the equipment used, refer to the following procedure:

    a. For a vector network analyzer, first record the swept frequency response curve with no calibration applied. This will be used for verifying that the analyzer is in the appropriate linear region (not overloaded) and has enough dynamic range. Perform a calibration of the analyzer to normalize out the response of the cable loop. This calibration will serve as the source reference test. While a full two-port calibration is desirable to provide the lowest measurement uncertainty and account for standing wave issues, etc., flexing of cables, movement of rotary joints, and other variations may make the calibration less accurate in practice. A through response normalization, while having a higher level of uncertainty specified by the manufacturer, may actually be more accurate in practice due to the cable variations involved. Refer to step 5 below for information on estimating these effects.

    b. For scalar swept frequency devices (scalar network analyzers, spectrum analyzers with tracking generators, etc.) record the swept frequency response curve of the cable loop. If the analyzer contains a scalar calibration or trace math function, it may be used to subtract this reference curve from subsequent measurements.

    c. For discrete signal generator and receiver combinations, tune the receiver and signal generator to each frequency and record the reading of the receiver.

    Note: For swept and list-based measurements using instruments such as network analyzers or spectrum analyzer/tracking generator combinations, care shall be taken to ensure that the measured (received) signal is tracking properly with the transmitted signal to avoid measuring larger losses than the actual path loss. Informative Reference Material *describes this phenomenon in more detail and provides recommended validation procedures.*

5. Prior to proceeding to the next test step, move the cables around and monitor the frequency response. Any gross changes in response indicate bad cables or connections and should be rectified prior to continuing. Minor variations (fractions of a dB) are expected and should be accounted for in the measurement uncertainty of the reference measurement.

6. Record the measurement results to a file that can be imported into a Microsoft Excel spreadsheet.

4.4.2   Measurement Step 2: Range Reference Test

The second step measures the frequency response of the reference antenna, range, and all cabling, connectors, switches, etc. between the reference port and the test port, as well as the cabling and equipment included in step 1. This step is required for each polarization of the receive antenna and for each separate signal path between the antenna under test (AUT) and any different test ports connecting to test equipment used for the DUT measurement. Only the paths used to record data (i.e., the paths to the receiver used for TRP measurements, or the output path from the communication tester for TIS measurements) need to be measured.

For each polarization and configuration, perform the following steps:

1. Connect the receiver or input port of the network analyzer to the test port connection to be characterized using the same cable configuration used to attach it to the reference port. Any cable adapters added or removed from the system to make the required connections must be accounted for as mentioned previously. Terminate any unused connections to the appropriate test equipment or by using 50 Ω loads.

2. Prior to connecting the source to the reference antenna, attach a 50 Ω termination to the reference port (or otherwise ensure no output from the signal generator) and record the noise floor of the analyzer or receiver at each frequency point. Use a frequency response sweep or discrete points as necessary based on the configuration. If available, use a max-hold function to obtain the maximum noise level for several sweeps.

3. Connect the reference antenna to the reference port and use a low dielectric support to hold the antenna in the middle of the quiet zone, boresight with the measurement antenna, and parallel to the polarization being characterized. For directional reference antennas, ensure that both the reference and measurement antennas are boresight to each other. Ensure that the support structure is out of the measurement path such that it has a minimal impact on the reference measurement.

4. Ensure all equipment has been powered on long enough to have stabilized. The equipment should normally have been left on from the cable calibration step. All settings of the equipment should be identical to those for the cable calibration. The power level of the signal generator must be the same as that for the reference sweep (unless a vector network analyzer is used to obtain relative power data) and must remain stable over time in order to obtain valid data.

5. Perform a frequency scan or sweep to cover the required test frequencies and record the result. Ensure that the received signal is below the compression point of the receiver (linear region) and at least 20 dB above the noise floor as measured in step 2 above in order to have less than 1 dB measurement uncertainty due to the noise. Depending on the equipment used, refer to the following procedure:

    a. For a vector network analyzer, record a frequency response curve with the calibration applied. This curve is the desired range response measurement.

    b. For scalar swept frequency devices (scalar network analyzers, spectrum analyzers with tracking generators, etc.) record the swept frequency response curve of the cable loop. If the analyzer has been configured to automatically subtract the cable calibration reference curve, then the resulting curve is the desired range response measurement. If not, the resulting curve is the range response plus the cable contribution, which will be subtracted out later.

    c. For discrete signal generator and receiver combinations, tune the receiver and signal generator to each frequency and record the reading of the receiver. The resulting curve is the range response plus the cable contribution, which will be subtracted out later.

    Note: For swept and list-based measurements using instruments such as network analyzers or spectrum analyzer/tracking generator combinations, care shall be taken to ensure that the measured (received) signal is tracking properly with the transmitted signal to avoid measuring larger losses than the actual path loss. Informative Reference Material *describes this phenomenon in more detail and provides recommended validation procedures.*

6. Record the measurement results to a file that can be imported into a Microsoft Excel spreadsheet.

4.4.3   Calculating the Range Reference Path Loss

Once the data has been acquired as described above, it's necessary to convert it to a loss value and combine it with the reference antenna gain in dBi to obtain the total path loss to be used as the reference correction. Once this value has been determined, it can be added to the power readings of the test equipment to represent the reading relative to an isotropic source.

Use Equation 4.1-5 to determine the path loss. Table 4.4.3-1 shows a sample table for recording the data for one polarization and signal path. For data acquired using calibrated analyzers as described above, the frequency response curve generated by the second measurement is actually $P_{RX} - P_{RX}'$ in dB, so the negative of it represents a loss value. Subtracting that value from the reference antenna gain provides the total path loss. Work backwards as necessary to fill in the columns. Note that with calibration applied, the noise floor reference measurement will also have P_{RX}' subtracted from it. For vector network analyzers, all measured values are relative numbers, so the various reference values will be in dB rather than dBm.

Table 4.4.3-1 Example Range Reference Measurement Data Record

Band	Frequency (MHz)	Cable Ref. (dBm)	Test Port (dBm)	Noise Floor (dBm)	Test Port - Cable (dB)	Test Port - Noise (dB)	Ref. Ant. Gain (dBi)	Path Loss (dB)
3GPP Band 71, TX low	617							
3GPP Band 71, RX low	634.5							
3GPP Band 71, TX mid	652							
3GPP Band 71, RX mid	663							
3GPP Band 71, TX high	680.5							
3GPP Band 71, RX high	698							
3GPP Band 12, TX low	699							
3GPP Band 12, RX low	729							
3GPP Band 12, TX mid	707.5							
3GPP Band 12, RX mid	737.5							
3GPP Band 12, TX high	716							
3GPP Band 12, RX high	746							
3GPP Band 17, TX low	704							
3GPP Band 17, RX low	734							
3GPP Band 17, TX mid	710							
3GPP Band 17, RX mid	734							
3GPP Band 17, TX high	716							

Band	Frequency (MHz)	Cable Ref. (dBm)	Test Port (dBm)	Noise Floor (dBm)	Test Port - Cable (dB)	Test Port - Noise (dB)	Ref. Ant. Gain (dBi)	Path Loss (dB)
3GPP Band 17, RX high	734							
3GPP Band 29, RX low	717							
3GPP Band 29, RX mid	722.5							
3GPP Band 29, RX high	728							
3GPP Band 13, TX low	777							
3GPP Band 13, RX low	746							
3GPP Band 13, TX mid	782							
3GPP Band 13, RX mid	751							
3GPP Band 13, TX high	787							
3GPP Band 13, RX high	756							
3GPP Band 14, TX low	788							
3GPP Band 14, RX low	758							
3GPP Band 14, TX mid	793							
3GPP Band 14, RX mid	763							
3GPP Band 14, TX high	798							
3GPP Band 14, RX high	768							
3GPP Band 26, TX low	814							
3GPP Band 26, RX low	859							
3GPP Band 26, TX mid	831.5							
3GPP Band 26, RX mid	876.5							
3GPP Band 26, TX high	849							
3GPP Band 26, RX high	894							
Cellular (3GPP Band 5), TX low	824	-10.43	-57.78	-99.42	47.35	41.64	1.56	48.91
Cellular (3GPP Band 5), RX low	869	-10.75	-59.46	-101.71	48.71	42.25	1.57	50.28
Cellular (3GPP Band 5), TX mid	836.5	-11.12	-56.61	-98.3	45.49	41.69	1.57	47.06
Cellular (3GPP Band 5), RX mid	881.5	-11.21	-56.48	-97.64	45.27	41.16	1.54	46.81

Band	Frequency (MHz)	Cable Ref. (dBm)	Test Port (dBm)	Noise Floor (dBm)	Test Port - Cable (dB)	Test Port - Noise (dB)	Ref. Ant. Gain (dBi)	Path Loss (dB)
Cellular (3GPP Band 5), TX high	849	-11.43	-57.57	-99.93	46.14	42.36	1.49	47.63
Cellular (3GPP Band 5), RX high	894	-11.47	-59.44	-96.52	47.97	37.08	1.45	49.42
MBS (M-LMS Band)	925.977							
GNSS (L5 Band)	1166.22							
GNSS (L1, E1 Band)	1575.42							
PCS (3GPP Band 2), TX low	1850	-15.72	-72.53	-102.42	56.81	29.89	1.85	58.66
PCS (3GPP Band 2), RX low	1930	-15.91	-71.31	-100.9	55.4	29.59	1.88	57.28
PCS (3GPP Band 2), TX mid	1880	-16.2	-70.96	-97.71	54.76	26.75	1.91	56.67
PCS (3GPP Band 2), RX mid	1960	-16.12	-71.25	-103.61	55.13	32.36	1.84	56.97
PCS (3GPP Band 2), TX high	1910	-16.35	-72.75	-102.09	56.4	29.34	1.79	58.19
PCS (3GPP Band 2), RX high	1990	-16.41	-73.41	-98.9	57	25.49	1.71	58.71
3GPP Band 25, TX low	1850							
3GPP Band 25, RX low	1930							
3GPP Band 25, TX mid	1882.5							
3GPP Band 25, RX mid	1962.5							
3GPP Band 25, TX high	1915							
3GPP Band 25, RX high	1995							
3GPP Band 70, TX low	1695							
3GPP Band 70, RX low	1995							
3GPP Band 70, TX mid	1702.5							
3GPP Band 70, RX mid	2002.5							
3GPP Band 70, TX high	1710							
3GPP Band 70, RX high	2010							
3GPP Band 70, DL only RX high	2020							
AWS-1 (3GPP Band 4), TX low	1710							
AWS-1 (3GPP Band 4), RX low	2110							

Band	Frequency (MHz)	Cable Ref. (dBm)	Test Port (dBm)	Noise Floor (dBm)	Test Port - Cable (dB)	Test Port - Noise (dB)	Ref. Ant. Gain (dBi)	Path Loss (dB)
AWS-1 (3GPP Band 4), TX mid	1732.5							
AWS-1 (3GPP Band 4), RX mid	2132.5							
AWS-1 (3GPP Band 4), TX high	1755							
AWS-1 (3GPP Band 4), RX high	2155							
3GPP Band 66, TX low	1710							
3GPP Band 66, RX low	2110							
3GPP Band 66, TX mid	1745							
3GPP Band 66, RX mid	2145							
3GPP Band 66, TX high	1780							
3GPP Band 66, RX high	2180							
3GPP Band 66, DL only RX high	2200							
3GPP Band 30, TX low	2305							
3GPP Band 30, RX low	2350							
3GPP Band 30, TX mid	2310							
3GPP Band 30, RX mid	2355							
3GPP Band 30, TX high	2315							
3GPP Band 30, RX high	2360							
3GPP Band 7, TX low	2500							
3GPP Band 7, RX low	2620							
3GPP Band 7, TX mid	2535							
3GPP Band 7, RX mid	2655							
3GPP Band 7, TX high	2570							
3GPP Band 7, RX high	2690							
3GPP Band 41, TRX low	2496							
3GPP Band 41, TRX mid	2593							
3GPP Band 41, TRX high	2690							

Band	Frequency (MHz)	Cable Ref. (dBm)	Test Port (dBm)	Noise Floor (dBm)	Test Port - Cable (dB)	Test Port - Noise (dB)	Ref. Ant. Gain (dBi)	Path Loss (dB)
3GPP Band 48, TRX low	3550							
3GPP Band 48, TRX mid	3625							
3GPP Band 48, TRX high	3700							
3GPP Band 46, RX low	5150							
3GPP Band 46, RX mid	5537.5							
3GPP Band 46, RX high	5925							

4.5   Range Reference Measurement Data File

Data shall be supplied in a format accessible (i.e. readable) for additional examination and computation as outlined in Table 4.5-1.

Table 4.5-1 Sample Range Reference Measurement Data File Format

Measurement Date:	May 1, 2003							
Reference Antenna(s):	SD-1234 (Cell Band), SD-4567 (PCS Band)							
Polarization:	Theta							
Signal Path:	Theta Polarization to Spectrum Analyzer (TRP)							
Band	Freq. (MHz)	Cable Ref. (dBm)	Test Port (dBm)	Noise Floor (dBm)	Test Port - Cable (dB)	Test Port - Noise (dB)	Ref. Ant. Gain (dBi)	Path Loss (dB)
Cellular (3GPP Band 5)	824	-10.43	-57.78	-99.42	47.35	41.64	1.56	48.91
Cellular (3GPP Band 5)	836.5	-10.75	-59.46	-101.71	48.71	42.25	1.57	50.28
Cellular (3GPP Band 5)	849	-11.12	-56.61	-98.30	45.49	41.69	1.57	47.06
PCS (3GPP Band 2)	1850	-15.72	-72.53	-102.42	56.81	29.89	1.85	58.66
PCS (3GPP Band 2)	1880	-15.91	-71.31	-100.90	55.40	29.59	1.88	57.28
PCS (3GPP Band 2)	1910	-16.20	-70.96	-97.71	54.76	26.75	1.91	56.67
Polarization:	Phi							
Signal Path:	Phi Polarization to Spectrum Analyzer (TRP)							

Band	Freq. (MHz)	Cable Ref. (dBm)	Test Port (dBm)	Noise Floor (dBm)	Test Port - Cable (dB)	Test Port - Noise (dB)	Ref. Ant. Gain (dBi)	Path Loss (dB)
…	…	…	…	…	…	…	…	…

Polarization:		Theta						
Signal Path:		Theta Polarization to Communication Tester (TIS)						

Band	Freq. (MHz)	Cable Ref. (dBm)	Test Port (dBm)	Noise Floor (dBm)	Test Port - Cable (dB)	Test Port - Noise (dB)	Ref. Ant. Gain (dBi)	Path Loss (dB)
Cellular (3GPP Band 5)	869	-11.21	-56.48	-97.64	45.27	41.16	1.54	46.81
Cellular (3GPP Band 5)	881.5	-11.43	-57.57	-99.93	46.14	42.36	1.49	47.63
Cellular (3GPP Band 5)	894	-11.47	-59.44	-96.52	47.97	37.08	1.45	49.42
PCS (3GPP Band 2)	1930	-16.12	-71.25	-103.61	55.13	32.36	1.84	56.97
PCS (3GPP Band 2)	1960	-16.35	-72.75	-102.09	56.40	29.34	1.79	58.19
PCS (3GPP Band 2)	1990	-16.41	-73.41	-98.90	57.00	25.49	1.71	58.71

Polarization:		Phi						
Signal Path:		Phi Polarization to Communication Tester (TIS)						

Band	Freq. (MHz)	Cable Ref. (dBm)	Test Port (dBm)	Noise Floor (dBm)	Test Port - Cable (dB)	Test Port - Noise (dB)	Ref. Ant. Gain (dBi)	Path Loss (dB)
…		…	…	…	…	…	…	…

4.6 Alternate Scenarios

In some cases, it may be desirable to combine the transfer of a precision power calibration (i.e. using a reference power meter) to the measurement equipment along with the range reference measurement into one measurement step. This can have the advantage of reducing the total uncertainty that would be entailed in two separate measurement steps; one to perform the range reference and the second to transfer the power calibration. This section describes two possible scenarios envisioned for performing this type of transfer.

4.6.1 TRP Reference

By using the reference power meter for the reference measurement in step 4 of Section 4.4.1 the absolute power calibration of the reference power meter can be transferred to the measurement receiver used in Section 4.4.1. The delta between the two measurements now contains not only the path loss

CTIA
Certification™

terms of the range reference measurement, but the deviation between the absolute power readings of the two instruments at their relative input levels. Note that this calibration transfer does not account for any non-linearity of the receiver(s) and is most accurate if the power level at the reference antenna is near the power level to be measured in the DUT.

4.6.2   TIS Reference

For TIS measurements, the desired measurement quantity is received power of the DUT at a given error rate. A one-step substitution measurement can be performed (assuming the power sensor can be attached directly to the reference antenna such that no additional cable loss need be accounted for) to transfer a received power calibration to the communication tester along with the range reference measurement. In this case, Section 4.4.1 can be skipped, and the system configured as in Section 4.4.1 with the power sensor now connected to the reference antenna and the communication tester transmitting through the signal path to be qualified. The signal strength is measured out of the reference antenna for a given output level of the communication tester and the resulting difference becomes the path loss correction for received power. Note that this calibration transfer does not account for any non-linearity of the communication tester's signal generator or the power meter. Ideally, the source power calibration is most accurate if the power level received at the reference antenna is near the sensitivity level of the DUT, although the sensitivity level of the power meter may have a larger contribution to the overall uncertainty in that case. Note also that the power meter and sensor must be suitable for measuring the active signal generated by the communication tester in order to perform this measurement.

If additional cabling is required to reach the power sensor, that additional cabling is first used to connect the power sensor to the output of the communication tester according to the steps in Section 4.4.1 before proceeding to the steps in Section 4.4.2..

4.6.3   Ripple Based Calibration

Since a single range path loss measurement receives the full error contribution due to any reflections within the test environment (chamber ripple), alternate methods that minimize this error contribution may be used to reduce the measurement uncertainty.

One method for averaging out the ripple effect is to actually perform the equivalent of a ripple test using the sleeve dipole at all frequencies of interest. The dipole is offset from the center of rotation and a single pattern measurement cut is performed for the polarization of interest using a maximum of 5 degree step size. After correcting for the path length variation, any chamber induced ripple will result in an oscillation around the desired center position path loss. Taking the linear average of the resultant data provides a good estimate of the ripple-free path loss, although the likelihood of summing over a non-integral number of wavelengths will still result in a small frequency dependent bias.

This method can typically be used to calibrate both polarizations of a measurement system, provided any unnecessary support structure is removed during the calibration process to minimize the impact on the ripple during the calibration. Note that since ripple cannot be eliminated from the measurement system through calibration, this has no impact on the ripple contribution to the EUT measurement uncertainty, but only serves to minimize its impact on the range calibration.

Another common method of minimizing ripple contribution is to remove the impact of reference gain from the measurement by performing an efficiency-based calibration. This involves performing a spherical pattern measurement of the reference antenna, using a maximum of 15 degree step size, to determine the measured efficiency and then using the reference efficiency rather than the reference gain to determine the net path loss. Since the dipole can only be uniquely polarized along the theta polarization, a separate transfer standard step is required to obtain the delta between the theta and phi polarizations of the measurement antenna. To minimize the ripple contribution to the transfer, a horn is typically used, pointed along the phi axis. Rotating between 0 and 90 degrees in phi changes the polarization for theta = 0 degrees. Note that if an omni-directional antenna like the reference antenna were used as the transfer standard, the same ripple impact would apply for each of the two measurements, potentially doubling the

impact of ripple uncertainty on the phi polarization calibration. Even so, there can be expected to be some additional uncertainty embedded in the theta-to-phi transfer standard, in addition to that due to repeated measurements. It should also be noted that unless the dipole is also offset from the center of rotation, this method only has the effect of averaging ripple in the theta axis direction of rotation, convoluted with the theta dependence of the reference antenna pattern. Any ripple contribution in the phi direction remains constant. While it is generally assumed that the ripple cancels over the surface integral of the sphere, the SSD contribution in Section 2.10 of *CTIA 01.70* [1] can be expected to apply to this term.

4.7   Wideband Channels

For technologies like WCDMA and LTE, where the channel bandwidths can be several MHz, correcting the path loss at only the center frequency may result in a measurement error when the channel is not perfectly flat. In addition, LTE TRP complicates matters further by offsetting the occupied bandwidth to different portions of the selected channel. Thus, the center frequency of the channel may not even be a frequency that is measured. This error can generally be measured and corrected for by using the power average of the path loss across the occupied bandwidth. The average should be performed on the net path loss, including contributions from all cables, reference antenna gain, and other components to properly capture all standing wave contributions or other factors that would result in a non-flat channel. The calibration data must be taken with sufficient resolution to capture the frequency variation of the channel.

In cases where it is not possible or practical to correct for the average power level in the channel, an additional uncertainty contribution must be included as specified in *CTIA 01.70* [1]. This generally requires a detailed understanding of the channel shape to properly estimate the measurement uncertainty, making it more practical to correct for the error rather than adding an uncertainty term. In addition, if the average power is not used, the center frequency of the occupied bandwidth should be used. If that is also not possible or practical, then an additional measurement uncertainty term must be applied to address the frequency offset of the correction. Finally, the TIS result does not directly follow the average channel power, but rather is biased higher (worse) due to the portion of the bandwidth that reaches sensitivity first and starts introducing errors. Current indications are that this contribution is small for the channel flatness expected from a typical antenna pattern measurement system, but an appropriate contribution may be estimated as well.

Section 5   Test Site Characteristics and Quiet Zone Accuracy

5.1   Equipment Required

Details on the antenna radiation pattern symmetry can be found in Section 4 of *CTIA 01.90* [5].

1. Anechoic chamber and spherical positioning system to be characterized. For the purpose of these tests, this chamber must be large enough to allow the Measurement Antenna (MA) to be at least R (the minimum measurement distance specified in Table 5.3.4-1 for the frequency band being tested) from center of rotation of the DUT and the test site must be reasonably free of interference. This method is intended to characterize the effect of a variety of positioning systems on the required pattern tests. However, reasonable precautions should be taken to avoid designs that would reflect significant radiated energy back into the test region or absorb significant energy out of the test region. Such systems may cause significant error in the measurement results and defeat the purpose of this test.
2. Sleeve dipole probe antennas with less than ±0.1 dB of asymmetry in the azimuth plane pattern for each frequency called out in Section 3.
3. Loop probe antennas with less than ±0.1 dB of asymmetry in the azimuth plane pattern for each frequency called out in in Section 3.

   Note: It is necessary that the above antennas be optimized for the respective frequencies as indicated in Section 3. The asymmetry specification for purposes of this measurement may be stated more specifically as the pattern shall not deviate from a perfect circle by more than 0.1 dB (0.2 dB peak-to-peak). Sleeve dipoles and center fed balanced loop antennas are recommended since the cable and feed point may be arranged in such a way that interactions with the measurement are minimized. The asymmetry specification holds only at the frequency at which the ripple test is performed (see Table 3-1). The gain and efficiency of this antenna is immaterial since the measurement seeks to determine deviations in the measured antenna pattern caused by reflections within the measurement chamber.

4. Reference horn if the range reference is being performed using a horn antenna. The same horn used for the range reference measurement should be used for this procedure. If unavailable, using a horn of the same serial model is acceptable.
5. Low dielectric constant support structure (e.g. Styrofoam) for positioning the probe antennas.
6. Measurement antenna(s) (e.g., horn or dipole used during antenna measurements).
7. Network analyzer or signal generator/measurement receive.

5.2   Terminology and Coordinate Systems

This test procedure has been designed to be as generic as practical in order to produce similar results for any test system. The principal goal is to qualify the behavior of the quiet zone from as many orientations as practical.

Starting from the classical spherical coordinate system shown in Figure 5.2-1 (a), the phi (ϕ) axis is defined as being along the z-axis. Treating this as the coordinate system of the DUT is the equivalent of assuming the DUT is mounted directly to the phi-axis rotator. Then as the phi axis rotates, the orientation of the theta axis varies with respect to the DUT (see Figure 5.2-1 b).
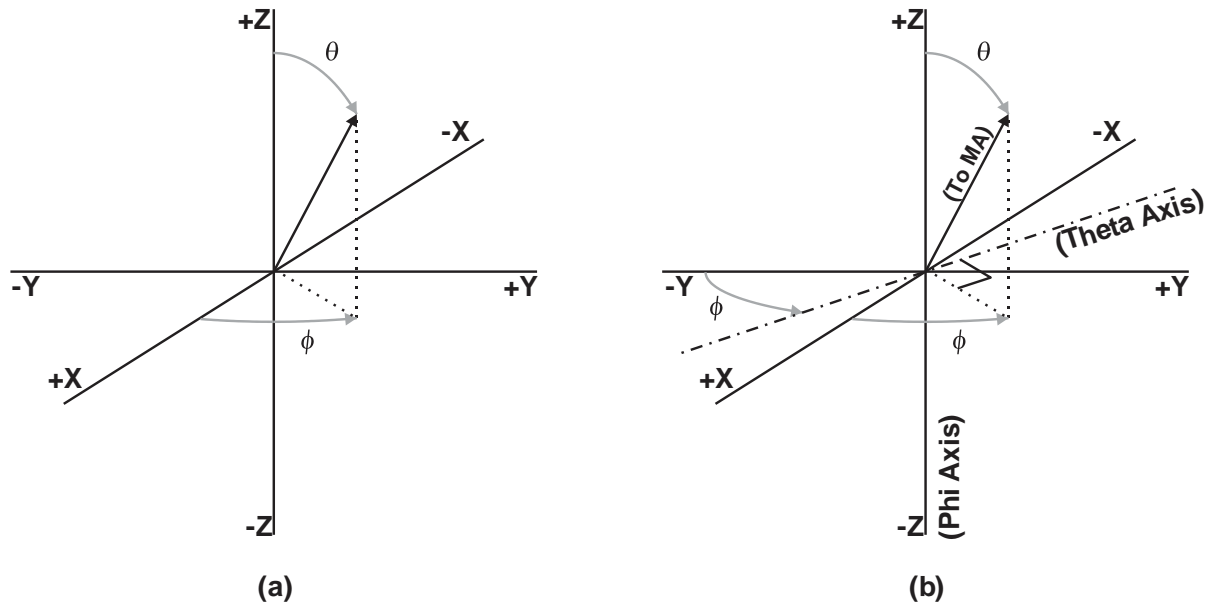
Figure 5.2-1 Spherical Coordinate System

In conjunction with defining the spherical coordinate system, it is necessary to define the two polarizations to be used for measuring total field at each point. The polarizations are identified in terms of the two rotational axes, such that the phi polarization is along the direction of motion when the phi axis rotates and the theta polarization is along the direction of motion when the theta axis rotates (see Figure 5.2-2).
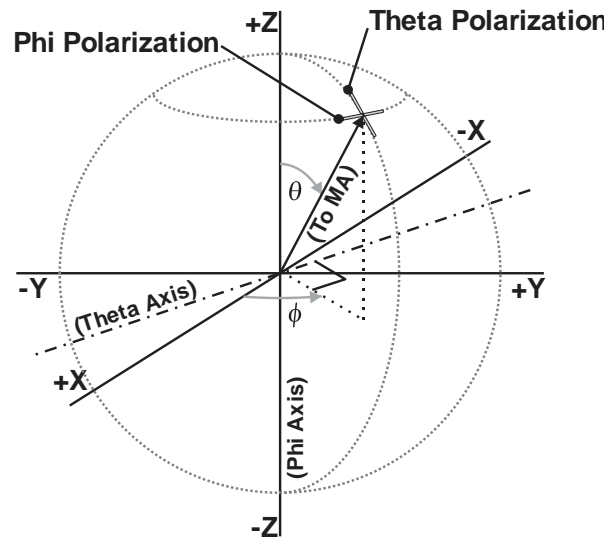
Figure 5.2-2 Measurement Antenna Polarizations

The test plan assumes that the DUT will be supported by some sort of structure along the –z-axis, which is likely to obstruct or obscure the measurement of the data point at the $\theta = 180°$ point. The resulting spherical coverage required for a pattern test (based on 15 degree steps) is given in Figure 5.2-3, which shows that the whole 3D surface is included in the testing, with the exception of the area for which $|\theta| = 165°$. The ripple test is intended to cover the same range of angles for each axis as are required to perform a pattern measurement. Thus, the theta-axis ripple test only extends to $\theta = 165°$.
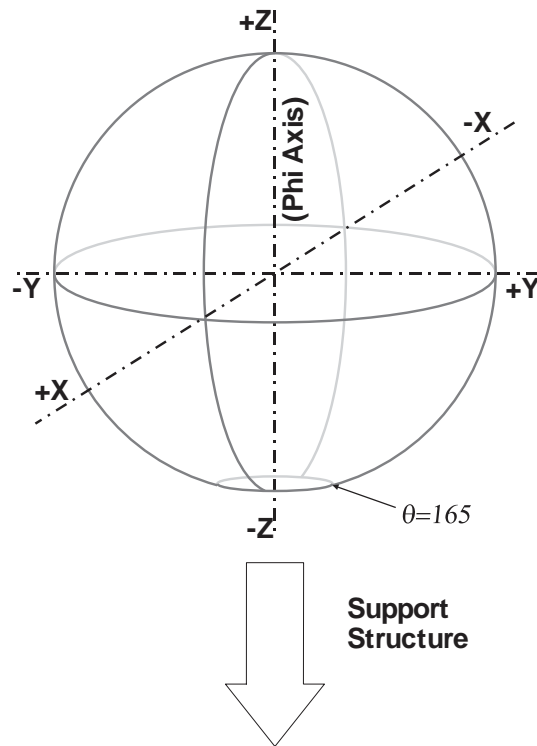
Figure 5.2-3 Spherical Coverage and Orientation of Support Structure with Respect to Coordinate System

For the purposes of these tests, two principal categories of positioning systems will be defined, based on expected methods of performing spherical pattern tests. These are distributed-axes systems and combined-axes systems. Distributed-axes systems move the measurement antenna about the DUT and phi-axis positioner (Figure 5.2-4a) and are representative of most conical cut method systems. Combined-axes systems mount the phi-axis positioner on the theta-axis positioner to rotate the DUT along two axes (Figure 5.2-4b). Examples of this type of system include so-called multi-axis positioning systems and the manual great-circle cut method. The ripple test is intended to cover the same range of angles and perform an equivalent measurement no matter what the design of the positioning system.
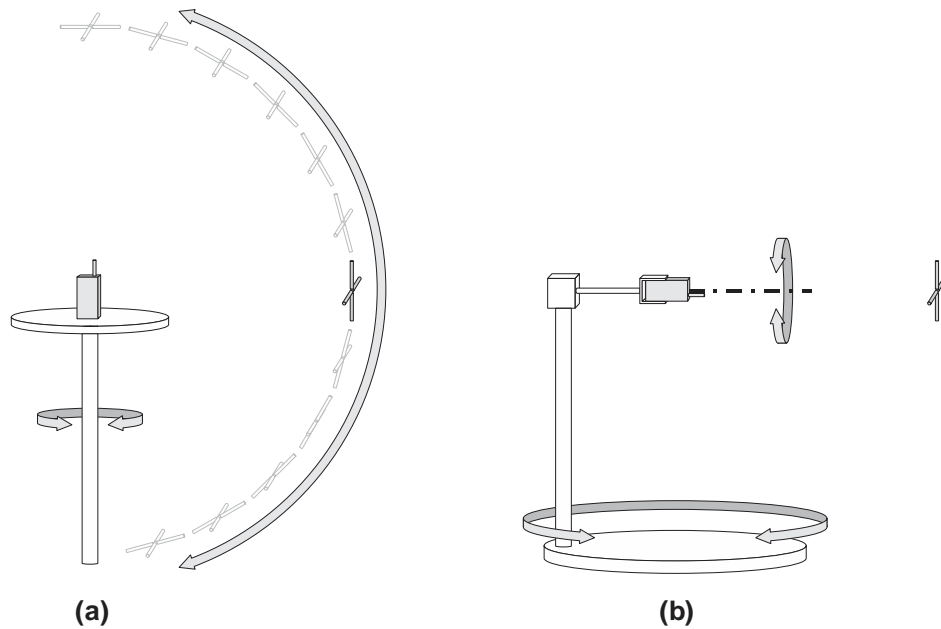
Figure 5.2-4 Illustrations of Typical Distributed-Axes System (a) and Combined-Axes System (b)

5.3   Basic Measurement Procedure

There are two main parts to the measurement procedure; the phi-axis ripple test and the theta-axis ripple test. This procedure shall be followed to verify the performance of the test system for each variation in the mounting system (i.e., free-space vs. head/hand phantom) to be used in normal testing. All required mounting structure and test equipment required for normal testing shall be in place, subject to the allowances specified below. Note that for manual great circle cut systems, it may be necessary to test each different support used to position the DUT to different phi angles.

It is necessary to ensure the symmetry of the probe antennas used to perform the test. This may be certified by a qualified calibration lab prior to their use or may be verified onsite provided sufficient symmetry exists in the probe antenna support structure to demonstrate the required symmetry. The measurements outlined above will be used to determine the uncertainty related to ripple for Radiated Power and Receiver Performance measurements as well as the Range Reference Measurement. These measurements will provide results representative to the ripple uncertainty which can be expected when using a dipole for the range reference measurement, but not when using a horn. A horn is more directional than sleeve dipoles and magnetic loops therefore for a well-designed system the impact of ripple on the range reference measurement is lower when using a horn. If the lab is using a horn for the range reference measurement, and choses, an additional ripple test can be performed. The lab is still required to perform the theta and phi axis ripple test to determine the ripple uncertainty for the Radiated Power and Receiver Performance measurements.

5.3.1   Probe Antenna Symmetry Test

This test is intended for qualification of the symmetry of the probe antennas. It is not considered a direct part of the ripple test, but rather a certification step to ensure that the probe may be used to satisfy the ripple test requirements. As such, the system configuration may be modified from the ripple test configuration as required to perform this verification.

For each probe antenna to be verified, repeat the following steps:

1. Mount the probe antenna at the center of a dielectric support such that the probe's axis is centered along the positioner's axis of rotation and the axis of rotation points through the nulls in the pattern of the dipole or loop. (Normally this test would be done using the phi axis of the positioner, but either axis is acceptable as long as the desired result is achieved). Ensure that there is no wobble in the orientation of the probe through a 360° rotation of the axis.
2. Place the measurement antenna in the co-polarized position (parallel to the axis of a dipole and tangential to the loop) a distance at least R (the minimum measurement distance specified in in Section 5.3, the frequency band being tested) meters away from the probe antenna. Adjust the elevation of the measurement antenna to be at boresight with the center of the probe antenna.
3. Attach a signal source to a coaxial cable feeding the probe antenna and set the frequency to the appropriate channel. Set the amplitude to a level appropriate for the measurement receiver. Connect a measurement receiver to the measurement antenna. Ensure that all coaxial cables are dressed to minimize effects upon the measurement results.
4. Rotate the probe antenna about its axis and record the signal received by the measurement antenna at every 2 degrees of azimuth for a total of 360°.
5. Record the measurement results to a file that can be imported into a Microsoft™ Excel spreadsheet.
6. Repeat steps 1 through 6 above for each probe antenna.

    Note: The sleeve dipole and loop antennas may be combined into one reference assembly, thus allowing the two data sets to be taken conjointly.

The total ripple observed in this symmetry test should be less than ±0.1 dB from the midpoint (0.2 dB peak-to-peak) in order for the associated probe antenna to be used for the remaining tests. In cases where it is not possible to use a dipole with the desired symmetry (e.g. where a smaller than resonant dipole is needed due to mechanical constraints of the positioning system) a dipole with a larger measured asymmetry value may be used provided the asymmetry error in excess of ±0.1 dB is combined with the corresponding surface standard deviation (SSD) or maximum ripple measurement results by the root-sum-of-squares (RSS) method. For example, assume that the (+, -) position of the phi-axis ripple test requires the use of a dipole with an asymmetry of ±0.3 dB and measures an SSD of ±0.5 dB, then the reported result for that position would be $((0.3 - 0.1)^2 + 0.5^2)^{\frac{1}{2}} = \pm0.54\,\mathrm{dB}$. The maximum dipole asymmetry allowed with this method shall be ±0.5 dB.

5.3.2   Phi-Axis Ripple Test

The phi-axis ripple test covers a cylindrical quiet zone 300 mm in diameter around the phi axis and 300 mm long. Each probe antenna is oriented with its axis parallel to the phi axis at a total of six positions defined by three positions along the phi axis (one at the center of the quiet zone and one each ± offset along the phi axis), combined with one 150 mm offset perpendicular to the phi axis for each axial offset. At each position, the phi axis is rotated 360° with the measurement antenna positioned at theta = 90° to record the ripple. Each position is labeled by its radial and axial offset from the center position, (R, Z), using 0, +, or – to represent the appropriate offset in each direction. See Figure 5.3.2-1 for additional information.

Figure 5.3.2-1 Phi-Axis Test Geometry

For each polarization and band, repeat the following steps:

1. Place the measurement antenna and any associated theta-axis positioner at theta = 90° such that the measurement antenna is boresight with the center of the quiet zone. The measurement antenna should be at the same separation distance to be used for actual pattern measurements. This distance must be at least R (the minimum measurement distance specified in Section 2 for the frequency band being tested) meters away from the center of the quiet zone. Select or adjust the polarization to correspond to the polarization (theta or phi) to be tested.

2. Mount the probe antenna to the phi-axis positioner using a low permittivity dielectric support. Use the sleeve dipole for the theta polarization and the loop for the phi polarization. At each of the six offset positions, ensure that the axis of the probe is parallel to the phi axis of rotation.

3. Attach a signal source to a coaxial cable feeding the probe antenna and set the frequency to the appropriate channel. Set the amplitude to a level appropriate for the measurement receiver. Connect a measurement receiver to the measurement antenna. The received signal during the ripple test measurement should be at least 40 dB above the noise floor or noise errors greater than 0.1 dB will result. Ensure that all coaxial cables are dressed to minimize effects upon the measurement results.

4. Rotate the probe antenna about the phi axis and record the signal received by the measurement antenna at every 2 degrees of azimuth for a total of 360°.

5. Record the measurement results to a file that can be imported into a Microsoft® Excel spreadsheet.

6. Record test parameters including: (a) the distance between the measurement and probe antennas, (b) cable losses and other losses associated with the measurement setup, (c) the power of the signal source at the probe antenna connector, and (d) the noise level of the receiver with no signal applied.

7. Repeat steps 1 through 6 above for each probe antenna (polarization and band) for each of the 6 test positions, offsetting 150 mm ±3 mm from the center of the quiet zone in each direction along the phi axis and radially from the center.

5.3.3 Theta-Axis Ripple Test

The theta-axis ripple test covers a quiet zone sphere 300 mm in diameter. Each probe antenna is oriented with its axis parallel to the theta axis at a total of seven positions defined by two 150 mm offsets along each Cartesian axis. At each position, the theta axis is rotated from –165° to 165° with the measurement antenna positioned at phi = 0°, or for two separate tests from 1-165° with the measurement antenna positioned at phi = 0° and again at phi = 180°, to record the ripple. Each position is labeled by its offset from the center position along each axis, (X, Y, Z), using 0, +, or – to represent the appropriate offset in each direction. See Figure 5.3.3-1 for additional information.
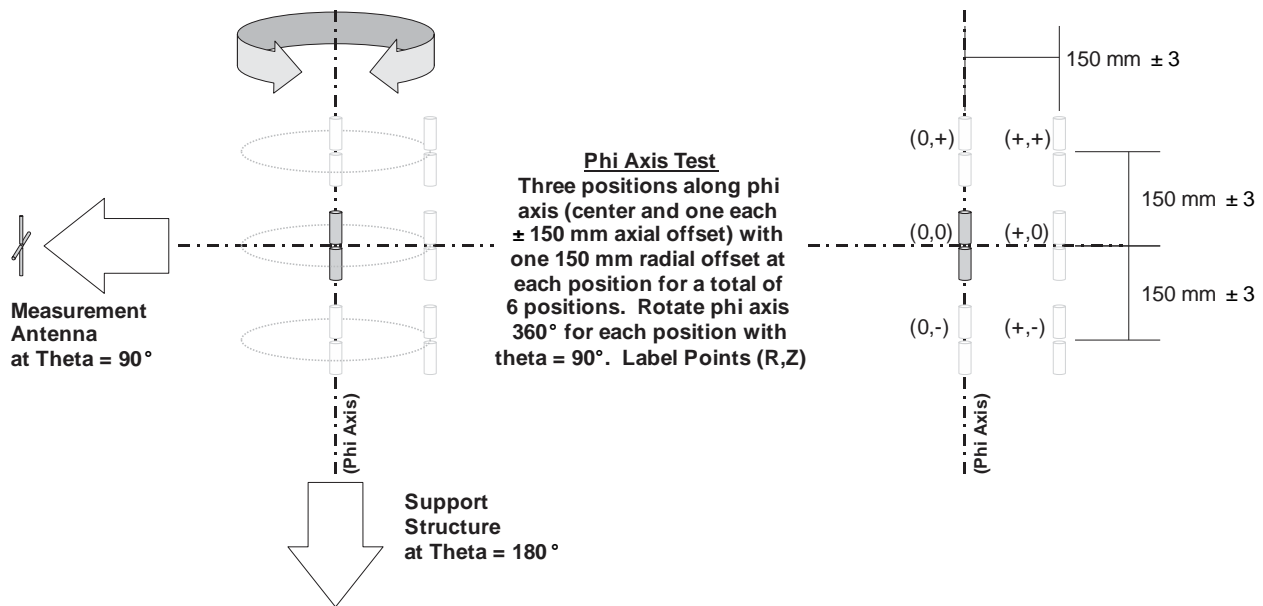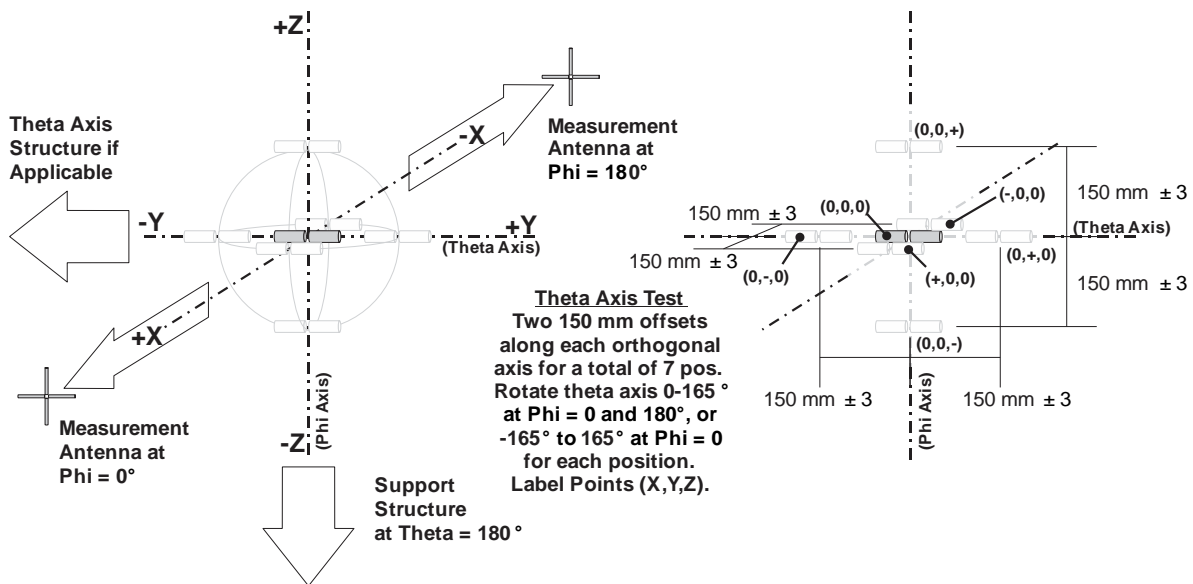

Figure 5.3.3-1 Theta-Axis Test Geometry

For each polarization and band, repeat the following steps:

1. Place the measurement antenna such that it is boresight with the center of the quiet zone. The antenna should be at the same separation distance to be used for actual pattern measurements. This distance must be at least R (the minimum measurement distance specified in Section 2 for the frequency band being tested) meters away from the center of the quiet zone. Select or adjust the polarization to correspond to the polarization (theta or phi) to be tested.

2. With the phi-axis positioner set to 0° (or for both phi = 0 and 180° in cases where the theta positioner range of motion is less than ±165°) mount the probe antenna with its axis parallel to the theta axis of rotation using a low permittivity dielectric support. Use the sleeve dipole for the phi polarization and the loop for the theta polarization. At each of the seven offset positions, ensure that the axis of the probe is parallel to the theta axis of rotation. In cases where the theta positioner range of motion is less than ±165°, the probe antenna and associated cables should maintain the same orientation with respect to the phi-axis positioner structure for both the phi = 0 and 180° test cases. (That is, the probe should be mounted such that it rotates with the phi positioner.)

3. Attach a signal source to a coaxial cable feeding the probe antenna and set the frequency to the appropriate channel. Set the amplitude to a level appropriate for the measurement receiver. Connect a measurement receiver to the measurement antenna. The received signal during the ripple test measurement should be at least 40 dB above the noise floor

or noise errors greater than 0.1 dB will result. Ensure that all coaxial cables are dressed to minimize effects upon the measurement results.

4. Rotate the probe antenna about the theta axis and record the signal received by the measurement antenna at every 2 degrees of azimuth for a total of 330°, or two separate tests of 164°.

   Note: To cover the same range of angles at 2° steps, the range of the two individual tests is reduced by one degree since the zero degree position is not measured.

5. Record the measurement results to a file that can be imported into a Microsoft☐ Excel spreadsheet.

6. Record test parameters including: (a) the distance between the measurement and probe antennas, (b) cable losses and other losses associated with the measurement setup, (c) the power of the signal source at the probe antenna connector, and (d) the noise level of the receiver with no signal applied.

7. Repeat steps 1 through 6 above for each probe antenna (polarization and band) for each of the 7 test positions, offsetting 150 mm ±3 mm from the center of the quiet zone along each of the six cardinal directions.

5.3.4   Allowances and Adjustments

When implementing these tests on actual positioning systems, it is possible that there will be interference issues between the required test positions and the mechanical support structure required to hold the DUT or head/hand phantom during a test. This section details a list of allowances whereby the test system may be modified slightly from its normal test configuration in order to perform the ripple tests. Where possible, the alterations to the system should be minimized, and the final acceptability of any adjustment shall be the decision of the appropriate CTIA Certification subject matter expert (SME).

1. The portion of the support structure required to mount the DUT to the phi-axis positioning structure for the free-space test may be removed to clear the region of the quiet zone for the ripple test for both axes. The tester should be prepared to show that the structure removed has a negligible impact on the free-space pattern measurement of the DUT, compared to the remaining structure included in the ripple test.

2. Support materials with a dielectric constant less than 1.2 may be removed to a maximum distance of 250 mm outside the quiet zone (400 mm from the center).

3. An adapter plate comprising up to 13 mm of dielectric material with a permittivity less than 4.5 and residing wholly within the footprint of the base of the head phantom base may be considered part of the head phantom and removed with the head phantom for the purposes of the ripple test. In addition, any support structure used to hold the hand phantom should be removed, because a separate uncertainty term is used to address its effect.

4. For the phi-axis ripple test, where mechanical interference with support structure may prevent rotation of the probe antennas around the phi axis, the phi-axis positioning structure may be moved away from the quiet zone the minimum distance required to perform the (X,–) position tests. It should not be necessary to move the support for the remaining phi-axis positions.

5. To avoid near-field effects that may incorrectly bias the ripple test, no remaining support material with a dielectric constant greater than 1.2 should be within 75 mm of any point on the physical surface of the antenna portion of any probe. This is primarily expected to be an issue for the theta-axis test where loops and dipoles may be expected to physically intersect with any remaining head phantom support. To accommodate this possibility

without eliminating a required test point, the test point closest to the phi-axis support (0,0,–) may be substituted with one of the following tests, in order of preference:

    a. The maximum of the two points defined by offsetting 150 mm ±3 mm in either direction parallel to the theta axis (Y-axis) from the (0,0,–) point, labeled as (0,+,–) and (0,–, –), may be substituted for (0,0,–).

    b. If both of those points cannot be measured, either:

        i. The maximum of the two points defined by offsetting 150 mm ±3 mm in either direction along the direction perpendicular to both the theta and phi axes (X-axis) from the (0,0,–) point, labeled as (+,0,–) and (–,0,–), may be substituted for (0,0,–).

<p align="center">OR</p>

        ii. The phi-axis positioning structure may be moved away from the quiet zone the minimum distance required to provide the required clearance from the surface of the probe antennas
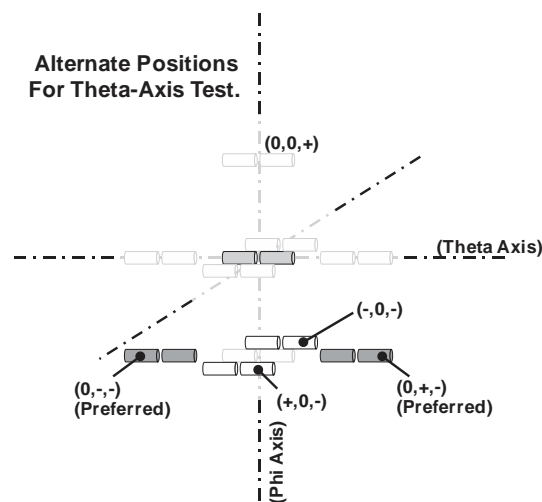
Figure 5.3.4-1 Illustration of Alternate Probe Positions Allowed for Theta-Axis Test

6. In case the θ-axis or ϕ-axis positioning systems cannot accommodate 2° angular resolution, a coarser angular sampling is allowed provided the number of offset positions along the cardinal axes is increased accordingly. In any case, the sample spacing shall not exceed 15°. The offset positions shall be computed in the following manner:

    a. Determine the ratio of the achievable angular resolution to the nominally specified 2° resolution.

    b. Round this ratio up to the next whole number.

    c. Divide 150 mm by the number obtained above and round to the nearest 5 mm. This will be the offset increment.

    d. Starting from the center, create the list of offset positions along the cardinal axes, each position separated by the offset increment. The last offset will be exactly 150 mm, even if the distance between the penultimate and last offset positions will be less than one increment (See examples in Table 5.3.4-1).

Consider the following acceptable examples for various angular resolutions.

Table 5.3.4-1 Example Scenarios for Reduced Angular Resolution Ripple Tests

Angular Resolution (Deg)	Rounded Ratio of Resolution Relative to 2°	Offset Increment (mm)	X-Offsets (mm)	Y-Offsets (mm)	Z-Offsets (mm)
2	1	150	±150	±150	±150
5	3	50	±50, ±100, ±150	±50, ±100, ±150	±50, ±100, ±150
10	5	30	±30, ±60, ±90, ±120, ±150	±30, ±60, ±90, ±120, ±150	±30, ±60, ±90, ±120, ±150
15	8	20	±20, ±40, ±60, ±80, ±100, ±120, ±140, ±150	±20, ±40, ±60, ±80, ±100, ±120, ±140, ±150	±20, ±40, ±60, ±80, ±100, ±120, ±140, ±150

5.4 Additional Ripple Test Requirements for Notebook-Sized Test Volumes

Prior to certification testing of notebooks or similar devices not fitting within a 300 mm diameter sphere, additional ripple tests will be required. The quiet zone shall be probed following the methods described in Section 5.2 and Section 5.3 but with added probe antenna offsets corresponding to the largest volume for which the test system will be authorized. Additional allowances have been incorporated in the test procedure to accommodate ripple testing with commonly used positioners and fixtures previously certified for handset testing. The overall results shall be used in estimating measurement uncertainty for these larger devices. To have the most accurate uncertainty estimates for different types of test objects, it is recommended that the ATL provides separate uncertainty calculations for handset measurements and notebook measurements.

The following subsections describe changes and additions to the tests described in Section 5.3 for a notebook type device with maximum physical dimension, D. For notebook testing, D shall be assumed to be 500 mm, which accounts for the maximum distance from corner to corner in the largest available "desktop replacement" notebooks. Notebooks with large form factors typically are wider than tall and have the embedded antennas located in the display. For these reasons and to accommodate existing positioner systems, the ripple test will assume that there will be no source of radiation at $Z < -150$ mm. The effective ripple scan volume will be a cylinder of diameter $D = 500$ mm and axial extension from $Z = -150$ mm to $Z = 210$ mm. See Figure 5.4-1 for an illustration of the alternate test volume for notebooks.

CTIA 01.73, Version 4.0.4
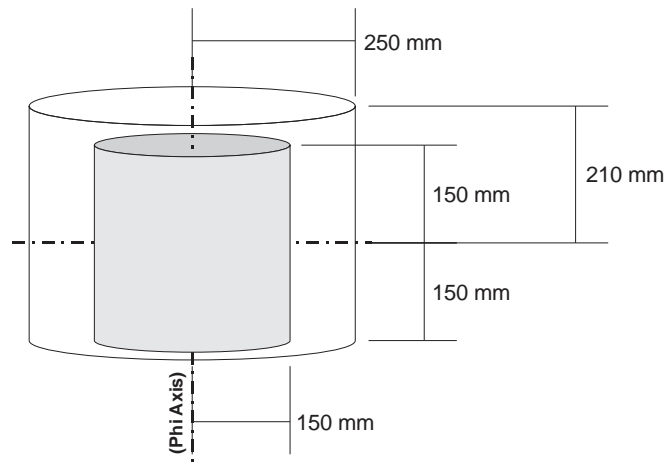
Figure 5.4-1 Illustration of the Increase in Test Volume for Notebooks

5.4.1   Probe Antenna Symmetry Test

Provided all ripple tests are performed using the same probe antennas, no additional testing is required to validate the probe antenna symmetry.

5.4.2   Extensions to Phi-Axis Ripple Test

Perform the test as described in Section 5.3.2 for all probe antennas and all bands, but at four additional probe antenna offsets along the radial and axial directions. The four supplementary (R, Z) positions will then be at (0, +210 mm), (+250 mm, –150 mm), (+250 mm, 0), (+250 mm, +210 mm).
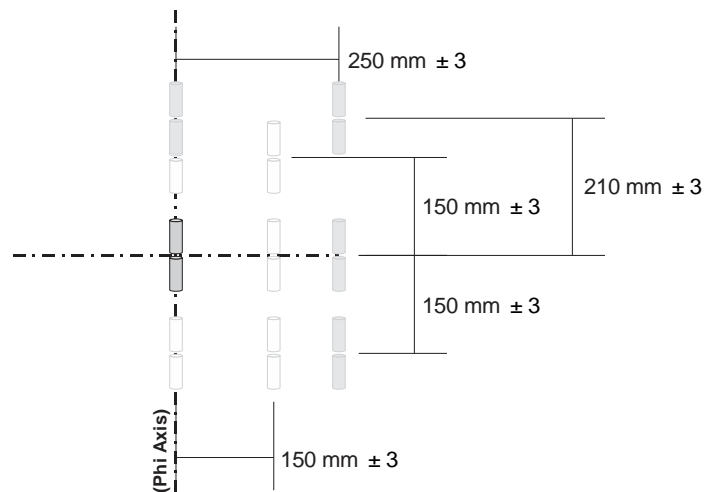
Figure 5.4.2-1 Illustration of the Additional Phi-Axis Ripple Test Locations for Notebooks

5.4.3 Extension to Theta-Axis Ripple Test

Perform the test as described in Section 5.3.3 for all probe antennas and all bands, but at five additional offset positions. The five supplementary positions will be along the cardinal axes at (X, Y, Z) coordinates given by (±250 mm, 0, 0), (0, ±250 mm, 0), and (0, 0, +210 mm).
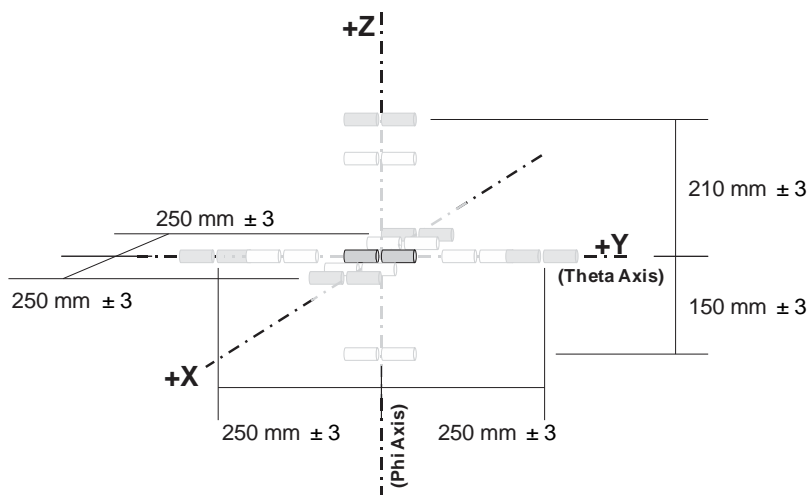
Figure 5.4.3-1 Illustration of the Additional Theta-Axis Ripple Test Locations for Notebooks

5.4.4 Additions to Allowances and Adjustments

This section describes modifications to the allowances that are given in Section 5.3.4 that will be made to accommodate the ripple test in practical automated systems. Where possible, the alterations to the system should be minimized, and the final acceptability of any adjustment shall be the decision of the appropriate CTIA Certification subject matter expert (SME).

1. The portion of the support structure required to mount the DUT to the phi-axis positioning structure for the free-space test may be removed to clear the region of the quiet zone for the ripple test for both axes. The tester should be prepared to show that the structure

removed has a negligible impact on the free-space pattern measurement of the DUT, compared to the remaining structure included in the ripple test.

2. Support materials with a dielectric constant less than 1.2 may be removed to a maximum distance of 250 mm outside the quiet zone (400 mm from the center).

3. An adapter plate comprising up to 13 mm of dielectric material with a permittivity less than 4.5 and residing wholly within the footprint of the notebook base may be considered part of the notebook and removed for purposes of the ripple test. Additional dielectric brackets and fixtures necessary to maintain screen notebook and display position will also be removed for the purposes of the ripple test, provided the dielectric material has a permittivity of less than 4.5, and these materials protrude less than 13 mm beyond any surface of the notebook, and such fixtures are not physically located within 100 mm of the tested antenna(s) in the device.

4. For the phi-axis ripple test, where mechanical interference with support structure may prevent rotation of the probe antennas around the phi-axis, the phi-axis positioning structure may be moved away from the quiet zone the minimum distance required to perform the (+250 mm, −150 mm) position tests. It should not be necessary to move the support for the remaining phi-axis positions.

5. To avoid near-field effects that may incorrectly bias the ripple test, no remaining support material with a dielectric constant greater than 1.2 should be within 75 mm of any point on the physical surface of the antenna portion of any probe. This is primarily expected to be an issue for the theta-axis test where loops and dipoles may be expected to physically intersect with any remaining SAM phantom support. As this ripple test has been limited to −150 mm offsets along the Z-axis, the following text is identical to the text in Section 5.3 except that for clarity, the "+/−" notation has been replaced with specific coordinates. The test point closest to the phi-axis support (0, 0, −150 mm) may be substituted with one of the following tests, in order of preference:

    a. The maximum of the two points defined by offsetting 150 mm ±3 mm in either direction parallel to the theta axis (Y-axis) from the (0,0, −150 mm) point, labeled as (0, +150 mm, −150 mm) and (0, −150 mm, −150 mm), may be substituted for (0, 0, −150 mm).

    b. If both of those points cannot be measured, either:

        i. The maximum of the two points defined by offsetting 150 mm ±3 mm in either direction along the direction perpendicular to both the theta- and phi-axes (X-axis) from the (0, 0, −150 mm) point, labeled as (150 mm, 0, 150 mm) and (−150 mm, 0, −150 mm), may be substituted for (0, 0, −150 mm).

        or

        ii. The phi-axis positioning structure may be moved away from the quiet zone the minimum distance required to provide the required clearance from the surface of the probe antennas.

6. In case the θ-axis or φ-axis positioning systems cannot accommodate 2° angular resolution, a coarser angular sampling is allowed provided the number of offset positions along the cardinal axes is increased accordingly. In any case, the sample spacing shall not exceed 15°. The offset positions shall be computed in the following manner:

    a. Determine the ratio of the achievable angular resolution to the nominally specified 2° resolution.

    b. Round this ratio up to the next whole number.

    c. Multiply this ratio by 0.4 to account for the increase in radius of the test volume.

    d.   Round this ratio up to the next whole number.

    e.   Divide 100 mm by the number obtained above and round to the nearest 5 mm. This will be the offset increment.

    f.   Starting from 150 mm, create the list of offset positions along the cardinal axes, each position separated by the offset increment calculated above. The last offset will be exactly 250 mm for the X- and Y-axes and 210 mm for the +Z-axis, even if the distance between the penultimate and last offset positions will be less than one increment.

5.5 Reference Horn Ripple Test Procedure

If a horn is being used for the range reference measurement, the following procedure can be performed to quantify the effect of ripple on the range reference measurement, in addition to the theta and phi axis test.

A depiction of the typical ripple test set up with the horn is shown in Figure 5.5-1 below.
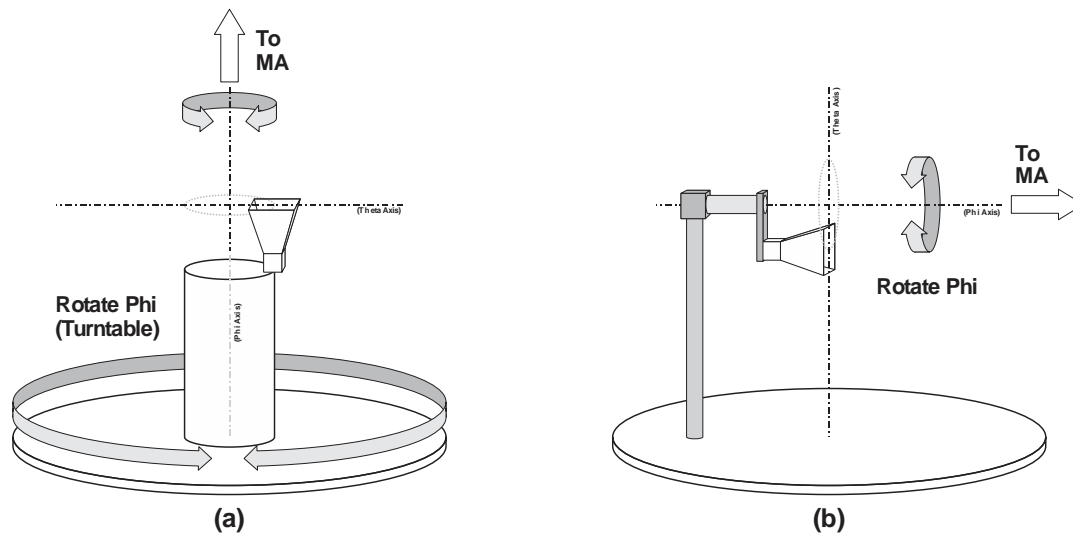
Figure 5.5-1 Horn Configured for Range Reference Measurement in Distributed Axes System (a), and a Combined Axes System (b)

The first measurement is performed with the horn in the standard position for the range reference measurement. The following measurements are performed with the horn offset from the center of the measurement system. The offset will be referred to as 'r' or a radial offset. The mast which is used should be the same as used for the range reference measurement. For the radial offset measurement additional low dielectric fixtures/mounts may be used. A low perturbation fixture should be used to ensure that the side lobes of the antenna do not impact the ripple test results.

For the measurement, the horn will be rotated in phi and therefore will capture the ripple for both x and y offsets.

The x and y offsets will capture the ripple that impacts the range reference measurement therefore there is no need to perform measurements offset in z.

For each measurement rotate the horn 360 degrees and measure the power in both the theta and phi polarizations every 5 degrees.

Note: This angular spacing was determined using the highest (5925 MHz) and lowest (617 MHz) quiet zone measurement frequency in the current test plan and estimating the size of the reference antenna (maximum dimension of 50 cm).

The horn shall first be measured in the standard position for the range reference measurement then moved radially for four separate measurements, with r being a uniform step with the final position in r being λ/2 of the lowest frequency at which the horn is used (for the range reference measurement).

Note: This spacing ensures that the highest frequency, 5925 MHz, will be measured at roughly every λ/2 for a reference antenna operating down to the lowest measurement frequency, 617 MHz. For example, 0.66 λ at 3.7GHz for a reference antenna that is measuring down to 700 MHz, which means the maximum radial offset of the antenna will be 0.214 meters.

The measurement shall be performed following the same method used to perform the range reference measurement, for example, measure the same point in theta which is normally measured during the range reference measurement.

5.6   Applying the Ripple Test Procedure to Specific Systems

The procedure presented in the previous sections should be applicable to any fully automated spherical pattern measurement system. This section provides several illustrations to assist in interpretation of the requirements for different system types.
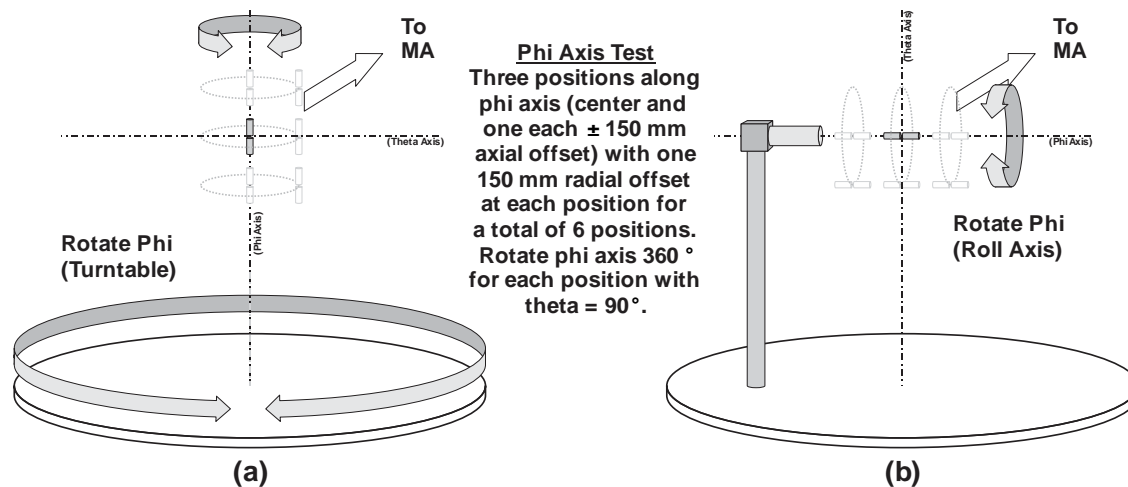
Figure 5.6-1 Phi-Axis Test Geometry for a Typical Distributed-Axes System (a), and a Typical Combined-Axes System (b)

Rotate Theta (Measurement Antenna)

To MA

(Theta Axis)

(Phi Axis)

Theta Axis Test
Two offsets along each orthogonal axis for a total of 7 pos. Rotate ±165 degrees for each postion.

(a)

To MA

(Phi Axis)

(Theta Axis)

Rotate Theta (Turntable)

(b)
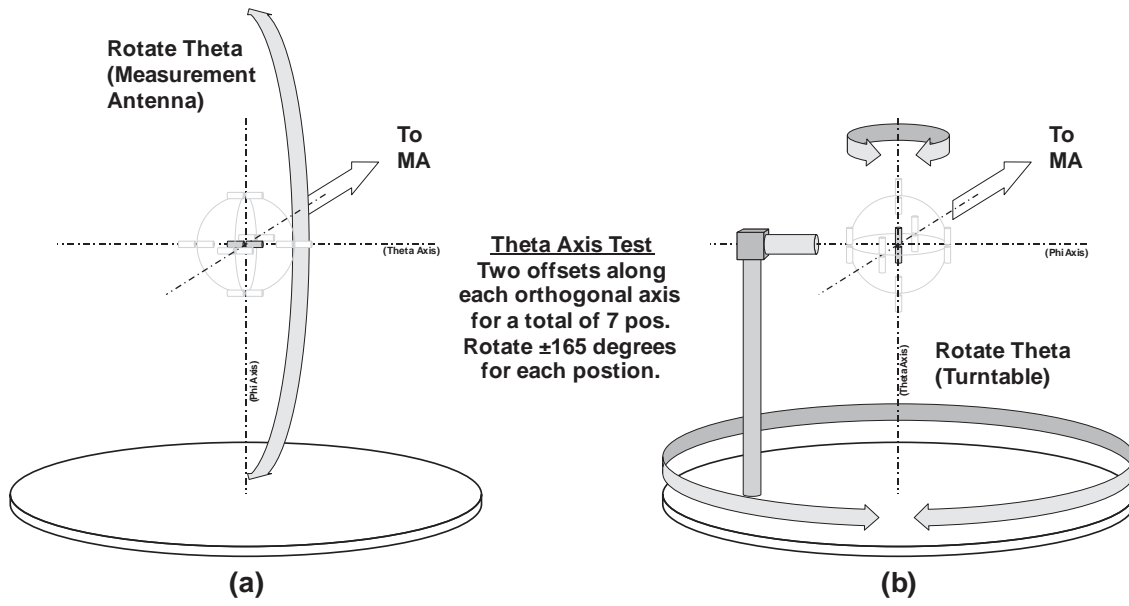
Figure 5.6-2 Theta-Axis Test Geometry for a Typical Distributed-Axes System (a), and a Typical Combined-Axes System (b)

CTIA
Certification™

Procedure allows the removal of a certain amount of low dielectric material and minor adjustments to location of positioning equipment to accommodate test.

Rotate Phi (Turntable)

(Phi Axis)

(Theta Axis)

To MA

(a)

Rotate Phi (Roll Axis)

(Phi Axis)

(Theta Axis)

To MA

(b)
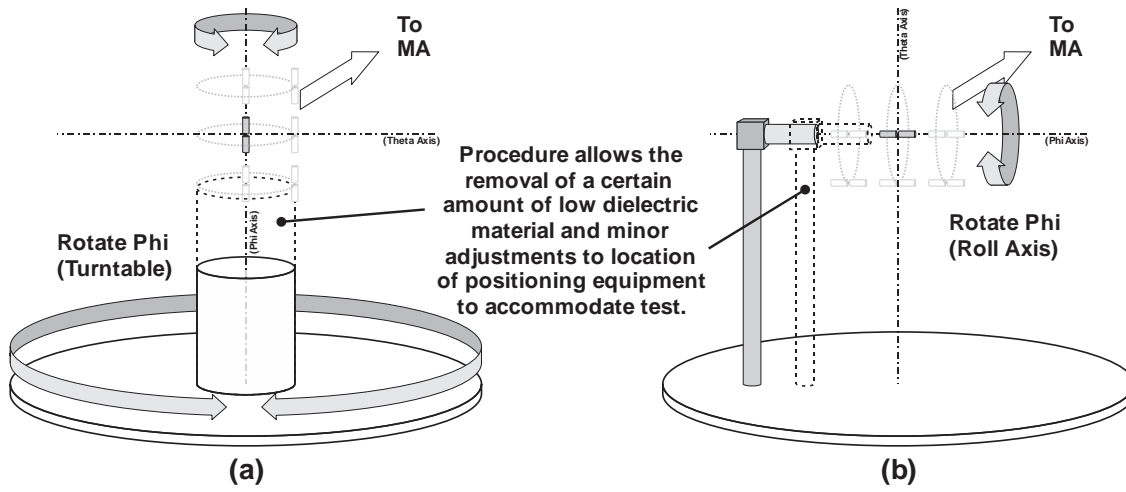
Figure 5.6-3 Example Illustrating Some Allowed Alterations of Test Setup for Phi-Axis

CTIA Certification™
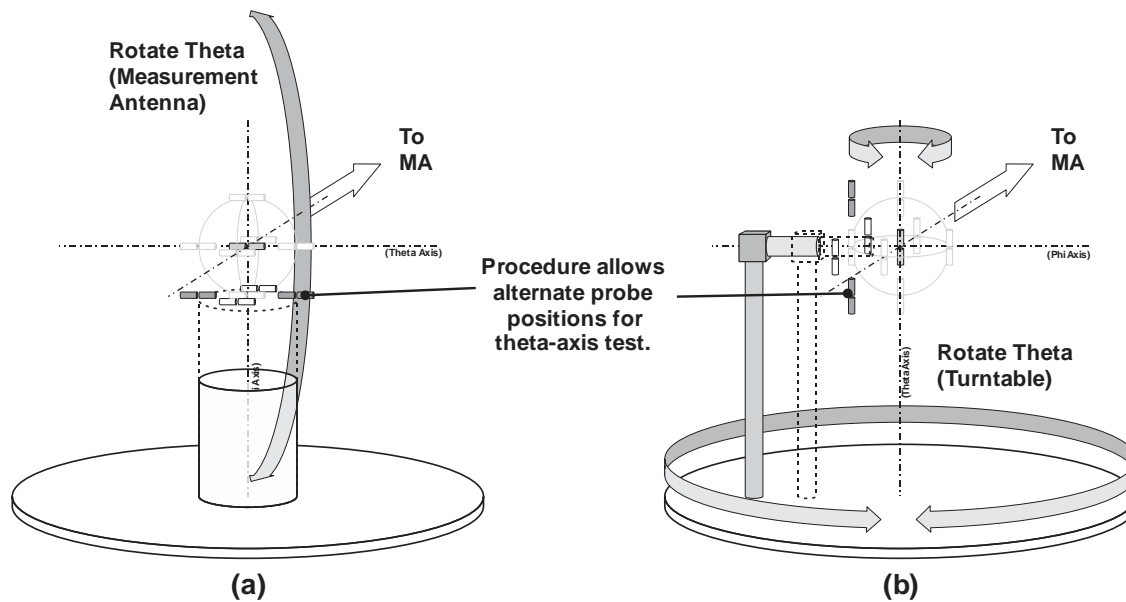
Figure 5.6-4 Example Illustrating Alternate Positions and Allowed Alterations for Theta-Axis Test

5.7   Analysis

1. Adjust the off-axis ripple measurements to correct for distance variation using the equation for the Law of Cosines.

    Note: For long range lengths where this adjustment may be considered negligible, it is not required to apply the correction.

2. Plot the corrected patterns using polar coordinates.
3. Use the procedures defined in *CTIA 01.70* [1] to calculate the resulting measurement uncertainty due to the ripple test results.
4. The plot and calculated results are to be supplied as part of the ATL authorization process.

Law of Cosines Adjustment Method (for Far-Field testing)

For coplanar antennas, the Law of Cosines may be used to determine the distance between antennas as one is rotated about a center axis. Since each ripple test measurement is self-referencing, minor differences in elevation will have only second or third order effects on the result. Refer to Figure 5.7-1 to aid in understanding this discussion.

Note: This illustration is a view from the perspective of looking down on vertically oriented antennas from above.

$$d^2 = r^2 + l^2 - 2rl \cos(\alpha)$$
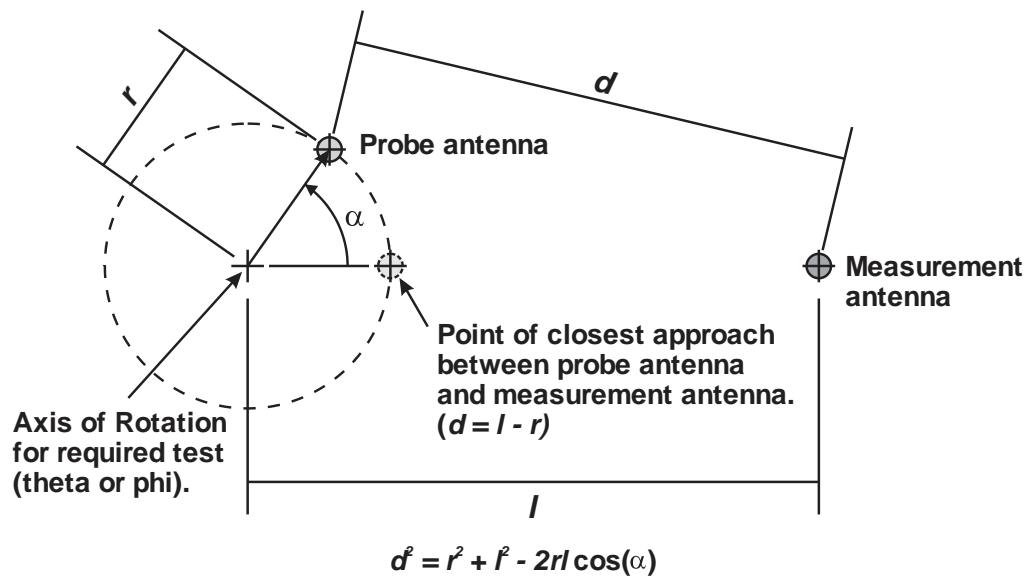
Figure 5.7-1 Geometry for Law of Cosines Range Length Adjustment

- Let l be the distance measured between the axis of rotation and the measurement antenna

- Let r be the measured distance that the probe antenna is offset from the axis of rotation.

- Let α be the rotation angle of the probe antenna where 0-degrees is the point where the probe antenna is closest to the measurement antenna and 180-degrees is the point where the probe antenna is farthest away from the measurement antenna. This is either the theta or phi angle for the associated ripple test, with the required angular offset

- applied (i.e. $\alpha = \theta + 0, 90,$ or $180°$). The corrections for the phi-axis test may be simplified by starting with the probe antenna closest to the measurement antenna so that $\alpha = \phi$.

- Let d be the calculated distance between the probe antenna and the measurement antenna. Then d may be calculated from the Law of Cosines as follows:

Equation 5.7-1

$$d^2 = r^2 + l^2 - 2rl \cos(\alpha)$$

- Adjust the measured signal power to account for distance variation using the following equation:

<div align="right">Equation 5.7-2</div>

$$P_{adj}(dBm) = P_{meas}(dBm) + 20\log(d/l)\,(dB)$$

Note: Parameter r and l must be carefully measured and recorded to enable accurate application of this technique.

Section 6 Reverberation-Chamber Precharacterization Procedure

6.1 Methodologies Used in Chamber Characterization and DUT Performance Assessment

6.1.1 Methodology – Reverberation Chamber Configuration and Measurement of S-Parameters

This configuration is required to determine the chamber's coherence bandwidth, chamber precharacterization, and reference power transfer function. The measurement and post-processing steps required for determining the chamber power transfer function are the same for the precharacterization and reference measurement steps. These steps are described below:

1. The following objects shall be placed into the test volume of the reverberation chamber: the reference antenna, measurement antenna, fixture for the DUT (if utilized), and RF absorber and/or phantom(s), as described in Sections 6.2.2 (proximity effect test), 6.2.3 (uncertainty due to lack of spatial uniformity) or *CTIA 01.21* [3] (reference measurement and DUT measurements). Additional objects may be required, as described in the appropriate subsection. The same antennas shall be used for both the precharacterization and reference measurement steps. The reference antenna shall be placed in the test volume of the chamber in such a way that it undergoes the same stirring sequence that the DUT antenna will undergo during the TRP or TIS measurements and is a minimum of 0.5λ from any walls, mode-stirrers, or other metallic objects [12]. Directional reference antennas shall be pointed away from both the DUT and the measurement antennas. This configuration ensures that the loss in the chamber, which determines the power transfer function, is the same during both the reference power transfer function characterization and the DUT measurement.

2. Calibrate the vector network analyzer with a full two-port calibration so that the vector S-parameters between the ports of the measurement antenna and the reference antenna can be measured. See *CTIA 01.21* [3].

3. Connect the antennas to the cables and measure the full set of vector two-port S-parameters for N mode-stirring samples. The mode-stirring samples shall be collected in stepped mode. For each mode-stirring sample, the complex S-parameters shall be stored for later calculations.

4. The stirring sequence may consist of mechanical stirring, antenna-position stirring, polarization stirring, and other stirring methods. Frequency averaging is used across the channel bandwidth specified in Table 3-5.

5. The number and type of mode-stirring samples N in the chosen stirring sequence should be selected in such a way that they yield an acceptably low contribution to the total measurement uncertainty. To meet the specified uncertainty, the labs shall use more than 100 independent samples, preferably 200 or 400. As well, position stirring may be more effective in reducing uncertainty than mechanical stirring for devices in loaded chambers because of the potential reduction in spatial uniformity caused by the DUT. To reduce the number of samples required, the samples shall meet the correlation requirements defined in Section 6.2.2 (see Equation 6.2.2-2). In this case, the samples are considered "uncorrelated," whereby one sample is not related to another with respect to proximity, frequency step, and/or mechanical stirrer position. The number of uncorrelated samples, which is a subset of all samples, contributes to the random component of the expanded uncertainty. The number of uncorrelated samples depends on the frequency, size of chamber, size and shape of stirrers, the level of loading by absorbing objects, and whether or not frequency stirring is used.

6.1.2   Methodology – Calculation of Chamber Coherence Bandwidth

The coherence bandwidth calculated and averaged over the complete stirring sequence shall be larger than the channel over which the DUT will be measured to prevent test-set-up-induced errors in DUT measurements. Coherence bandwidth is found from S-parameter measurements made over a complete stirring sequence. It is a function of the chamber configuration, including the antennas and loading. The coherence bandwidth for DUT tests shall not be narrower than the values given in Table 3-4.

Figure 6.1.2-1 illustrates an example calculation of the normalized correlation function for a reverberation chamber. The expectation in Equation 6.1.2-1 was calculated over several different offsets between 0 and ±100 MHz from the center frequency and the results plotted to generate the correlation curve.
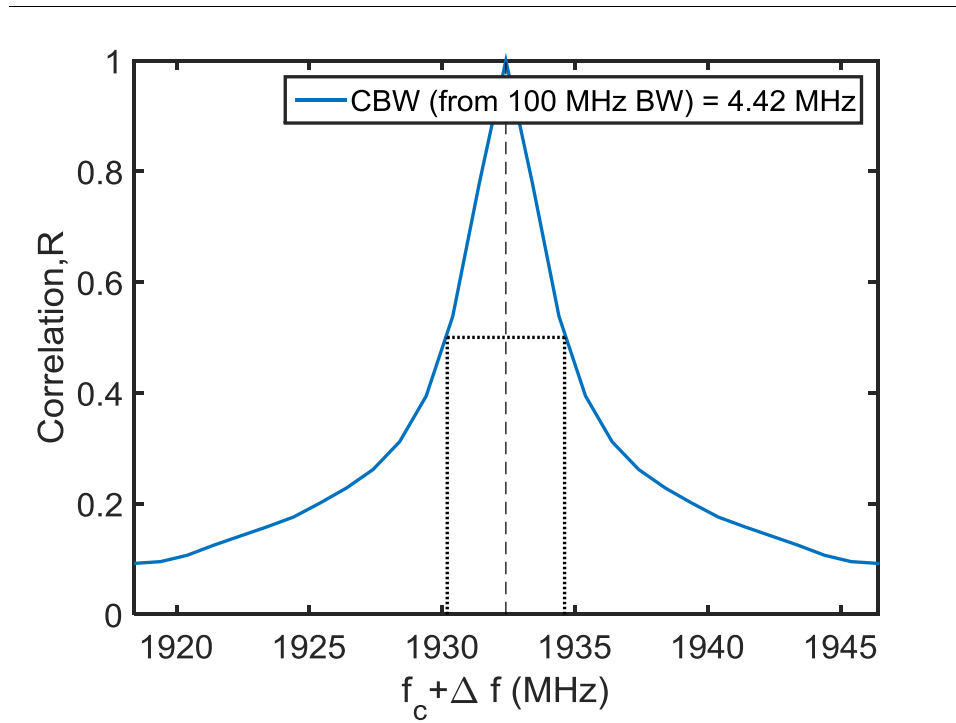
Figure 6.1.2-1 Illustration Of The Frequency Correlation Averaged Over Multiple Mode-Stirring Samples. The Coherence Bandwidth Corresponding to a Threshold Of 0.5 Is Shown by the Dotted Line

If the coherence bandwidth must be increased to meet the specifications in Table 3-4 the reverberation chamber shall be loaded with RF absorbing material, and Steps 1 through 4 below carried out iteratively until the coherence bandwidth meets the specification. Because loading the reverberation chamber also increases measurement uncertainty, it is important to ensure that the uncertainty limit is not exceeded when tuning the chamber to a specific coherence bandwidth.

The methodology for determining the coherence bandwidth for a particular reverberation-chamber set-up is as follows:

1. Using the stirring sequence chosen for device testing, measure the transmission parameter S_{21} for each mode-stirring sample n and reference antenna location t. A minimum value of $T = 1$ reference antenna locations shall be used. The VNA frequency step for this test shall be at most 100 kHz.

2. Calculate the complex autocorrelation function, R, given by Equation 6.1.2-1 or each mode-stirred sample nk, at lag, i, over a 100 MHz bandwidth for the center frequency, f_c, of each band to be evaluated.

Equation 6.1.2-1

$$R(i, n_k) = \sum_{j=\max(1, i+1)}^{\min(M, M+i)} S_{21}(f_j, n_k) S_{21}^*(f_{j-i}, n_k),$$

Where $S_{21}(f_j, n_k)$ corresponds to the measured complex S_{21} at frequency step f_j with M frequency points measured within the bandwidth of interest, BW, so that $f_1 = f_c - BW/2$ and $f_M = f_c + BW/2$. The index n_k is the mode-stirring sample (out of N). The index, i, corresponds to one of several frequency step offsets (lags) over the bandwidth of interest (here $BW = 100\ MHz$) where $-(M-1) \le i \le (M-1)$. The frequency lag shown in Figure 6.1.2-1 is given by, $\Delta f = i\left(\frac{f_M - f_1}{M-1}\right)$. The asterisk denotes complex conjugation. For $BW = 100$ MHz, the complex autocorrelation function will span 200 MHz. The autocorrelation is implemented in most numerical programs. Assuming the S_{21} data are contained in a matrix called `data_complex` with M rows of frequency steps and N columns of stirring-sequence samples, a routine may be written as

```
    M = number of frequency steps;
    N = number of stir sequence steps;
    R = empty matrix for autocorrelation values with size (2*M-1 rows, N
columns);
    for idx = 1 to N
         R_temp = autocorrelation of data_complex over all rows for column
idx. This will be an array 2*M-1 in length;
         R(all 2*M-1 rows,column idx)=R_temp. This fills the column of R;
    end
```

The variable `R` is a matrix of autocorrelation values where the lags are the rows and the columns are still the mode-stirring samples.

3. Average the autocorrelation functions from Equation 6.1.2-1 over all N mode-stirring samples at each frequency point giving the expectation of the N channels. Normalize the expectation values to a maximum of 1. A routine for this step may be written as

```
R_ave_comp = mean across columns of R;
R_ave_norm = R_ave_comp/(maximum of R_ave_comp);
R_ave_mag = absolute value of R_ave_norm
```

where `R` was defined in step 2, `R_ave_comp` is a vector comprised of the mean of the autocorrelation values over mode-stirring sample, `R_ave_norm` is `R_ave_comp` with each element divide by the maximum complex value in `R_ave_comp`, and `R_ave_mag` is the normalized magnitude of the mean autocorrelation function.

4. Determine the coherence bandwidth for the current loading condition from the frequency band that exceeds the threshold value. The threshold value shall be 0.5. An example routine may be,

```
Deltafreq = vector of frequency steps that is 2*M-1 in length
with 0 as its center midpoint;
midpoint = index of the midpoint of Deltafreq
threshold = 0.5;
pnt1 = interpolate R_ave_mag versus Deltafreq at threshold for
     points with index 1 to midpoint;
```

```
pnt2 = interpolate R_ave_mag versus Deltafreq at threshold for
        points with index midpoint to 2*M-1;
CBW = pnt2-pnt1;
```

Where `Deltafreq` is a vector of lags for the autocorrelation calculation, the interpolation is used to determine the location of the intercept with the `threshold` at 0.5, and `CBW` is the coherence bandwidth.

6.1.3   Methodology – Determination of the Reverberation Chamber's Power Transfer Function

The power transfer function G_{ref} for a given reverberation chamber configuration is estimated from T sets of the proposed stirring sequence, where each of the T sets is conducted at spatially uncorrelated reference antenna positions (see Equation 6.2.2 2 and [13]) as specified in Section 6.2.3, step 1. At each location, one sample *t* of the chamber's power transfer function is determined from the mean of the measured transmission parameter S_{21}, where the mean is calculated over all frequencies F and mode-stirring samples N. The power transfer function is then calculated from the mean of the samples that were measured at the multiple locations, transformed to dB and reported in dB. The standard deviation of these samples is also used to find the component of uncertainty due to lack of spatial uniformity in Section 6.2.3. This quantity is also reported in dB.

For example, if a proposed stirring sequence consists of N=200 mode-stirring samples, the measurement of G_{ref} is carried out for T different, unique sets of this 200-sample stirring sequence at T uncorrelated reference antenna positions. Correlation is defined in Equation 6.2.2 2. For large-form-factor devices or small-form-factor IoT devices with a phantom, it may be necessary to increase T_{cal} (see *CTIA 01.21* [3]) to ensure that the uncertainty in a measurement that uses a given stirring sequence does not exceed the level specified in *CTIA 01.21* [3]. Uncertainty may also be reduced by increasing the number of mode-stirring samples that define a stirring sequence or modifying the stirring sequence.

For each channel to be tested, the estimate of the power transfer function $G_{ref,t}$ of the reverberation chamber shall be calculated by the following equation (see [14][15]):

Equation 6.1.3-1

$$G_{ref,t,lin} = \frac{\frac{1}{NF}\sum_{n=1}^{N}\sum_{f=1}^{F}|S_{21}(f,n)|^2}{e_{mismatch,meas}\; e_{mismatch,ref}\; \eta_{meas}\; \eta_{ref}}$$

where $e_{mismatch,meas}$ is the mismatch of the measurement antenna, $e_{mismatch,ref}$ is the mismatch of the reference antenna, η_{meas} is the radiation efficiency of the measurement antenna, and η_{ref} is the radiation efficiency of the reference antenna. The calculation is performed in linear units. Note that value of the mismatch and radiation efficiency of the measurement antenna is not required, because it will be the same during both the reference and DUT measurements and, therefore, will not affect the final results. These values are included for consistency with published literature. The term $e_{mismatch}$ can be found from $1 - |<< S_{11} >_F>_N|^2$ of the antenna in question, where <.> represents the averages over *N* mode-stirring samples and *F* frequencies across the channel bandwidth to be tested given in *CTIA 01.21* [3]. $G_{ref,t,lin}$ represents the *t*th power transfer function (obtained from *NF* samples) of a particular reverberation chamber configuration, corrected for mismatch of both the measurement antenna and the reference antenna, as well as the radiation efficiency of the reference antenna.

The power transfer function is then given by:

Equation 6.1.3-2

$$G_{ref,lin} = \frac{1}{T_{val}} \sum_{t=1}^{Tval} G_{ref,t,lin}$$

where T_{val} = T_{prox} (Section 6.2.2), T_{pre} (Section 6.2.3), or T_{cal} (*CTIA 01.21* [3])

1. Measure S-parameters over a full stirring sequence, as specified in Section 6.1.1.
2. Calculate the power transfer function for the tth reference antenna location, $G_{ref,t,lin}$ from Equation 6.1.3-1. The power transfer function $G_{ref,lin}$ is the mean of these T estimates given in Equation 6.1.3-2. The standard deviation of the T_{pre} power transfer functions found in Section 6.2.3 for the loading condition used in the DUT measurement is used to estimate the uncertainty due to the lack of spatial uniformity, as given in Section 6.2.3. The calculation is performed in linear units and reported in dB as:

$$G_{ref}\,[dB] = 10 \log_{10}(G_{ref,lin}).$$

6.2 Test Procedures Used in Chamber Precharacterization

These tests shall be conducted prior to use of the chamber and repeated annually or whenever the chamber configuration changes, with the exception of changes in loading within the limits specified in Section 6.2.3. These tests shall be conducted in each band for which the reverberation chamber is to be used. These test frequencies are outlined in Table 3-3, with the frequency bandwidths outlined in the specific precharacterization tests defined in this section.

6.2.1 Test Procedure – Cable Assembly Loss Measurement

This measurement step will calibrate the power loss of the cable(s) needed to connect the instrument used to measure the received power from the measurement antenna during TRP measurements, and to generate the power radiated by the measurement antenna during TIS measurements. This instrument is normally a base station emulator, but can also consist of a base station emulator connected to power meter or spectrum analyzer through a power splitter. To measure the loss in this cable (and splitter, if used), proceed with the following steps:

1. Connect the cable assembly (which may include a power splitter whose third port is terminated in 50 Ω) between the two ports of the network analyzer. The VNA must be calibrated at its two input ports, rather than at the ends of the cables that connect to the measurement and calibration antennas. Alternatively, the cable assembly may be connected between the two reference planes shown in *CTIA 01.21* [3] and the VNA calibration from the reference measurement may be used.
2. Measure the transmission S-parameter (S_{21} or S_{12}) of the cable assembly.
3. Save the power transfer values $G_{cable} = |S_{21}|^2$ for the test frequencies where the measurements will be conducted.

6.2.2 Test Procedure – Chamber Precharacterization of Proximity Effect

The proximity effect refers to the loss of power that occurs when radiation from the reference or DUT antenna is absorbed in a lossy material without undergoing any reflections in the chamber. The proximity effect test ensures that this loss does not exceed the variance due to the lack of spatial uniformity in the chamber for a given loading condition [16]. This precharacterization test is not required for testing small-form-factor IoT devices in free space. This precharacterization is also not required if the chamber has

already been precharacterized for a physically larger device than the small-form-factor device plus phantom.

Refer to Figure 6.2.2-1 for large-form-factor (LFF) devices and Figure 6.2.2-2 for small-form-factor (SFF) devices to be tested with a phantom for the following steps.

1. RF absorbers whose surface area represents (a) the largest DUT to be tested or (b) the largest phantom to be tested, or (c) the phantom itself, are placed in the chamber at the locations that will be used during the DUT measurements. For chambers with turntables, this is typically on the turntable, directly across from the reference antenna. For chambers without turntables, the location is not critical, but should be within the test volume.
2. Place the reference antenna at the location intended for DUT measurements, as shown in Figure 6.2.2-1 (a) for LFF devices or Figure 6.2.2-2 (a) for SFF devices to be tested with a phantom by the distance "Aux1". This is Position 1 for the test. Orient the reference antenna in one of three orthogonal orientations and at one of three heights corresponding to $z = 0$, $z = Z_{max}$, and $z = Z_{max}/2$ ($T_{prox} = 9$). Directional antennas shall be oriented away from the absorber.
3. The power transfer function G_{ref} (see Section 6.1.3) and the standard uncertainty due to lack of spatial uniformity $u_{G_{\mathrm{ref}}}$ for this chamber set-up are estimated from a minimum set of $T_{prox} = 9$ uncorrelated power transfer function measurement samples. The interval G_{ref} ± 2.31 $u_{G_{\mathrm{ref}}}$ [dB] is calculated, where

Equation 6.2.2-1

$$u_{\mathrm{Gref}}[dB] = \frac{\sigma_{\mathrm{Gref}}^{i}[dB]}{\sqrt{T_{\mathrm{prox}}}}$$

and $\sigma_{\mathrm{Gref}}^{i}$ [dB] is defined in Section 6.2.3 (see also *CTIA 01.70* [1]). A single 10 MHz band located at the center frequency in each technology band to be measured shall be tested for the Proximity Effect. These test frequencies are given in Table 3-3. The frequency step shall correspond to that determined in Table 3-5. The total loading shall provide a coherence bandwidth equal to or greater than that specified in Table 3-4.

4. The reference antenna is then positioned closer to and, if a directional antenna is being used, aimed toward the lossy object (absorber and/or phantom), as shown in Figure 6.2.2-1 (b) for large-form-factor devices or Figure 6.2.2-2 (b) for small-form-factor devices with a phantom. This is Position 2 for the test. The reference antenna is moved toward the lossy object and far enough from the last set of power transfer function measurements that all samples from the two sets shall be uncorrelated. This is verified by use of Pearson's cross correlation function calculated over stirring sequences made at Position 1 and Position 2 for each of the $T_{prox} = 9$ power transfer function measurement samples [15].

Equation 6.2.2 2

$$\rho_{c,t}(f) = \left| \frac{\sum_{n=1}^{N}\left[\left(S_{21,1} - \langle S_{21,1}\rangle_N\right)\left(S_{21,2} - \langle S_{21,2}\rangle_N\right)^{*}\right]}{\sqrt{\sum_{n=1}^{N}\left[\left|S_{21,1} - \langle S_{21,1}\rangle_N\right|^{2}\right]}\sqrt{\sum_{n=1}^{N}\left[\left|S_{21,2} - \langle S_{21,2}\rangle_N\right|^{2}\right]}} \right|,$$

where $\rho_c(f)$ is averaged over the F measured frequencies in the channel. A threshold value of 0.3 shall not be exceeded for this average value. If any of the $T_{prox} = 9$ positions are correlated, then a new auxiliary Position 2 shall be selected that is farther from Position 1.

5. A minimum set of $T_{prox} = 9$ auxiliary power transfer function measurement samples shall be acquired. A new transfer function $G_{\mathrm{ref,aux}}$ is calculated from the auxiliary measurements by use of Equation 6.1.3-1 and Equation 6.1.3-2.

6. The standard uncertainty is calculated and the interval corresponding to $G_{\mathrm{ref,aux}} \pm 2.31\,u_{G_{\mathrm{ref,aux}}}$ [dB] is calculated, see Equation 6.2.2-1. If this interval overlaps with the interval $G_{\mathrm{ref}} \pm 2.31\,u_{G_{\mathrm{ref}}}$ [dB], the proposed antenna placement in step 2 is deemed acceptable. If these intervals do not overlap, the reference antenna must be placed farther from the lossy object or objects at a new Position 1. The procedure is then repeated until an acceptable antenna placement is found for Position 1 and Position 2. The distance corresponding to the minimum acceptable reference antenna placement shall also be maintained between the reference antenna and any absorber used to load the chamber.

7. For chambers with turntables, the minimum radius for the test volume, R_{min}, shall be determined as the distance from the reference antenna location in the Aux_2. measurement, shown in Figure 6.2.2-1 ((b) or Figure 6.2.2-2 (b), to the center of the turntable. See CTIA 01.21 [3] further definition of the test volume. For chambers without turntables, the minimum distance for the valid, R_{min}, shall be the distance Aux_2.
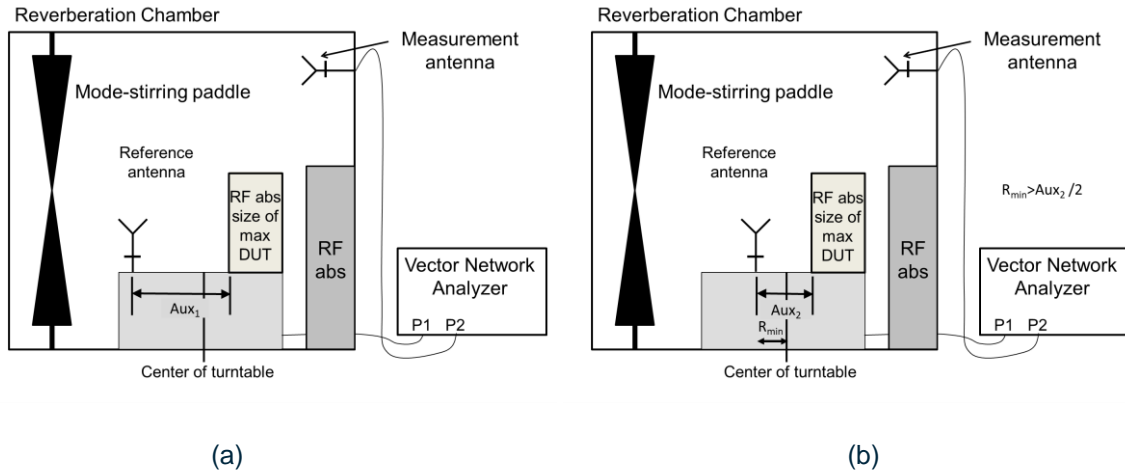
CTIA
Certification

Figure 6.2.2-1 Side View Of The Reverberation Chamber Set-Up to Measure the Proximity Effect for a Large-Form-Factor IoT Device Given Chamber Set-Up
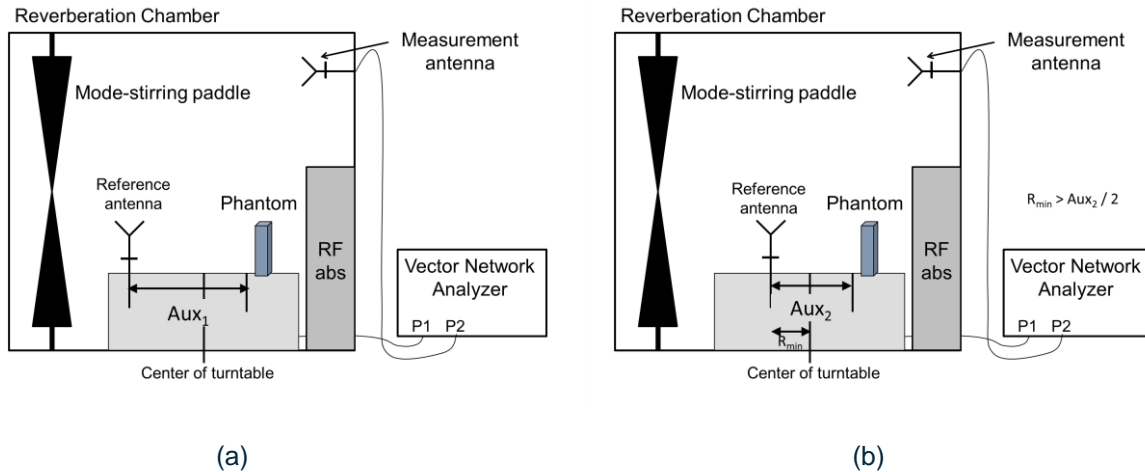

Figure 6.2.2-2 Side View Of The Reverberation Chamber Set-Up to Measure the Proximity Effect for a Given Chamber Set-Up for a Small-Form-Factor IoT Device With a Phantom

As shown in Figure 6.2.2-1, RF absorbers whose surface area represents the largest DUT to be tested shall be placed in the location of the DUT. In Figure 6.2.2-2, the phantom or simulated phantom represented by RF absorbers whose surface area represents the largest phantom to be tested shall be placed in the location of the DUT. In (a), the omnidirectional reference (transmit) antenna (used as an example) is placed a nominal distance (Aux_1) from the simulated large-form-factor DUT. In (b), to test for the proximity effect, the reference antenna is moved closer to the simulated DUT equidistant from the center of the turntable (distance of Aux_2). If the reference antenna is directional, it is oriented toward the DUT. Note that only stepped-mode-stirring is supported in this test plan.

6.2.3   Test Procedure – Chamber Precharacterization of Uncertainty due to Lack of Spatial Uniformity

In a theoretically ideal reverberation chamber, the average transmission between two antenna ports is the same regardless of the location or orientation of the antennas inside the valid test volume. The uncertainty due to lack of spatial uniformity serves to quantify how much the actual environment deviates from this ideal. Because this uncertainty may require a large work effort to determine, estimation is allowed based on a precharacterization test campaign separate from the DUT measurement.

A major driver of this uncertainty is the loading condition of the chamber. In a precharacterization measurement, the chamber shall be configured with RF absorbers, antennas and phantoms (if used) in the positions where they will be located during a DUT TIS/TRP measurement. In place of an actual DUT, RF absorber having dimensions equal to or exceeding those of the maximum-size DUT or phantom to be tested shall be placed in the location of the DUT. Alternatively, the actual phantom to be used in device tests may be utilized, in which case only the largest combination of phantoms to be tested simultaneously is required to be utilized. The amount and position of all RF absorber or the phantom shall be specified/documented so that it can be faithfully replicated in an DUT test. Precharacterization measurements can be made for loading that corresponds to the maximum-size DUT (or DUT-plus phantom combination) to be tested, or measurements can be made for several such loading conditions representing the expected range of loading under use conditions. The latter is expected to provide lower uncertainty for smaller test objects, because in general, lower amounts of loading provide lower measurement uncertainty.

The precharacterization procedure consists of measuring the power transfer function under one or more loading conditions. The corresponding coherence bandwidth and uncertainty due to lack of chamber spatial uniformity are determined for each loading condition. If multiple loading conditions are used, measure all loading conditions for each reference antenna position and/or orientation before moving the reference antenna to the next position. This ensures that the reference antenna position is exactly the same for every loading condition. These data shall be tabulated for future use of the reverberation chamber.

1. Place the reference antenna at one of four locations and one of three orthogonal orientations at each location ($T_{pre} = 12$). For chambers with turntables, the reference antenna shall be placed at $r = R_{min}$ (see Section 6.2.2) and $r = R_{max}$, and at two heights corresponding to the $z = 0$ and $z = Z_{max}$ of the test volume. For chambers without turntables, the reference antenna shall be placed at the two opposite corners of a cube at $z = 0$ of the test volume and then at the other two corners at $z = Z_{max}$ of the test volume.

2. Configure the chamber to measure S parameters and calibrate the VNA as described in Section 6.1.1.

3. Determine the maximum chamber loading, that is, the loading that is required to create a coherence bandwidth that exceeds the channel to be measured. This is typically done iteratively by loading the chamber with increasing amounts of RF absorber, plus the phantom, if used, measuring S parameters over a mode-stirring sequence and then calculating the coherence bandwidth from Section 6.1.2.

   Note that if a user encounters an DUT or phantom that presents more loss to the chamber than the one simulated during this precharacterization step, the user will need to determine the additional uncertainty due to lack of spatial uniformity with the steps outlined below.

4. Perform S-parameter measurements over a complete stirring sequence in each frequency band of interest for a set of loading cases. The loading cases correspond to numbers of blocks of RF absorber (or the exposed surface area of the RF absorber) ranging from zero (or a small amount of) RF absorber to the maximum RF absorber in approximately equal increments. The finer the loading increment tested, the more accurately the uncertainty can be estimated.

5. For each loading condition i, where i is greater than or equal to one, calculate the coherence bandwidth as specified in Section 6.1.2.

6. For each loading condition i, calculate the reference power transfer function, $G_{ref,lin}^i$ as specified in Section 6.1.3. Equation 6.1.3-2 with a minimum of $T_{pre} = 12$ reference measurement samples as specified in step 1. This calculation shall be carried out at the

center frequency for each channel to be tested, averaging the F measured frequencies over the channel bandwidth specified in Table 3-5 for each airlink technology to be supported by the chamber.

For each loading condition i and for each transmission standard to be tested, calculate the standard deviation $\sigma_{G_{ref,lin}^i}$ with Equation 6.2.3-1 using the channel bandwidths defined in Table 3-5 for all the available frequencies across each band.

Equation 6.2.3-1

$$\sigma_{G_{ref,lin}^i} = \sqrt{\frac{1}{(T_{pre}-1)}\sum_{t=1}^{T_{pre}}\left(G_{ref,t,lin}^i - G_{ref,lin}^i\right)^2}$$

The calculation is performed in linear units and reported in decibels. The decibel representation is found as:

$$\sigma_{G_{ref}^i}[dB] = 10\log_{10}\left(\frac{G_{ref,lin}^i + \sigma_{G_{ref,lin}^i}}{G_{ref,lin}^i}\right).$$

For each band, the highest value of $\sigma_{G_{ref}^i}[dB]$ shall be entered into the precharacterization table.

7. Create a table, where the first column corresponds to the operating band, the second column corresponds to the loading condition i (blocks of RF absorber or surface area of RF absorber, or each phantom-plus-absorber configuration), the third column corresponds to the coherence bandwidth, the fourth column corresponds to $\sigma_{G_{ref}^i}[dB]$. Columns two, three and four should be repeated for each loading configuration, where the superscript i increments for each loading configuration. This table will be used by future users of the chamber to estimate the coherence bandwidth and uncertainty due to lack of spatial uniformity under various loading conditions. An example of such a table is given in Table 6.2.3-1.

Table 6.2.3-1 Example Precharacterization Table Showing the Band, Loading Used, Coherence Bandwidth, Channel Bandwidth, and the Corresponding Uncertainty due to Lack of Spatial Uniformity

Band	# of Absorbers	Coherence BW (MHz)	Channel BW (MHz)	σ^{i}_{Gref} [dB]	# of Absorbers	Coherence BW (MHz)	Channel BW (MHz)	σ^{i+1}_{Gref} [dB]	# of Absorbers	Coherence BW (MHz)	Channel BW (MHz)	σ^{i+2}_{Gref} [dB]	# of Absorbers	Coherence BW (MHz)	Channel BW (MHz)	σ^{i+3}_{Gref} [dB]
Cellular (818-894 MHz)	0		0.20		2		0.20		4		0.20		6		0.20	
			1.20				1.20				1.20				1.20	
			2.40				2.40				2.40				2.40	
			3.80				3.80				3.80				3.80	
			10.00				10.00				10.00				10.00	
			20.00				20.00				20.00				20.00	

Note that the coherence bandwidth is calculated over a 100 MHz bandwidth at the center of each operating band, while G_{ref} is calculated over the channel bandwidth defined in Table 6.2.3-1 for all the available frequencies in each band. The worst case for $\sigma_{G_{ref}}$ [dB] for each operating band is entered into the table for each loading condition.

Section 7   Amplitude Quality of Quiet Zone Procedure for 5G Millimeter-Wave Test Plan

This section outlines the test procedures to evaluate the amplitude variation within the quiet zone.

7.1   Minimum Measurement Distance

The quality of quiet zone validation shall be performed in the far-field of the UE antennas.

7.2   Equipment Required

The reference AUT that is placed at various locations within the quiet zone shall be a directive antenna with similar properties of typical antenna arrays integrated in DUTs. The required characteristics in terms of directivity and Half Power Beamwidth (HPBW) of the reference AUT are shown in Figure 7.2-1, Figure 7.2-2 and Figure 7.2-3.
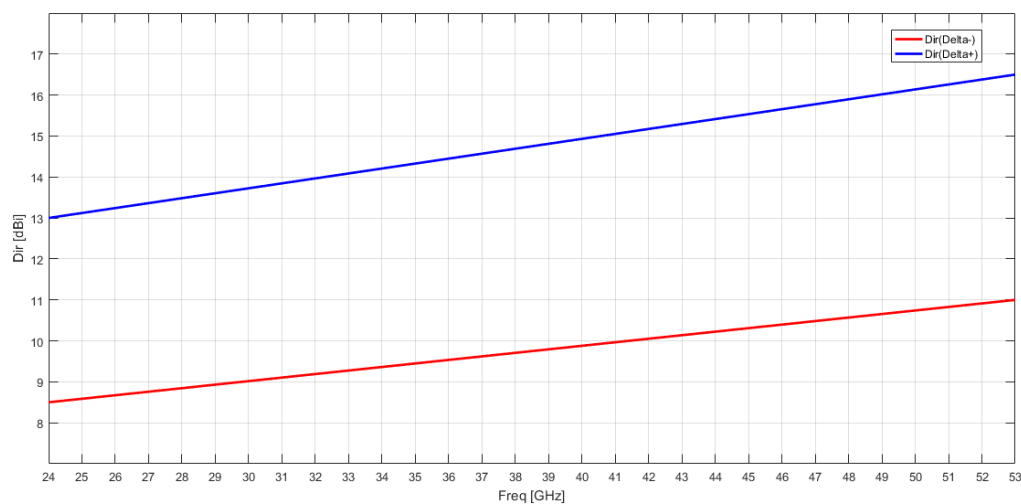

Figure 7.2-1 Directivity Mask
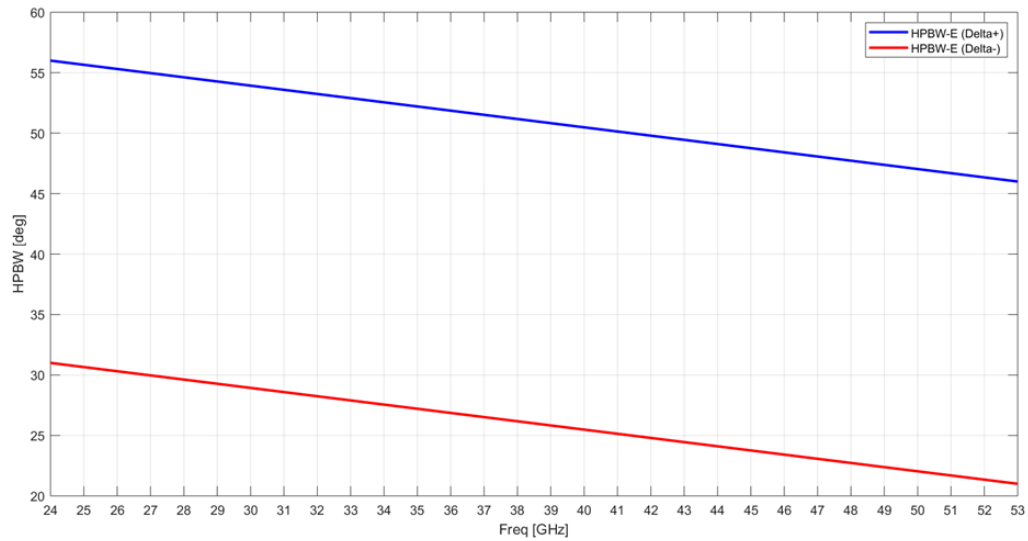
Figure 7.2-2 HPBW-E Mask
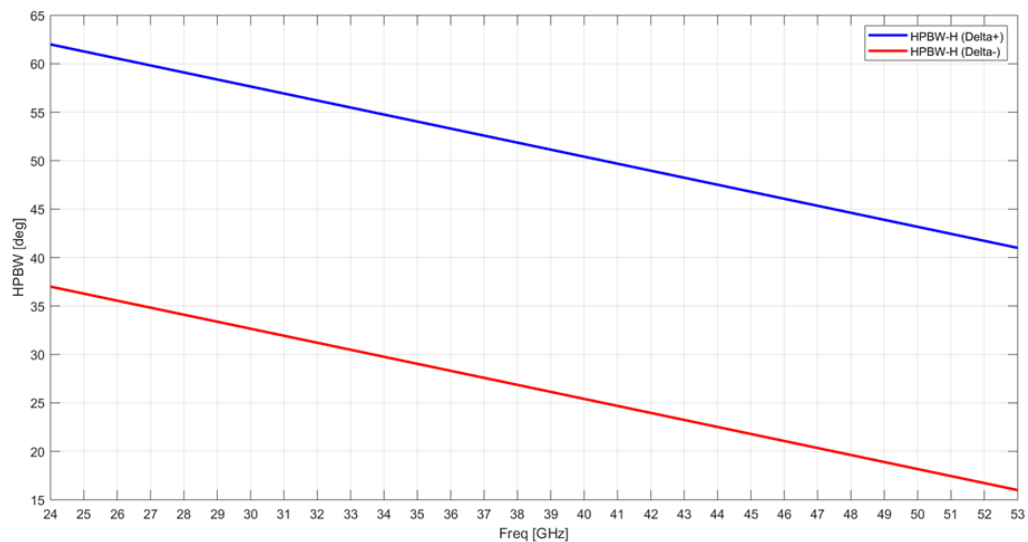
Figure 7.2-3 HPBW-H Mask

The AUT shall be symmetric on E and H planes.

The above masks for the reference antenna are met based on antenna vendors' calibration report or measurements performed by the lab.

For the measurement, a combination of signal generator and spectrum analyzer or a network analyzer can be used. The multi-port (with at least three ports) network analyzer is most suitable to reduce test time as both polarizations of the measurement antenna can be measured simultaneously, and multiple frequencies can be measured within a sweep.

7.3 Test Frequencies

The QoQZ test frequencies are outlined in Section 3.

7.4 Quality of Quiet Zone Measurement Procedure

This procedure describes the procedures for validating the QoQZ for the permitted far-field methodologies. This procedure is mandatory before the test system is commissioned for certification tests and characterizes the quiet zone performance of the anechoic chamber, specifically the effect of reflections within the anechoic chamber including any positioners and support structures. Additionally, it includes the effect of offsetting the directive antenna array inside a DUT from the center of the quiet zone, i.e., the center of rotation of the DUT and measurement antenna positioning systems as well as the directivity MU, i.e., the variation of antenna gains in the different direct line-of-sight links.

The spherical quiet zone is illustrated in Figure 7.4-1, which includes the definitions of center of quiet zone location, i.e., the geometric center of the positioning systems and the size, i.e., radius R.
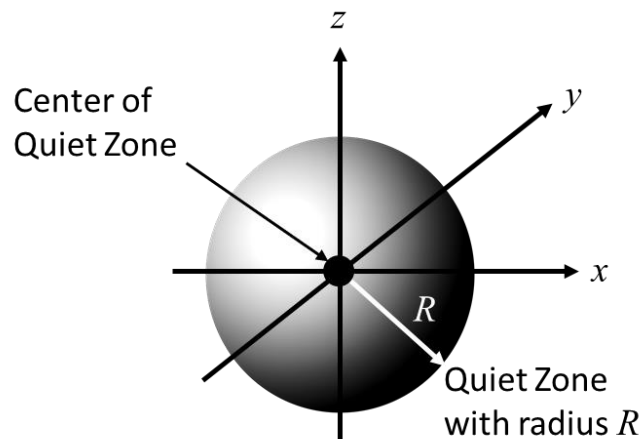

Figure 7.4-1 Quiet Zone Illustration

The outcome of the procedures can be used to estimate the following:

- Variation of the TRP measurements, spherical surface integrals of EIRP when the DUT is placed anywhere within the quiet zone and with the beam formed in any arbitrary direction inside the chamber.

- Variation of the EIRP/EIS measurements when the DUT is placed anywhere within the quiet zone and with the beam formed in any arbitrary direction inside the chamber.

The reference coordinate system defined in *CTIA 01.71* [6] Section 5.1, applies to this procedure.

The QoQZ measurements for integrated RF parameters such as TRP shall use 3D pattern measurements of the reference antenna patterns as they most closely resemble the 3D/spherical surface measurements/integrals of EIRP or EIS. Therefore, the QoQZ measurements for TRP metrics shall be based on efficiency measurements. On the other hand, the QoQZ measurements for single-directional EIRP and EIS metrics shall be based on gain measurements of the direct line-of-sight link between the reference AUT and the measurement antenna.

7.5 Reference AUT Orientations and Coordinate Systems

The reference AUT shall be positioned in a total of 7 different reference positions, shown in Figure 7.5-1.
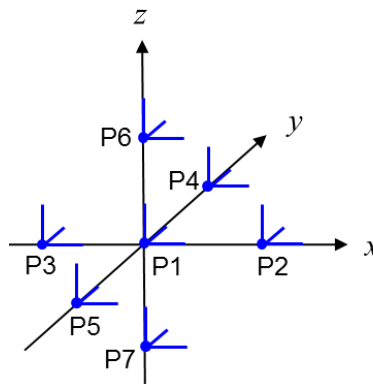
Figure 7.5-1 Reference AUT Positions

While position 1, P1, is the center of the quiet zone, the remaining positions, 2 through 7, are off-center positions each displaced by the radius of the quiet zone, R. The coordinates of the respective test points are shown in Table 7.5-1.

Table 7.5-1 Reference AUT Measurement Coordinates

Position	X	Y	Z
P1	0	0	0
P2	R	0	0
P3	$-R$	0	0
P4	0	R	0
P5	0	$-R$	0
P6	0	0	R
P7	0	0	$-R$

Due to the non-commutative nature of rotations, the order of rotations is important and needs to be defined when reference AUT orientations are tested. The reference orientation of the reference AUT is shown in Figure 7.5-2.
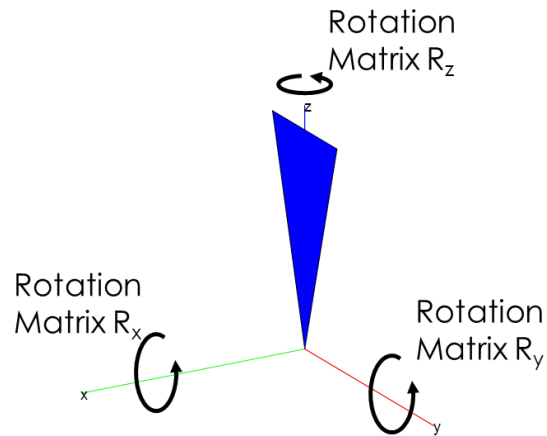
Figure 7.5-2 Illustration of Reference AUT Orientation

The rotations around the x, y, and z axes can be defined with the following rotation matrices:

$$R_x\,(\alpha) = \begin{bmatrix} 1 & 0 & 0 & 0 \\ 0 & \cos\alpha & -\sin\alpha & 0 \\ 0 & \sin\alpha & \cos\alpha & 0 \\ 0 & 0 & 0 & 1 \end{bmatrix}$$

$$R_y\,(\beta) = \begin{bmatrix} \cos\beta & 0 & \sin\beta & 0 \\ 0 & 1 & 0 & 0 \\ -\sin\beta & 0 & \cos\beta & 0 \\ 0 & 0 & 0 & 1 \end{bmatrix}$$

And:

$$R_z\,(\gamma) = \begin{bmatrix} \cos\gamma & -\sin\gamma & 0 & 0 \\ \sin\gamma & \cos\gamma & 0 & 0 \\ 0 & 0 & 1 & 0 \\ 0 & 0 & 0 & 1 \end{bmatrix}$$

with the respective angles of rotation, α, β, γ and:

$$\begin{bmatrix} x' \\ y' \\ z' \\ 1 \end{bmatrix} = R \begin{bmatrix} x \\ y \\ z \\ 1 \end{bmatrix}$$

Additionally, any translation of the reference AUT can be defined with the translation matrix:

$$T(t_x, t_y, t_z) = \begin{bmatrix} 1 & 0 & 0 & t_x \\ 0 & 1 & 0 & t_y \\ 0 & 0 & 1 & t_z \\ 0 & 0 & 0 & 1 \end{bmatrix}$$

with offsets t_x, t_y, t_z in x, y, and z, respectively and with:

$$\begin{bmatrix} x' \\ y' \\ z' \\ 1 \end{bmatrix} = T \begin{bmatrix} x \\ y \\ z \\ 1 \end{bmatrix}$$

The combination of rotations and translation is captured by the multiplication of rotation and translation matrices.

For instance, the matrix M:

$$M = T(t_x, t_y, t_z) \cdot R_x(\alpha) \cdot R_y(\beta) \cdot R_z(\gamma)$$

describes an initial rotation of the DUT around the z axis with angle γ , a subsequent rotation around the y axis with angle β, and a final rotation around the x axis with angle α. After those rotations, the DUT is translated by t_x, t_y, t_z in x, y, and z, respectively.

7.5.1   Distributed-axes System

The reference AUT positions inside a typical distributed-axes system are shown in Figure 7.5.1-1.
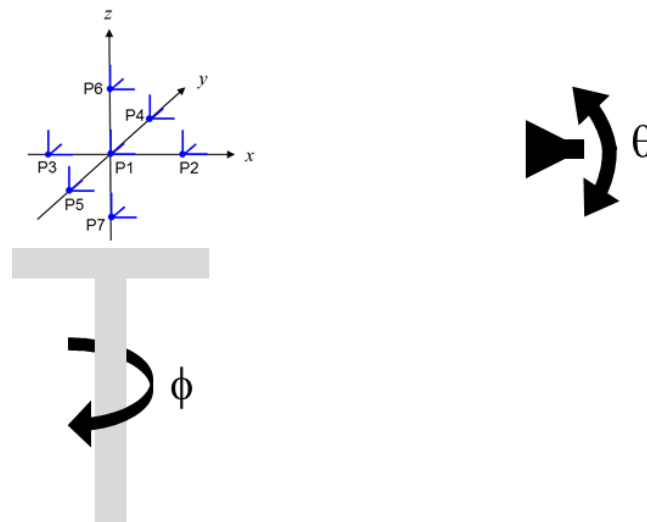
Figure 7.5.1-1 Reference AUT Measurement Positions for Distributed-Axes System

As different areas within the chamber could yield variations in the field uniformity inside the quiet zone caused by reflections, it is important to characterize the electromagnetic fields with the reference antennas uniformly illuminating the anechoic chamber.

Perform the reference measurements for the reference AUT placed at the 7 antenna positions with the antenna rotated around the y axis with 5 different angles β, i.e., $= \beta = 0°, 45°, 90°, 135°,$ and $180°$, and

rotated around the z axis with 8 different $\gamma = 0°, 45°, 90°, 135°, 180°, 225°, 270°,$ and $315°$. A graphical illustration of some sample reference AUT orientations is shown in Figure 7.5.1-2, the reference AUT placed at position 6, P6, for reference antenna polarization $\gamma_{pol} = 0°$ (illustrated in blue) and for the reference polarization $\gamma_{pol} = 90°$ (illustrated in red).

The matrix operation for the rotations and translation is defined as:

$$M = T(t_x, t_y, t_z) \cdot R_z(\gamma) \cdot R_y(\beta) \cdot R_{z,pol}(\gamma_{pol})$$

for the distributed-axes system.

Figure 7.5.1-2 Sample Reference AUT orientations for position 6, P6 for reference antenna polarizations $\gamma_{pol} = 0°$ and $\gamma_{pol} = 90°$

When facing the z-axis (along the turntable axis), $\beta = 0°$ and $\beta = 180°$, the antenna does not need to be evaluated for the 8 different rotations around the z axis. A single roll orientation is sufficient since those orientations are unique. Due to the pedestal, distributed-axes systems are not able to measure towards the $\beta = 180°$ direction; for those systems, the reference measurements at this reference AUT orientation can be skipped.

If the device re-positioning approach outlined in *CTIA 01.71* [6] Section 5.1, is adopted for the EIRP/EIS/TRP based conformance test cases, the QoQZ analysis is sufficient only for $\beta = 0°, 45°, 90°$.

The positioner relative coordinates/orientations with respect the measurement antenna/reflector in the initial position shall remain the same for each reference antenna orientation, e.g., in the sample distributed-axes system shown in Figure 7.5.1-2 the reference antenna shall be pointed towards the positioner for $\beta = 135°$ for the initial position of (θ, ϕ) of $(0,0)$.

7.5.2   Combined-axes System

The reference AUT positions inside a typical combined-axes system are shown in Figure 7.5.2-1.
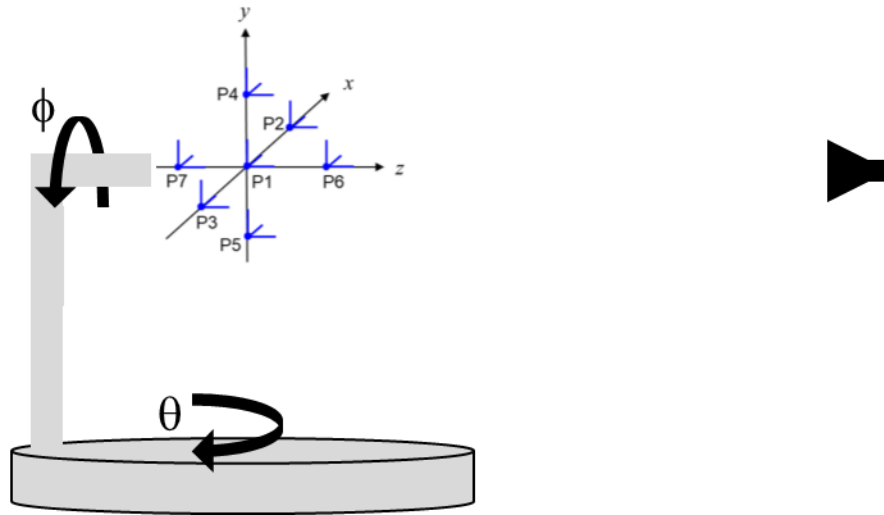
Figure 7.5.2-1 Reference AUT Measurement Positions for Combined-Axes System

Perform the reference measurements for the reference AUT placed at the 7 antenna positions with the antenna rotated around the x axis with 5 different angles α, i.e., $\alpha = -90°, -45°, 0°, 45°,$ and $90°$ and rotated around the y axis with 8 different angles $\beta = 0°, 45°, 90°, 135°, 180°, 225°, 270°,$ and $315°$. A graphical illustration of some sample reference AUT orientations is shown in Figure 7.5.2-2   with a reference AUT placed at position 4, P4, for the reference polarizations $\gamma_{\mathrm{pol}} = 0°$ (illustrated in blue) and $\gamma_{\mathrm{pol}} = 90°$ (illustrated in red).

The matrix operation for the rotations and translation is defined as

$$M = T(t_x, t_y, t_z) \cdot R_y() \cdot R_x(\alpha) \cdot R_{z,pol}(\gamma_{pol})$$

for the combined-axes system.
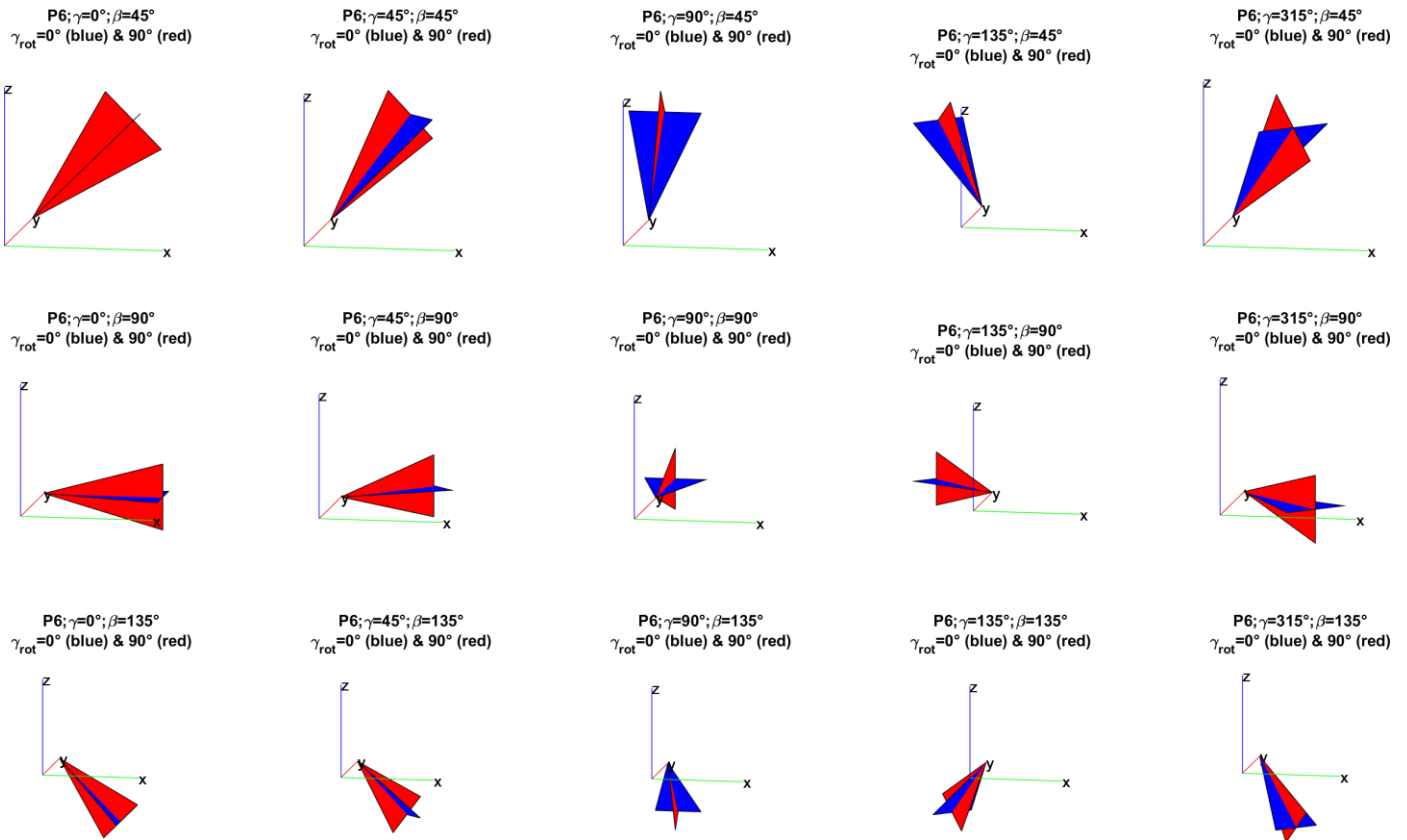
Figure 7.5.2-2 Sample Reference AUT Orientations for Position 4, P4, for Reference Antenna Polarization γ_{pol} = 0° and γ_{pol} = 90°

When facing the y axis (along the turntable axis), $\alpha = 90°$ and $\alpha = -90°$, the antenna does not need to be evaluated for the 8 different rotations around the y axis. A single rotation is sufficient since those orientations are unique. Due to the pedestal of the 2-axis positioner, combined-axes systems are not able to measure 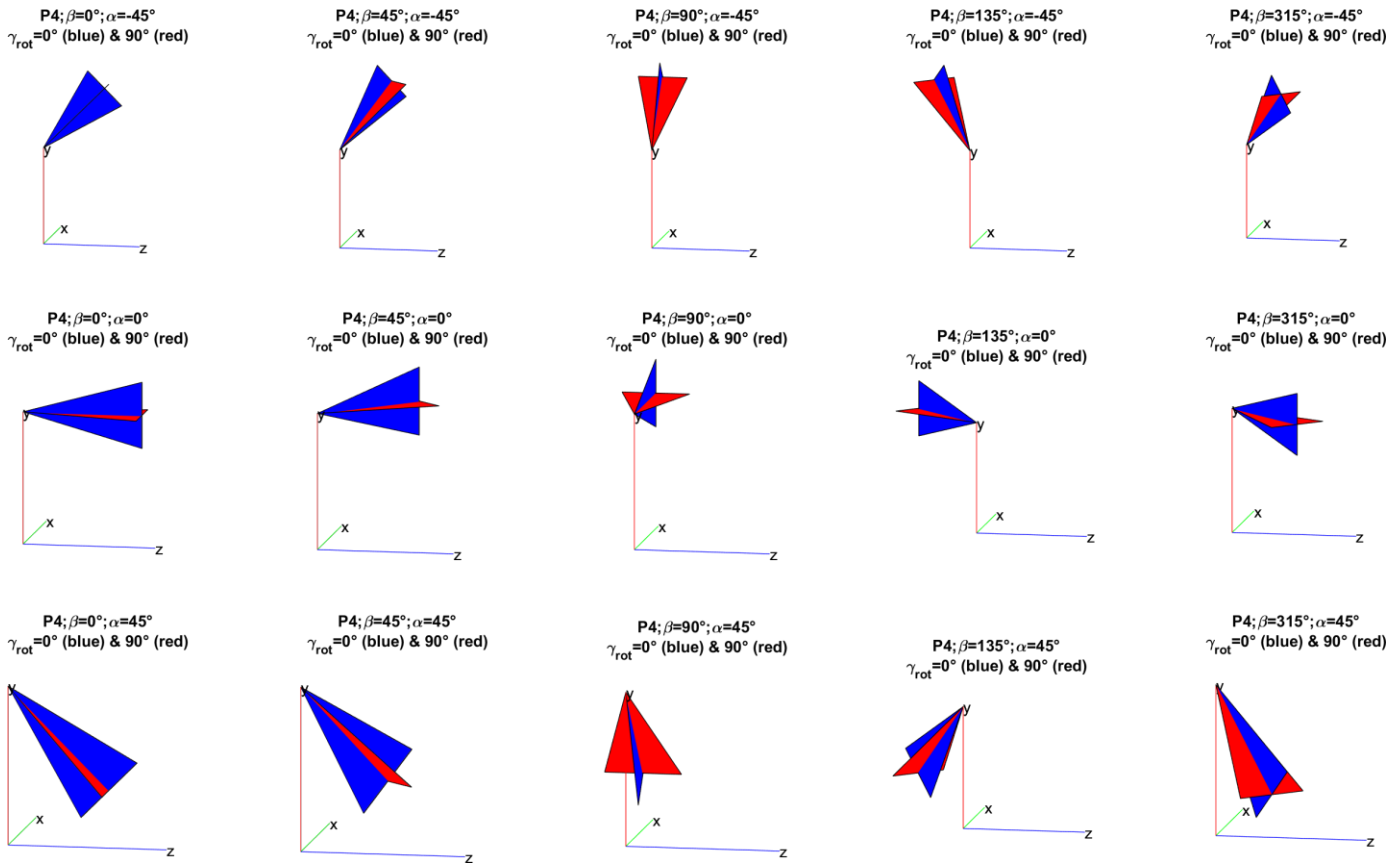towards the $\beta = 180°$ direction; for those systems, the reference measurements at this reference AUT orientation can be skipped.

If the device re-positioning approach outlined in *CTIA 01.71* [6] Section 5.1, is adopted for all EIRP/EIS/TRP based conformance test cases, the quality of quiet zone analysis is sufficient only for $\beta = 0°, 45°, 90°, 270°,$ and $315°$.

The positioner relative coordinates/orientations with respect to the measurement antenna/reflector shall remain the same for each reference antenna orientation, e.g., in the sample combined-axes system shown in Figure 7.5.2-1. The reference antenna shall be pointed towards the positioner for $\beta = 135°$ and $225°$ for the initial position of (θ, ϕ) of (0,0).

7.6   Statistical Analysis

The combined MU element related to the QoQZ for TRP and the offset between the UE's antenna array and center of the quiet zone is the standard deviation of the various efficiency measurement results that are based on the 7 different reference AUT positions, the respective reference AUT orientations, and the two reference AUT polarization orientations.

The combined MU element related to the QoQZ for EIRP/EIS, offset between UE antenna array and center of quiet zone, and directivity is the standard deviation of the single-point gain measurement results that are based on the 7 different reference AUT positions, the respective reference AUT orientations, and the two reference AUT polarization orientations.

Section 8   Phase Quality of Quiet Zone Procedure for 5G Millimeter-Wave Test Plan

This section outlines the test procedures to evaluate the phase variation within the quiet zone. Either the rotary scan procedure in Section 8.4 or the field probing procedure in Section 8.5 can be used to determine the largest phase variation.

8.1   Minimum Measurement Distance

The QoQZ validation has to be performed in the far-field distance of the UE antennas.

8.2   Equipment Required

The reference AUT that is placed at various locations within the quiet zone shall be a directive antenna with similar properties of typical antenna arrays integrated in DUTs. The characteristics in terms of directivity and HPBW of the reference AUT are the same as Section 7.2.

For the measurement, a network analyzer can be used. The multi-port (with three ports) network analyzer is most suitable to reduce test time as both polarizations of the measurement antenna can be measured simultaneously, and multiple frequencies can be measured in a sweep.

8.3   Test Frequencies

The QoQZ test frequencies are the same as those outlined in Section 7.4 for the amplitude QoQZ testing, i.e., Table 3-2 in Section 3.

8.4   Rotary Scan Procedure

With this approach, the phase behavior is characterized on multiple points on a circular trajectory within the quiet zone as illustrated in Figure 8.4-1.
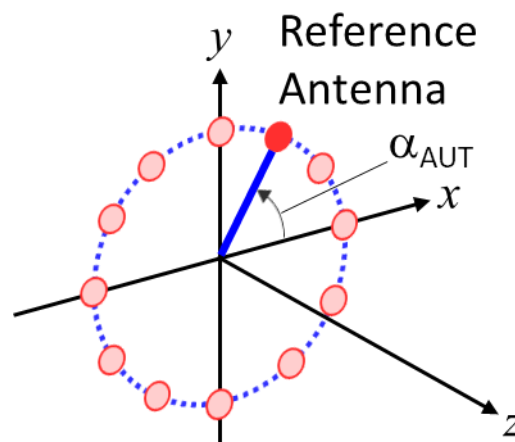
Figure 8.4-1 Characterization of the Phase Response Within the Quiet Zone Using a Rotary Scan

This measurement can be accomplished using a reference AUT connected to the end of a rotary arm scanning the circular path centered on the center of the quiet zone. Such a rotary movement can capture all of the impact on phase as in actual test cases since it uses the same positioning equipment used for such tests. For these scans, the reference AUT is directed towards the z axis and the rotary scan is performed within the x and y plane. For this test, a reference antenna with single polarization is sufficient but two orthogonal polarizations shall be tested, as outlined in Figure 8.4-2 for the reference antenna starting out in the H-Polarization (principal polarization aligned with x axis) and in Figure 8.4 3 for the

reference antenna starting out in the V-polarization (principal polarization aligned with y axis) at rotary angle, α_{AUT}, of 0°.
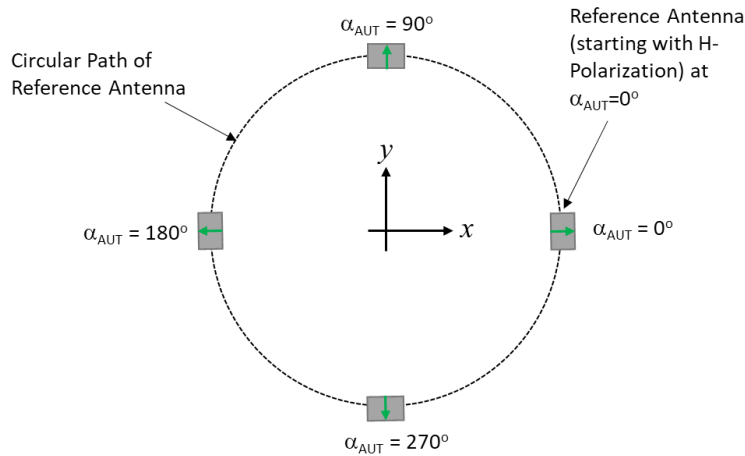
Figure 8.4-2 Sample Reference AUT Positions with Starting H-Polarization of Rotary Angle α_{AUT}, of 0°
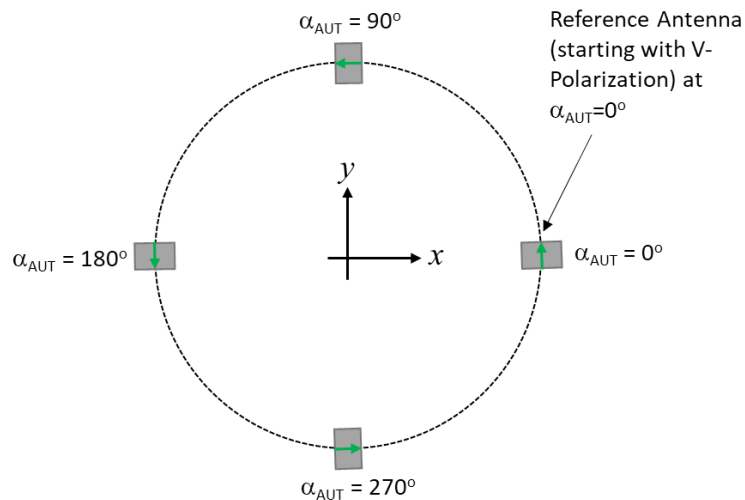
Figure 8.4-3 Sample Reference AUT Positions with Starting V-Polarization of Rotary Angle α_{AUT}, of 0°

Due to cross-polarization effects between the reference antenna and the feed antenna, e.g., the measurement is in a null for the H-Pol feed/measurement antenna when the reference antenna is at rotary angles 90° and 270° of Figure 8.4-3 the phases shall be measured at the H and V polarized ports of the feed/measurement antenna as a function of the rotary angle α_{AUT}. As illustrated in Figure 8.4-2 and Figure 8.4 3, the phase jumps by 180° for sets of reference AUT positions that are opposite from each other, which needs to be compensated in post-processing of the phase measurements. If the path loss calibration was performed without the phase, i.e., without full two-port calibration on both polarizations, a phase alignment between the H and V measurements is necessary to eliminate the fixed phase offset between both measurement paths, e.g., by performing phase measurements at rotary angle of $\alpha_{AUT} = 45°$. The two separate phase measurements can be combined into one curve by calculating the overall phase of the phasor, i.e.,

$$\beta = \angle[S_{1H}\cos(\alpha_{\text{AUT}}) + S_{1V}\sin(\alpha_{\text{AUT}})]$$

for the test when the reference AUT starts out with an H-polarization at of α_{AUT}, of 0°, see Figure 8.4-2, and

$$\beta = \angle[S_{1V}\cos(\alpha_{\text{AUT}}) + S_{1H}\sin(\alpha_{\text{AUT}})]$$

for the test when the reference AUT starts out with a V-polarization at of α_{AUT}, of 0°, see Figure 8.4-3. Here, β is the resulting phase variation on circular path while S_{1H} (S_{1V}) are the S-parameter measured at the H (V) port of the feed/measurement antenna and $\angle$ is the operator for the phase.

This procedure shall be performed at four fixed radii of $R = 15\ \text{cm}, 10\ \text{cm}, 5\ \text{cm},$ and $0\ \text{cm}$ at $z = 0$ as illustrated schematically in Figure 8.4-4. Additionally, rotary scans at $R = 0$ cm and the perimeter of the spherical quiet zone at offsets in $\pm z$ shall be evaluated, i.e., one rotary scan with 5 cm radius at $z = \pm 14.15$ cm, as illustrated in Figure 8.4-5. Each rotary scan shall be performed for rotary angle increments of every 0.5°.
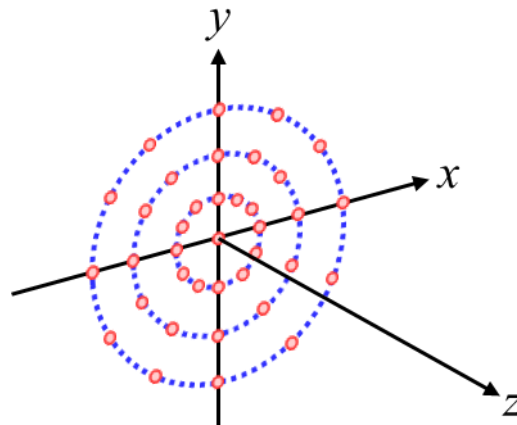
Figure 8.4-4 Rotary Scan at Four Fixed Radii at $z = 0$
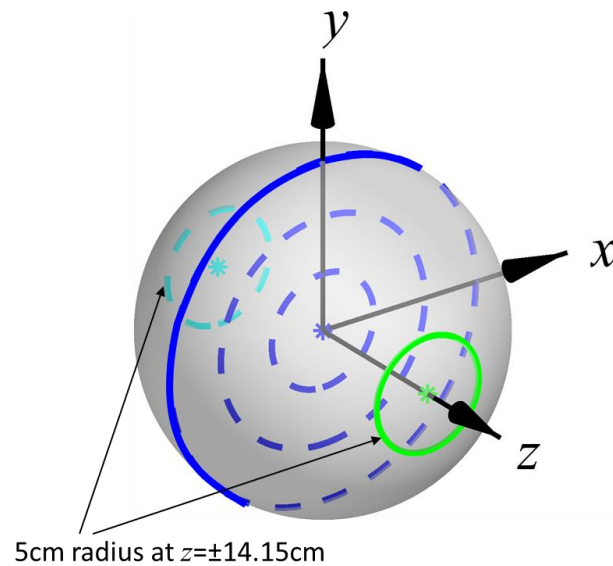
Figure 8.4-5 Rotary Scans Within Spherical Quiet Zone

The basic measurement procedure is therefore as follows:

1. Mount the reference AUT at fixed radius $R = 15$ cm at $z = 0$.

2. Align the principal polarization of the reference AUT with the x-axis (horizontal) at rotary angle α_{AUT}, of 0° (see Figure 8.4-2) with the antenna facing the z direction.

3. Perform S_{1H} and S_{1V} measurements every 0.5° in rotary angle α_{AUT}, for each test frequency outlined in Section 8.3.

4. Calculate the resulting phase variation on the circular path of radius R using Equation 8.4-1 and Equation 8.4-2.

5. Align the principal polarization of the reference AUT with the y-axis (vertical) at rotary angle α_{AUT}, (see Figure 8.4-3) with the antenna facing the z direction.

6. Perform S_{1H} and S_{1V} phase measurements every 0.5° in rotary angle α_{AUT} for each test frequency outlined in in Section 8.3.

7. Calculate the resulting phase variation on the circular path of radius R using Equation 8.4-2.

8. Mount the reference AUT at fixed $R = 10$ cm and repeat steps 2 through 7 and subsequently move to step 9.

9. Mount the reference AUT at fixed $R = 5$ cm and repeat steps 2 through 7 and subsequently move to step 10.

10. Mount the reference AUT at fixed $R = 0$ cm and repeat steps 2 through 7 and subsequently move to step 11.

11. Move the reference AUT at fixed radius $R = 0$ cm at $z = +14.15$ cm and repeat step 2 through 7 and subsequently move to step 12.

12. Move the reference AUT at fixed radius $R = 5$ cm at $z = +14.15$ cm and repeat step 2 through 7 and subsequently move to step 13.

13. Move the reference AUT at fixed radius $R = 0$ cm at $z = -14.15$ cm and repeat step 2 through 7 and subsequently move to step 14.

14. Move the reference AUT at fixed radius $R = 5$ cm at $z = -14.15$ cm and repeat step 2 through 7.

Alternatively, the use of a dual-polarized reference AUT is not precluded and a slightly modified procedure could be used.

The phase variations shall be evaluated for the combined rotary scans independently for each constant z, i.e., the phase variation due to the propagation in the z-direction shall not be compensated. The maximum phase variation for each fixed z is determined by combining (concatenating) all radial scans performed at given z, e.g., $R = \{15 \text{ cm}, 10 \text{ cm}, 5 \text{ cm}, 0 \text{ cm}\}$ at $z = 0$, and evaluating the total peak-to-peak variation. The maximum phase variation within the spherical quiet zone, $\Delta\beta_{max}$, shall be calculated and reported using:

Equation 8.4-3

$$\Delta\beta_{\text{max}} = \max \left[\begin{array}{c} \Delta\beta(R = \{15 \text{ cm}, 10 \text{ cm}, 5 \text{ cm}, 0 \text{ cm}\}, z = 0), \Delta\beta(R = \{5 \text{ cm}, 0 \text{ cm}\}, z = -14.15 \text{ cm}), \\ \Delta\beta(R = \{5 \text{ cm}, 0 \text{ cm}\}, z = 14.15 \text{ cm} \end{array} \right]$$

where $\Delta\beta_{max}$ is the maximum phase variation within concatenated rotary scans performed at position z, i.e.,

Equation 8.4-4

$$\Delta\beta(R, z) = \max[\beta(R, z)] - \min[\beta(R, z)]$$

Note that it is necessary to unwrap the phase if any β has rolled over a 360º boundary, e.g. -180º to +180º.

8.4.1   Phase QoQZ Fixture Correction

Small tilts in relation to the system coordinate system may be compensated due to minor misalignment of the fixture used for Phase QoQZ.

These misalignments between the plane wavefront and the reference antenna when applying the rotary scan procedure can be expressed in terms of x-axis tilt $\Delta\theta_x$ and y-axis tilt $\Delta\theta_y$. These tilts are shown in Figure 8.4.1-1 and Figure 8.4.1-2 where:

- The transparent disc represents the ideal xy plane aligned with the coordinate system with perfect alignment.

- The yellow pyramid represents a generic measurement antenna, while in CATR systems it is to be replaced by a feed and reflector system.

- The blue dots are examples of the test positions on each radius for the $z = 0$ plane.

- The orange disc represents, exemplary, an actual measurement plane (true QZ plane) with exaggerated tilt values, where $\Delta\theta_x = -15°, \Delta\theta_y = -10°$.
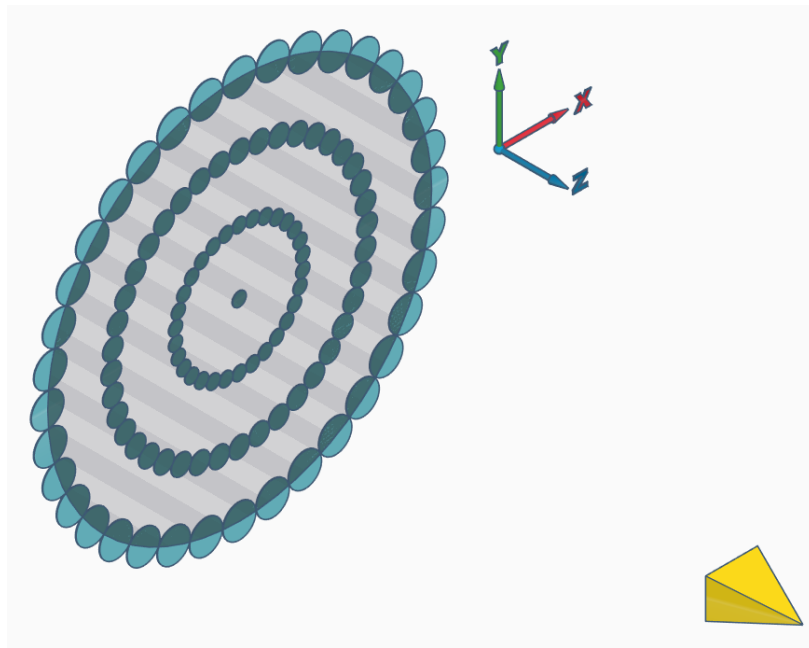
Figure 8.4.1-1 Target QZ Plane (at $z = 0$) with Perfect Alignment
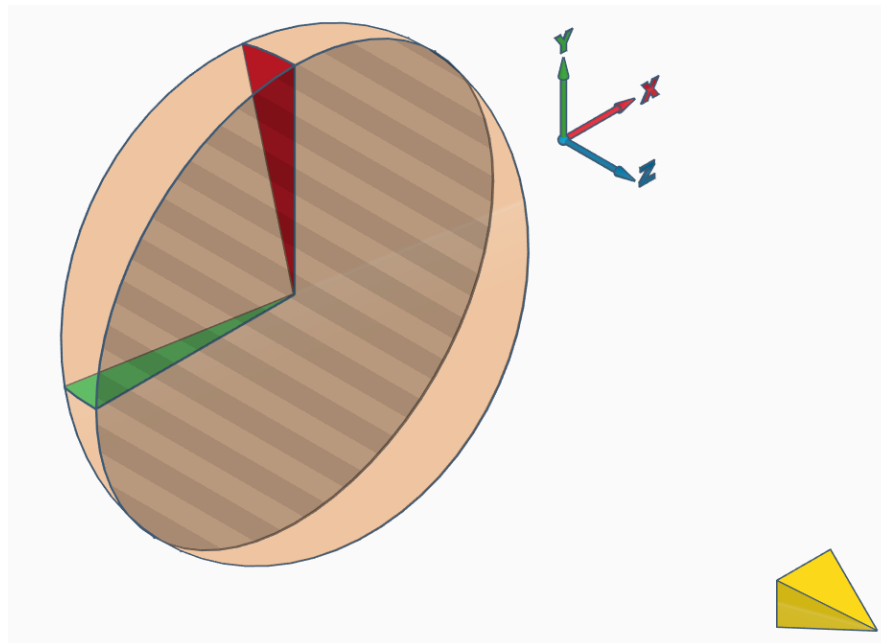

Figure 8.4.1-2 Definition of x-axis $\Delta\theta_x$ (Red) and y-axis $\Delta\theta_y$ (Green) Tilts

The tilt error correction for phase measurements can be expressed as:

$$\beta \approx \beta' + \left(R\cos(\alpha_{AUT})\tan(\Delta\theta_y)\frac{360°}{\lambda_k} - R\sin(\alpha_{AUT})\tan(\Delta\theta_x)\frac{360°}{\lambda_k} \right)$$

where:

- λ_k is the wavelength

The corresponding equation when the test starts with an H-polarization at of $\alpha_{AUT}, = 0°$, see Figure 8.4-2.

$$\beta \approx \angle[S_{1H}\cos(\alpha_{AUT}) + S_{1V}\sin(\alpha_{AUT})] + \left(R\cos(\alpha_{AUT})\tan(\Delta\theta_y)\frac{360°}{\lambda_k} - R\sin(\alpha_{AUT})\tan(\Delta\theta_x)\frac{360°}{\lambda_k}\right)$$

and when the test starts with a V-polarization of $\alpha_{AUT}, = 0°$, see Figure 8.4-3.

$$\beta \approx \angle[S_{1V}\cos(\alpha_{AUT}) + S_{1H}\sin(\alpha_{AUT})] + \left(R\cos(\alpha_{AUT})\tan(\Delta\theta_y)\frac{360°}{\lambda_k} - R\sin(\alpha_{AUT})\tan(\Delta\theta_x)\frac{360°}{\lambda_k}\right)$$

Tilt values $\Delta\theta_x$ and $\Delta\theta_y$ are found as an average result among all frequencies of minimizations per xy plane where, for each k (for each frequency) the optimum pair of tilts which minimizes the absolute difference (absolute maximum minimum variation) is found, and then the average for all frequencies is calculated:

$$\forall k\left(\Delta\theta_{x,k}, \Delta\theta_{y,k}\right) = \underset{\Delta\theta_x', \Delta\theta_y'}{\mathrm{argmin}}\left\{\left|\max_n\left(\beta\left(R, \alpha_{AUT,n}, \Delta\theta_x', \Delta\theta_y', \lambda_k\right)\right) - \min_n\left(\beta\left(R, \alpha_{AUT,n}, \Delta\theta_x', \Delta\theta_y', \lambda_k\right)\right)\right|\right\}$$

$$\Delta\theta_x = \frac{1}{K}\sum_{k=1}^{K}\Delta\theta_{x,k}$$

$$\Delta\theta_y = \frac{1}{K}\sum_{k=1}^{K}\Delta\theta_{y,k}$$

Alternatively, tilt values $\Delta\theta_x$ and $\Delta\theta_y$ can be found by calculating the planar least square fit as described in Section 8.5.1.

Same tilt correction values $\Delta\theta_x$ and $\Delta\theta_y$ shall be applied for all measurement frequencies, all radial scans (i.e. all z), and shall be documented together with maximum phase variation obtained after correction as part of the evidence for the declared QoQZ measurement uncertainty. The values $\Delta\theta_x$ and $\Delta\theta_y$ shall be bound within ±0.25º.

8.5   Field Probing Procedure

The phase variation is determined from a phase probe trace by measuring the full excursion of the phase over the aperture of the quiet zone and is recorded in degrees.

Any positioners and/or support structures used throughout any conformance tests shall be installed in the system so its impact on the phase variation is taken into account, i.e., the DUT positioner shall not be removed and its impact on the phase variation shall be taken into account, with the slide mounted to the location where the DUT is mounted. It is not recommended, but possible to mount the DUT positioner to the slide, in this case an additional alignment procedure is required to ensure that the DUT positioner is aligned to the x, y and z coordinates of the system.

The outcome of the procedures can be used to predict the variation of phase of the synthesized plane wave in the quiet zone. The reference coordinate system defined in in CTIA 01.71 [6] Section 5.1, applies to this procedure.

Evaluation of the IFF quiet zone is accomplished by directly sampling the phase characteristics of the quiet zone field using the antenna specified in Section 7.2 as reference antenna. The reference antenna is placed at various locations within the quiet zone and analysis of the data reveals the field phase variations as a function of frequency and quiet zone location.

The reference AUT is attached to a linear rail placed at the range centerline height at the front, middle and rear of the quiet zone. Field samples are collected as the antenna is scanned horizontally, vertically, and along $+45°$ and $-45°$ paths. In all scans, both polarizations [V, H] shall be measured.

The reference positions are shown in Figure 8.5-1. The phase shall be recorded in the xy plane, in increments of $\lambda/2$ or smaller for all positions that are contained within the spherical quiet zone at three different positions in z, i.e., within a circle of radius $R = 15\ cm$ at $z = 0$, and within a circle of radius $R = 5\ cm$ at $z = \pm14.15\ cm$. A calibration is performed for both polarizations at each z position, at $x, y = 0$, i.e., $(0,0,z)$. This in effect makes each point measured in r relative to $(0,0,z)$.
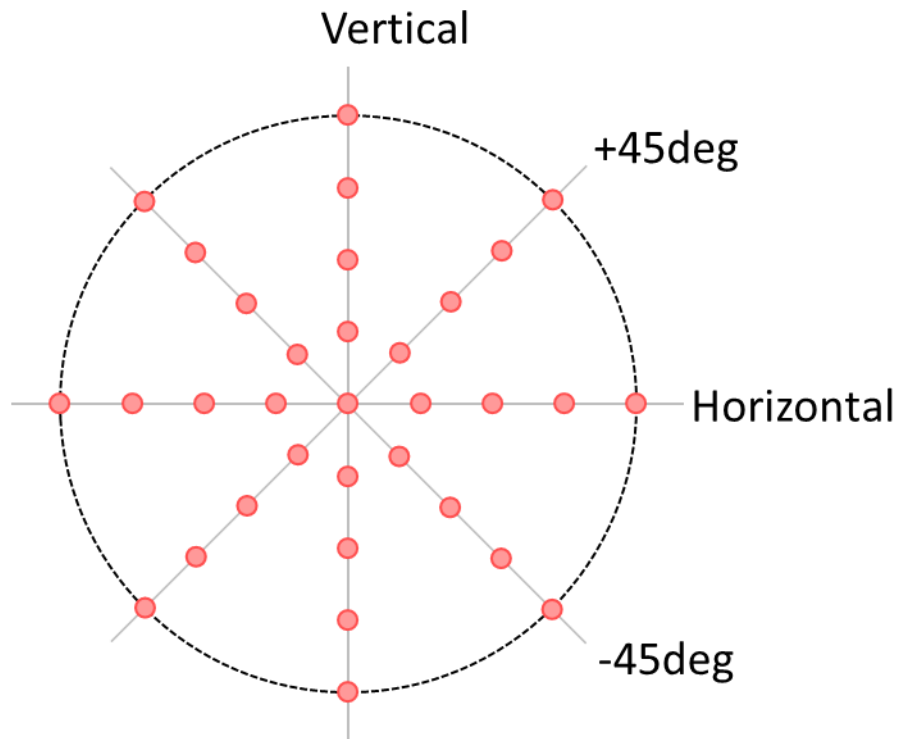
Figure 8.5-1 Field Probing Reference Positions

A summary of the configurations to be tested is shown in Table 8.5-1 for $z = 0$:

Table 8.5-1 Tested Configurations

Test Data No.	Field Probe Scan Direction	Probe Polarization	Feed Polarization	Phase Scan
1	Horizontal	H	H	β (Scan=1)
2	Horizontal	V	V	β (Scan=2)
3	Vertical	H	H	β (Scan=3)
4	Vertical	V	V	β (Scan=4)
5	+45º	H	H	β (Scan=5)
6	+45º	V	V	β (Scan=6)

Test Data No.	Field Probe Scan Direction	Probe Polarization	Feed Polarization	Phase Scan
7	-45º	H	H	β (Scan=7)
8	-45º	V	V	β (Scan=8)

The basic measurement procedure is as follows:

1. Align the axes of the positioner to the range coordinate system.

2. Mount the reference AUT at the position (0,0,0) -> center of coordinate system.

3. Align the AUT V polarization to the feed V polarization.

4. Measure the phase at (0,0,0). If using a Network Analyzer for the field probing procedure, this measurement can be a 2-port calibration in order to make all subsequent measurement points relative to this point.

5. Scan the AUT horizontally, vertically, $+45°$, and $-45°$ in the xy plane. Mount the horn such that it remains co-polarized with the feed through the duration of the scan.

6. Record S21V (co-polarized) for each position on all four lines (step 4) in the xy plane.

7. Change feed polarization to H-polarization.

8. Repeat step 2 to 5.

   a. At step 5, S21H (co-polarized) is recorded for each position on all four lines in the xy plane.

9. Move the AUT to next z position -> $z = +14.15\ cm$.

10. Measure the phase at (0,0,14.15 cm) as described in step 4.

11. Repeat steps 5 through 8.

12. Move the AUT to next z position -> $z = -14.15\ cm$.

13. Measure the phase at $(0,0,-14.15\ cm)$ as described in step 4.

14. Repeat steps 5 through 8.

Alternatively, the use of a dual-polarized reference AUT is not precluded and a slightly modified procedure could be used.

The phase variations shall be evaluated for the combined field probing scans independently for each constant z, i.e., the phase variation due to the propagation in the z-direction shall not be compensated. The maximum phase variation for each fixed z is determined by combining (concatenating) all 8 scans performed at given z, e.g., Scan={1, …, 8} at z=0, and evaluating the total peak-to-peak variation. The maximum phase variation within the spherical quiet zone, $\Delta\beta_{max}$, shall be calculated and reported using:

Equation 8.5-1

$$\Delta\beta_{\max} = \max[\Delta\beta(\text{Scan} = \{1, ... , 8\}, z = 0), \Delta\beta(\text{Scan} = \{1, ... , 8\}, z = -14.15\text{cm}), \Delta\beta(\text{Scan} = \{1, ... , 8\}, z = 14.15\text{cm})]$$

where $\Delta\beta$ is the maximum phase variation within the concatenated linear scans performed at position z, i.e.,

<div align="right">Equation 8.5-2</div>

$$\Delta\beta(\text{Scan}, z) = \max[\beta(\text{Scan}, z)] - \min[\beta(\text{Scan}, z)]$$

where β are related to the S-parameter measurements as follows: $\beta_i = \angle[S21_H]$ for for Scans 1, 3, 5, and 7, and $\beta_i = \angle[S21_V]$ for Scans 2, 4, 6, and 8.

Note that it is necessary to unwrap the phase if any β has rolled over a 360º boundary, e.g. -180º to +180º.

8.5.1 Phase QoQZ Fixture Correction

The phase error due to the fixture's manufacturing tolerances used during the phase measurement, when using the field probing method, may be corrected using the following method.

A small fixture misalignment in the z direction will create a phase error that will be proportional to the wavelength of the signal being measured. As the probe moves in the x or y direction across the quiet zone this phase will be proportional to the changes in the z direction, the frequency, and the location of the probe in the x or y axis.

In order to remove the misalignment error the next steps need to be followed:

1. At each z scan position (-14.15, 0, 14.15 cm), convert the data set to linearized phase as a function of x and y positions.

2. At each frequency, convert the phase data to a z value by multiplying by the wavelength and dividing by 360 degrees.

3. Calculate the least squares fit of the z data to a plane $z = Ax + By + C$.

4. Average the A and B values across all frequencies and all scans (i.e. all z). For the purpose of this calculation, the C value is immaterial.

5. Use the resulting average of the slopes A and B to calculate the angular error $\Delta\theta_x = \arctan(A)$ and $\Delta\theta_y = \arctan(B)$.

6. Use the average A and B values to compute the z plane values for all positions.

7. At each frequency, subtract the z plane values from the measured z values and convert the result back to linearized phase by multiplying by 360 degrees and dividing by the wavelength. The result is the phase variation with the linear component removed.

8. The difference between the maximum and minimum phase is the total phase variation at the corresponding frequency.

The same correction values A and B shall be applied for all measurement frequencies and scans (i.e. all z), converted to correction angles $\Delta\theta_x$ and $\Delta\theta_y$, and shall be documented together with maximum phase variation obtained after correction as part of the evidence for the declared QoQZ measurement uncertainty. The resulting correction angles in the x and y directions shall be bound within ±0.25º.

CTIA
Certification™

8.6 Maximum Phase Variation

The maximum phase variation $\Delta\beta_{max}$ (after fixture correction in case is applied) for the permitted methodology of IFF, determined either with the rotary scan or the field probing approach, shall be 22.5°. This maximum limit could be revisited based on OEM feedback on sensitivity of UE beam management to phase variation.

Section 9   Power Measurement Considerations

9.1   Power Measurement Equipment

In order to perform the power measurements required by this test, there are a number of considerations to take into account with regard to the test equipment used for these measurements. The recommended equipment for these power measurements is a spectrum analyzer, communication tester, or power meter. Any selected instrumentation should be specifically designed for measurement of wireless modulated waveforms.

Modern spectrum analyzers provide direct control over the parameters necessary to measure different communications signals and can make the required measurements with relatively low uncertainty contributions. However, older units may not be capable of performing the measurements within the tolerance necessary to meet the overall uncertainty requirement. For units with sufficient linearity and stability, it may be possible to use a transfer standard from a power meter or other more accurate device during the range reference measurement to reduce the total uncertainty associated with the analyzer.

Communication testers are convenient for use in power measurements since their receiver settings are normally correctly pre-configured for each protocol. Thus, the detailed considerations presented in the following sections have in general been handled by the manufacturer of the communication tester. Another convenience is that communication testers are commonly used for conducted power measurements and the use of the same equipment for the TRP measurement facilitates consistent comparisons between conducted and radiated performances. However, commonly used communication testers are designed for conducted tests and thus may require additional amplifiers to deal with the additional path losses associated with radiated tests.

Power meters are inherently broadband measurement receivers and as such require special precautions when used to measure OTA TRP. Modern power meters employ sampled diode detectors and digital signal processing techniques to enhance measurement accuracy and dynamic range. Detector video bandwidths have been extended to allow measurement of modulated wireless communications signals. Triggering capability has been improved to allow triggering from and measurement of burst modulated signals. These capabilities make power meters a viable alternative for OTA TRP measurement.

Other receivers may also be used to measure the received power provided it can be shown that they meet the necessary sensitivity, frequency discrimination, and waveform requirements for the respective communication technology.

9.2   General Measurement Requirements

This section lists general requirements and recommendations that should be addressed for all technologies and power measurement technologies. The primary goal is to ensure that uniform total radiated power measurements can be made within the expected uncertainty of the given device. The remaining sub-sections of this section contain guidance for measuring different types of signals and specific requirements for individual technologies. Those sections assume the use of a spectrum analyzer or a power meter for the required measurements, although other receiver technologies may be used, provided they are shown to produce equivalent results. Unless otherwise noted, RMS detector mode is assumed for the spectrum analyzer.

As with all RF measurements, special attention must be paid to the noise floor and compression levels of the instrumentation used. The wide dynamic range of signals expected for a typical ERP pattern measurement makes this difficult. The pulsed nature of wireless communication also places special demands on components such as preamplifiers and receiver front ends, which may perform fine for CW signals but produce harmonics or distortion for pulsed signals. The manufacturer's documentation for all components should be consulted to ensure that the expected level of performance can be obtained.

CTIA
Certification™

It is recommended that the peak signal received for a pattern be at least 40 dB above the noise floor. For a dipole this would result in a noise contribution of approximately 0.12 dB to the TRP, and just under 0.1 dB to the peak EIRP points. For antenna ranges for which the path loss would result in signal levels below this limit, either an appropriate preamplifier may be used (incorporating the necessary drift and linearity terms into the uncertainty budget), or the uncertainty budget must be increased to reflect the larger uncertainty due to the proximity to the noise floor. However, the total uncertainty of the measurement system may not exceed the limit given in *CTIA 01.01* [7]. In no case shall the peak signal for a pattern be allowed to be within less than 20 dB (1.1 dB TRP error for a dipole) of the peak noise floor (i.e. the total usable dynamic range must be greater than 20 dB) since the corresponding loss in resolution would reduce the usefulness of the EIRP pattern for comparison purposes.

Due to the modulated nature of the communication signal, specific dwell times are necessary to ensure repeatable measurements. The spectrum analyzer, power meter, or receiver must be able to support the required sweep times and specified number of uncorrelated data points to obtain the required measurement resolution for each technology. Software or firmware used to process the data must apply the appropriate digital filters to produce the required result.

Note: *Any external attenuation or amplification added to meet the above requirements must be included in the Range Reference Measurement, or added into the range correction as separate terms, and appropriate adjustments must be made to the total measurement uncertainty.*

For alternate receivers and power meters, they must support equivalent bandwidth and filter settings or functions that produce measurement results equivalent to those listed here.

9.2.1   Use of Spectrum Analyzers

Modern spectrum analyzers and signal analyzers have merged to a common hardware architecture, and differ only in acquisition type and digital signal processing (DSP). A mixer converts high RF frequencies to an intermediate frequency (IF), which is then digitized in an ADC. The LO to the mixer can be swept or fixed-tuned. Both RF and IF stages typically include gain/attenuation and filter blocks to optimize amplitude levels and filter unwanted signals/noise. The digital samples from the ADC are then processed in DSP according to the need, providing additional filtering such as resolution bandwidth (RBW) filters and signal detection or analysis. In spectrum analysis mode they process magnitude-only data, with signal detectors such as Peak and RMS that emulate traditional analog spectrum analyzers, while in signal analysis mode they process IQ data that has both magnitude and phase information, to yield demodulation measurements such as EVM. Spectrum analysis can be run in traditional frequency swept mode or zero span, while signal analysis is typically fixed tuned and uses the information bandwidth (sampling rate) of the receiver front end to capture a given channel width. For the purposes of this test plan, the RMS power over specific frequency bandwidths and time spans are of primary interest. Thus, the spectrum analysis mode is typically most applicable, although signal analysis modes may also be used successfully.

The traditional spectrum analyzer consists of a spectrum display that is tied to the output bits of the receiver's analog-to-digital converter (ADC). Different detectors are used to process each sample from the ADC to generate each data point on a trace. The sample detector takes a single ADC reading at each time or frequency point along a trace and returns that value as the displayed value. For other detectors, the ADC typically samples at some maximum rate and a processed result is displayed for each data point (commonly referred to as a "bin"). The number of samples taken per data point is given by the sweep time divided by the total number of points in the sweep and by the sample rate of the ADC. A peak detector returns the maximum value sampled during the portion of the sweep centered around each data point, while the RMS detector returns a linear average power of the available samples. Longer sweep times typically result in more samples per point and more accurate detector values. In addition to the sample rate of the ADC, the bandwidth filter will reduce the effective number of uncorrelated samples. The effective sample rate in samples per second is equivalent to the selected resolution bandwidth in Hz.

Since the vertical resolution of the display typically matches the available resolution of the ADC, the measured value is only accurate to the instrument specifications when the reading is within the graticule of the analyzer window. Points above or below that point are subject to compression and/or clipping effects that may not be apparent, especially when used with software automation. In addition, when using the RMS filter, the result can be biased even when the reported value is several dB from the top of the window, since some samples within the average may be clipped, resulting in a lower average value. Due to these limitations, the reference level and attenuation of the analyzer must be adjusted so that maximum signal level received during the pattern testing stays within the graticule. It is recommended that the peak signal remains at least 5 dB below the top of the window to avoid clipping unexpected peaks in the pattern. For tuned receiver type units, the settings must be adjusted as required so that the peak expected signal does not overdrive the receiver. Refer to the manufacturer's documentation to determine if the spectrum analyzer readings reported to software automation are valid when the signal is outside the bounds of the display.

9.2.2   Use of Communication Testers

Power may also be measured by using communication testers designed to perform maximum output power test cases as defined by 3GPP. Communication testers typically perform power measurements using a spectrum analyzer concept. The RF signal is down-converted to IF frequencies and processed using fast Digital Signal Processors (DSP). The bandwidth of the receiver filter is automatically set to that required by the respective protocol. E.g., for GSM a 500 kHz Gauss filter is used. As mentioned previously, additional external amplifiers and/or filters may be required to achieve sufficient dynamic range for radiated tests. Care should be taken to ensure that the communication tester receiver is capable of measuring the DUT radiated output power within the manufacturer declared measurement uncertainty considering the dynamic range necessary to accommodate additional path loss and antenna pattern variation. Communication testers with separate transmit and receive ports are most convenient for radiated tests. Otherwise, a single combined transmit/receive port would require a high isolation diplexer to split transmit and receive signals before amplification. In either case, it is important to verify that leakage from the output of the communication tester does not adversely affect measurements on the input ports.

9.2.3   Use of Power Meters

Unlike spectrum analyzers, power meters are broadband power measurement devices. They will combine the power of all signals present at the sensor into a single amplitude level. However, power meters are simple and inexpensive compared to spectrum analyzers, and data acquisition speed can be significantly faster, reducing overall TRP measurement times. Careful system design is required to insure that measurement error due to unwanted signals is kept below specified levels.

When power meters are used for TRP measurement, it is required to show that the coupling of the downlink power into the measurement antenna does not significantly affect the measured power, and is accounted for appropriately in the uncertainty budget. The power sensor shall be assumed to report the signal level as the sum of the voltages present, and it is recommended that the measurement system provide a minimum of 45 dB of uplink-to-downlink channel isolation to limit measurement error from this source to < 0.1 dB. Power meters not specifically designed or certified for wireless power measurements are prohibited.

Many sources of uncertainty impact the measurement of OTA TRP. These are covered in detail in *CTIA 01.20* [8] and *CTIA 01.70* [1]. Two sources of uncertainty require special attention when using power meters to determine OTA TRP:

- The ratio of uplink-to-downlink signal level (P_{UL}/P_{DL}) present at the power meter sensor

- The ratio of uplink signal level-to-noise (P_{UL}/N) present at the power meter sensor

9.2.3.1 Ratio of Uplink-to-Downlink Signal Level

A communication tester is used to place the DUT into a call on a specified channel and at a specified uplink channel power level. At least one downlink channel is required for DUT control and downlink traffic. In any practical OTA test chamber, some of the downlink channel energy will couple into the measurement antenna and will be present at the measurement receiver. If the receiver is a broadband power meter, the sensor will respond to the downlink channel energy as well as the uplink channel energy, producing measurement uncertainty. This source of uncertainty must be quantified and controlled.

TRP measurement uncertainty attributed to downlink power should be no greater than 0.1 dB. The level of isolation P_{UL}/P_{DL} required to achieve this uncertainty level is dependent on the characteristics of both the power sensor used and the signals being measured. Modern power meters use diode sensors almost exclusively. Diode sensors respond to voltage; they do not convert power to thermal energy. The power level reported with multiple signals present will depend on the level of coherency between the various signals. In the worst case, the diode sensor will add the peaks of the signals on a voltage basis. In this case, $P_{UL}/P_{DL} > 45$ dB is required to achieve an uncertainty level $U < 0.1$ dB.

In an OTA chamber, the downlink path from the communication tester to the DUT is established either through the measurement antenna, or through an auxiliary antenna mounted in the chamber for this specific purpose. In either case, some of the downlink channel energy will couple into the measurement receiver. It is instructive to examine these two system configurations to determine if the downlink signal level can be controlled to be greater than 45 dB below the uplink signal level expected during TRP measurements.

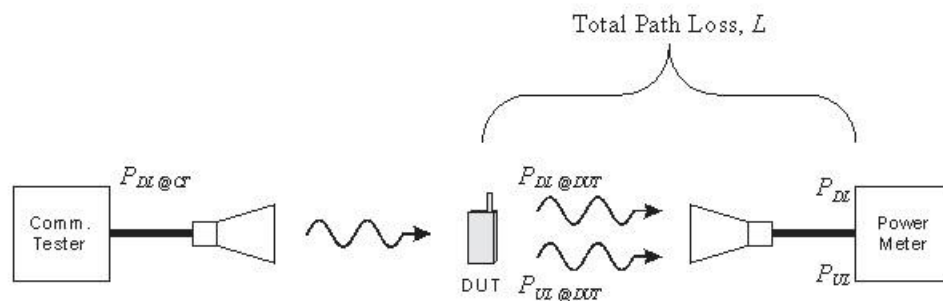Figure 9.2.3-1-1 Downlink Path Established Using an Auxiliary Antenna

Figure 9.2.3.1-2 shows a simplified diagram of an OTA system where the downlink path is established using an auxiliary antenna. For purposes of discussion, the auxiliary antenna is assumed to be located directly behind the DUT and in line with the measurement antenna. It is also assumed that the downlink and uplink channel signals are co-polarized.
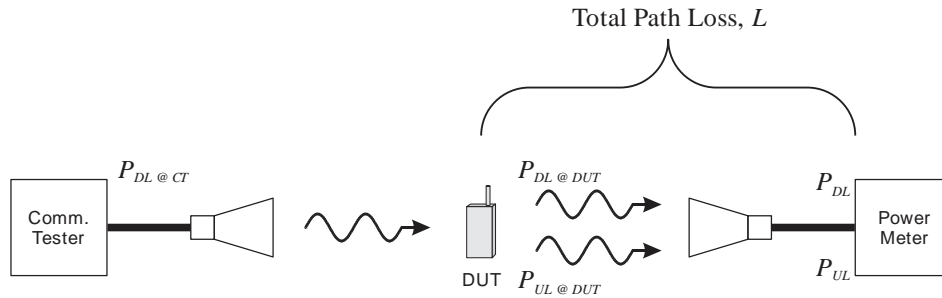
Figure 9.2.3.1-2 Use of Auxiliary Antenna for Downlink Channel

In this configuration, the downlink channel signal will propagate past the DUT and directly into the measurement antenna, a worst-case situation. Assume that the downlink signal level arriving at the DUT is $P_{DL \, @ \, DUT}$ and that the uplink signal level transmitted by the DUT in the direction of the measurement antenna is $P_{UL \, @ \, DUT}$. Since both the downlink and uplink channel signals must travel over the same path through the measurement antenna to the power meter sensor, and since both will be in the same frequency range, both will be attenuated by the same amount when they arrive at the power meter sensor. Thus, the ratio P_{UL}/P_{DL} at the sensor will be the same as the ratio $P_{UL \, @ \, DUT}/P_{DL \, @ \, DUT}$ at the DUT.

For typical DUTs, $P_{DL \, @ \, DUT}$ is in the range -80 to -50 dBm to maintain a connection with the DUT. Similarly, $P_{UL \, @ \, DUT}$ is typically in the range 0 to + 30 dBm, depending on the spatial orientation of the DUT. Thus:

Equation 9.2.3.1-1

$$10 \log_{10} \left(\frac{P_{UL}}{P_{DL}} \right) = 10 \log_{10} \left(\frac{P_{UL \, @ \, DUT}}{P_{DL \, @ \, DUT}} \right) = P_{UL \, @ \, DUT} (\text{dB}) - P_{DL \, @ \, DUT} (\text{dB}) = 50 \text{ to } 110 \text{ dB}$$

This range of values shows that this system configuration can satisfy the 45 dB isolation requirement.

Figure 9.2.3.1-3 shows a simplified diagram of an OTA system where the downlink path is established through the measurement antenna. A power splitter/combiner is used to couple the communication tester to the measurement antenna for DUT control. The power meter is connected to the opposite port of the splitter/combiner to measure the uplink channel signal transmitted by the DUT.
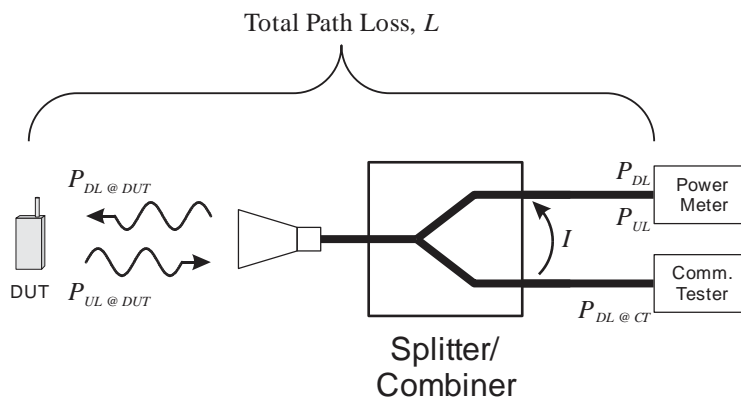
Figure 9.2.3.1-3 Use of Measurement Antenna for Downlink Channel

In this configuration, neglecting the cable losses between the splitter/combiner and the test equipment, the downlink channel signal travels to the DUT over the same path as the uplink channel signal and will experience approximately the same losses denoted as L. The downlink channel signal level appearing at the power meter sensor is dependent on the isolation of the splitter/combiner used, including any mismatch contribution from reflections at the measurement antenna or elsewhere in the system, and is denoted as I. The ratio P_{UL}/P_{DL} can be expressed as:

<div align="right">Equation 9.2.3.1-2</div>

$$10 \log_{10}\left(\frac{P_{UL}}{P_{DL}}\right) = 10 \log_{10}\left(\frac{P_{UL\,@\,DUT}/L}{P_{DL\,@\,CT}/I}\right) = 10 \log_{10}\left(\frac{P_{UL\,@\,DUT}\,I}{P_{DL\,@\,DUT}\,L^2}\right)$$
$$= P_{UL\,@\,DUT}(\text{dB}) - P_{DL\,@\,DUT}(\text{dB}) - 2L(\text{dB}) + I(\text{dB})$$

Using the same range of values for $P_{UL\,@\,DUT}$ and $P_{DL\,@\,DUT}$ as was used above, and assuming L=40 dB and I=30 dB:

$$10 \log_{10}\left(\frac{P_{UL}}{P_{DL}}\right) = 0 \text{ to } 60 \text{ dB}$$

This range of values shows that this system configuration probably will not satisfy the 45 dB isolation requirement for all spatial orientations of the DUT.

9.2.3.2   Ratio of Uplink Signal Level-to-Noise

Section 9.2 above requires that the peak DUT EIRP level must be at least 20 dB above the system noise floor and it is recommended that the peak level be at least 40 dB above the system noise floor.

Power meters using diode detectors as the power sensor are available with residual noise floors of -70 dBm or less. Diode detectors produce an output voltage proportional to input power level. Below about -30 dBm, the output voltage is proportional to the square root of the input power; at higher power levels the response becomes highly nonlinear and can vary significantly from device to device. To maximize instrument operating range, newer power meters have built in calibration circuitry which calibrates the sensor for operation in the nonlinear range from -30 to +20 dBm. Thus, the working dynamic range of these power meters is 90 dB.

In order to meet the noise floor requirements stated above, the peak EIRP level present at the power meter detector must be at least -50 dBm, with a recommended level of -30 dBm. These levels can be achieved with current OTA system configurations.

Wireless communications systems in use today use digital modulation techniques almost exclusively. These complex modulation formats are generally transmitted as a burst (GSM) or as a spread spectrum signal resembling noise (CDMA). Accurate measurement of the power level of these signals requires sampling the signal at a fast enough rate to reproduce the signal. For burst modulated signals, it is necessary to synchronize the duration of the measurement to the burst so that only the significant central region of the burst is captured. For spread spectrum signals, the signal must be sampled over the full extent of the channel spectrum to capture the true peak and average power levels.

The complex nature of wireless signals originally required the use of high-speed sampling spectrum analyzers (or communication testers) to accurately measure the levels of the signals transmitted by a DUT. However, newer power meters from several manufacturers have been designed specifically for wireless modulation formats. Power meters used for OTA TRP tests shall meet or exceed the following requirements:

- Minimum sampling rate of 2.5 MHz.

- Triggering modes to allow triggering from the rising edge of a burst modulated signal.

- Gating, delay and holdoff features to allow selection of the central region of pulses and bursts and collection of over 750,000 data samples over the selected region.

- Power sensors specifically designed for measurement of wireless modulation formats with wide video bandwidths.

9.3   Common Modulations and Waveforms

The signals to be measured for a wireless device can generally be subdivided based on signal bandwidth (narrowband vs. wideband) and temporal signature (e.g. continuous vs. pulsed). As wireless technologies have advanced, channel bandwidths have grown from just wide enough to handle voice traffic (e.g. 200 kHz) to many MHz in span. At the same time, these large channels can be subdivided into subchannels where measurement techniques remain similar to those for narrower channels. The signals may also be subdivided in time, making measurements more challenging, especially for broadband signals. Ideally, the entire channel bandwidth is sampled continuously allowing for subdividing in time if needed, but swept signal approaches may also be used for wide channels.

Note that all of the power measurement techniques described here are generally applicable for measuring any sort of RF communication signal, whether uplink or downlink, and thus apply both to measuring the transmit power of a DUT as well as validating the transmit power of a communication tester or other downlink signaling.

9.4   Total Channel Power

If a spectrum analyzer supports sufficient resolution bandwidth to accurately measure the broadband signal in a zero-span sweep, then it may be used as a broadband power measurement device using an RMS or sample detector rather than requiring integrated channel power measurements. For a Gaussian RBW filter shape, the RBW must be at least three times the channel bandwidth to obtain broadband power readings within 0.1 dB of the actual channel power. Newer spectrum analyzers often offer rectangular or flat-top filter options, which typically converge to the correct value when the RBW setting is something greater than 120% of the channel bandwidth. For the purposes of this test plan, broadband power measurements may be performed using a Gaussian RBW of at least $f_{Gaussian}$ or a flat top RBW filter of at least $f_{flat\,top}$ with VBW set to the maximum supported by the spectrum analyzer.

In a typical spectrum analyzer, the sample detector records one sample from the analog to digital converter (ADC) at each point on the trace. Each trace point represents an instantaneous picture (sample) of the signal level at that point in time. The linear power average of this data provides an acceptable measurement of the average power in the spread spectrum signal. However, the stability of this result is dependent on the number of points measured. The use of an RMS detector over a sufficient time frame provides a lower noise sweep, since the RMS detector performs the linear power average at each point on the trace for the period of time available to measure that point. Increasing the sweep time allows the RMS detector to average more samples together for each point on the trace. In signal analysis mode, the IQ analyzer records every sample from the ADC. For wide information bandwidths, this can produce a tremendous amount of data over the required dwell times, making data transfer for subsequent post processing problematic. Ideally the signal analyzer will provide onboard mechanisms for measuring the RMS channel power and stability over the required dwell times.

For the purposes of characterizing mobile transmit power, it is required to determine the average power of the signal envelope for a minimum dwell time of T_{dwell}. For a complete spherical pattern, where over 350 individual measurements are used to determine the average performance (TRP) it is considered acceptable to reduce the individual measurement dwell time to $T_{short\,dwell}$. Assuming the DUT is stable

CTIA
Certification

and the test equipment operates as expected, this will introduce a negligible additional uncertainty to the measurement. However, in the event of a conflict, the T_{dwell} dwell time shall be considered the reference.

The spectrum analyzer shall be set for zero-span in free-run mode with resolution bandwidth of $f_{Gaussian}$ or $f_{flat\ top}$ (depending on the RBW filter shape used) and a video bandwidth set to the maximum supported by the spectrum analyzer (3 MHz is the minimum VBW allowed). Using an RMS detector, the sweep time shall be set to at least T_{dwell} for single point tests and at least $T_{short\ dwell}$ for complete pattern tests. When using a sample detector, this time period may be broken up into several smaller sweeps, if desired, to increase the accuracy of the sample average, but the total time of all sweeps shall be at least T_{dwell} for single point tests and at least $T_{short\ dwell}$ for complete pattern tests. The received signal must be stable for the entire trace in order to record a valid result. A stable trace is defined as all points remaining within a ±0.5 dB window. For the sample detector, the running average of 20% of the total number of points must remain within a ±0.5 dB window.

If a power meter is used, it shall be capable of measuring the average power of modulated signals with complex modulation formats. The power meter sensor must have a minimum video bandwidth of at least 120% of the channel bandwidth, f_{span}. The power meter triggering shall be set to free-run and the sampling time set to T_{dwell} or greater for single point tests and at least $T_{short\ dwell}$ for complete pattern tests. The received signal must be stable for the entire trace in order to record a valid result. A stable trace is defined as all points remaining within a ±0.5 dB window. Power meters using diode detectors are sampling detectors, and the comments pertinent to sampling detectors in the above paragraph apply to these detectors.

9.5 Integrated Channel Power

Since many spectrum analyzers are limited to only 3 MHz RBW, a zero-span power measurement is usually not appropriate for wideband technologies. For accurate measurement of wideband channels using spectrum analyzers with limited bandwidth, an integrated channel power (ICP) measurement must be used to determine the total power in a channel. This is done by scanning the entire channel bandwidth using a narrow resolution bandwidth and then summing the power spectral density (scaled trace data points) across the measured bandwidth. A resolution bandwidth (RBW) from 0.5 to 3.0% of the total bandwidth is typically used to ensure that the band is sampled with sufficient resolution. The following equation is then used to compute the resulting channel power.

$$P = \frac{CBW}{NBW} \times \frac{1}{N} \sum_{i=1}^{N} P_i$$

Where P_i is the power of each data point in the trace, represented in linear units, CBW is the bandwidth of the channel, NBW is the noise bandwidth represented by the measurement of each data point in the trace, N is the number of points in the sweep, and P is the resulting channel power, again in linear units. Some spectrum analyzers may have this function built in as an optional measurement mode, but it's simple to perform this measurement without needing that additional functionality. The noise bandwidth is roughly equivalent to the resolution bandwidth setting of the spectrum analyzer, however, depending on the shape of the RBW filter implementation in the analyzer, there can be as much as half a dB of deviation between the RBW setting and the NBW needed for the calculation. To address this, we can re-write Equation 9.5-1 to be:

$$P = \frac{CBW}{NBW} \times \frac{1}{N} \sum_{i=1}^{N} P_i = CF_{RBW/NBW} \frac{CBW}{RBW} \times \frac{1}{N} \sum_{i=1}^{N} P_i$$

where RBW is the resolution bandwidth used to sweep across the channel, and $CF_{RBW/NBW}$ is a correction factor to correct for the difference between the RBW and NBW. Spectrum analyzer manufacturers embed this correction factor in their internal ICP algorithms, but it's not normally published in a data sheet. See Section 9.5.1 for direction on how to determine this correction factor directly for any given instrument.

For the purposes of characterizing mobile transmit power using integrated channel power, the following considerations apply. Refer to the section for the specific technology for the specific criteria for that technology. For individual power measurements, a minimum sweep time of T_{sweep} is required. For a complete spherical pattern, where over 350 individual measurements are used to determine the average performance (TRP) it is considered acceptable to reduce the individual measurement dwell time to $T_{short\ sweep}$. Assuming the DUT is stable and the test equipment operates as expected, this will introduce a negligible additional uncertainty to the measurement. However, in the event of a conflict, the T_{sweep} dwell time shall be considered the reference.

The spectrum analyzer shall be set for f_{span} span in free-run mode with resolution bandwidth of f_{RBW} and a video bandwidth set to the maximum supported by the spectrum analyzer (3 MHz is the minimum VBW allowed). Using an RMS detector with a sample resolution of 5 μs or better, the sweep time shall be set to at least T_{sweep} for single point tests and at least $T_{short\ sweep}$ for complete pattern tests with a minimum of 401 data points per sweep. When using a sample detector, this time period may be broken up into several smaller sweeps, if desired, to increase the accuracy of the sample average, but the total time of all sweeps shall be at least T_{sweep} for single point tests and at least $T_{short\ sweep}$ for complete pattern tests. Whether using a sample detector or an RMS detector on a spectrum analyzer with a lower sampling rate, a total of at least 20,000 samples should be averaged across the band. The received signal must be stable for the entire trace in order to record a valid result. A stable trace is defined as a trace where no obvious signal drops to the noise floor are visible and where the running average over 10% of the span follows a smooth profile across the entire bandwidth, and, ideally, remains within a ±1.0 dB window over

the center P_{flat}% of the trace. Note that this last criterion also implies that the trace should be flat across the entire channel. Some DUTs may have bad band filters or notches in the frequency response of their antennas that cause the trace to slope across the channel bandwidth. It is critical to ensure that any such phenomena are due to the DUT and not due to a bad measurement antenna or other problem with the measurement system.

9.5.1   Determining the RBW/NBW Correction Factor

The integrated channel power formula is simply a weighted sum of the power measured in narrow frequency "windows" defined by the bandwidth filter of the spectrum analyzer. The assumption is that each point reports the power measured through a rectangular filter with a width defined by the noise bandwidth (NBW) value. To be statistically valid and capture the entire channel behavior, there must be enough measurement points so that each NBW window for each point touch without any gaps. In reality, however, the number of points is normally chosen such that the NBW overlaps at each point, requiring a weighting factor to average this out. Each point should represent a frequency range given by the channel bandwidth (CBW), divided by the total number of points. Thus, the power from each point with a width of NBW must be scaled by the factor:

Equation 9.5.1-1

$$\frac{CBW}{NBW} \times \frac{1}{N}$$

Figure 9.5.1-1 illustrates this concept.

WCDMA Trace vs. Running Average
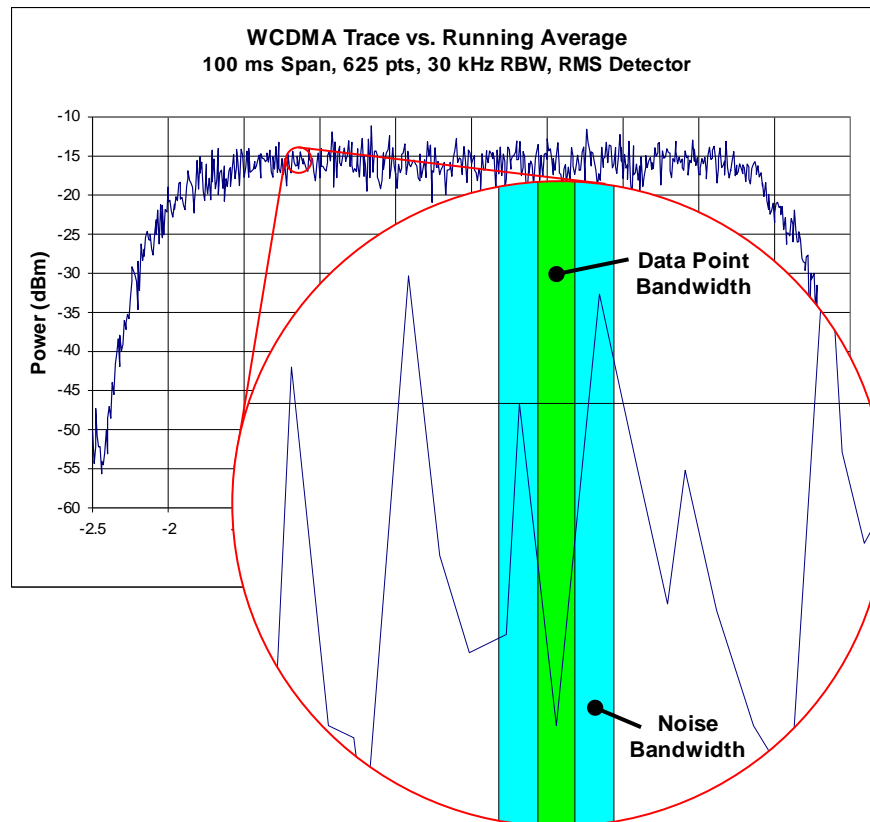**100 ms Span, 625 pts, 30 kHz RBW, RMS Detector**

Figure 9.5.1-1 Illustration of the Difference Between Noise Bandwidth and Data Point Width in the Integrated Channel Power Formula

On a physical spectrum analyzer, the resolution bandwidth filter is not a perfect rectangular filter as the noise bandwidth is assumed to be. Rather, the typical RBW filter is a Gaussian filter, where the bandwidth is defined at the half power level of the Gaussian curve.

Figure 9.5.1 2 illustrates the difference between an ideal Gaussian filter and a rectangular one, plotted on a linear power scale. While the tails of the Gaussian curve that extend outside the rectangular bandwidth are quite similar to the missing area near the peak of the filter, they do not cover the exact same amount of area. The result is that, for a broadband signal, an ideal Gaussian filter will read 0.28 dB higher than a rectangular filter with equivalent half power bandwidth. Thus, to use a Gaussian RBW filter for the integrated channel power calculation, a correction factor must be applied to address the difference in power reading between the applied filter and the desired rectangular filter shape.

Unfortunately, the RBW filters of a spectrum analyzer are never perfect Gaussian filters. The correction factor between RBW and NBW can often be as much as 0.5 dB. Therefore, to obtain a suitable correction factor for use in Equation 9.5.1-1, it is necessary to determine the difference for the given spectrum analyzer directly. Newer spectrum analyzers may also offer the use of a rectangular or flat top filter shape instead of Gaussian. While this will normally reduce the required correction factor significantly, these filters are also never perfectly rectangular and thus still require some level of correction factor.
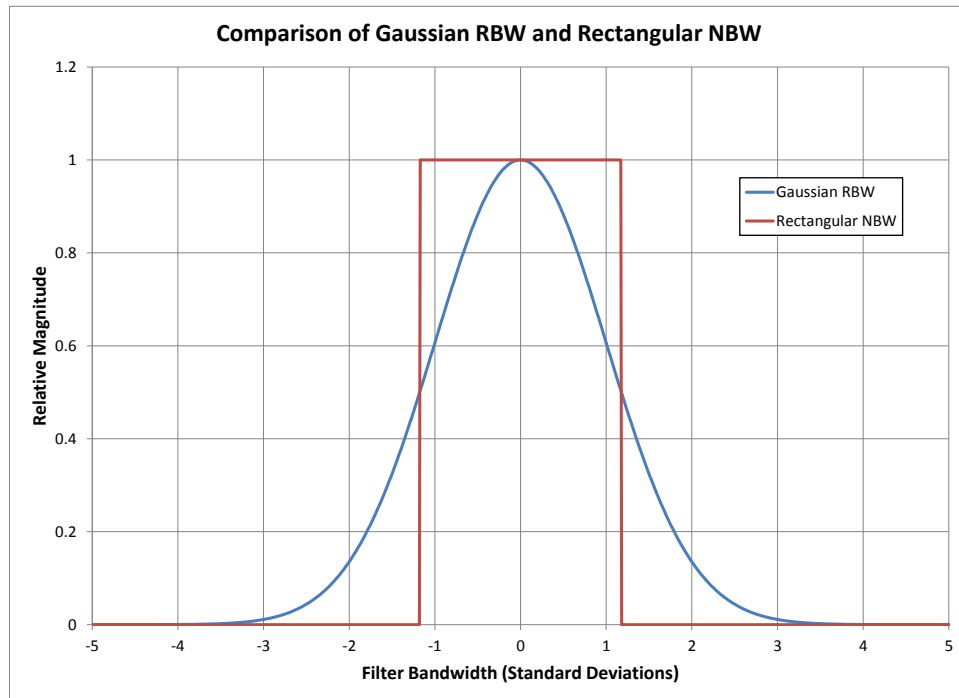
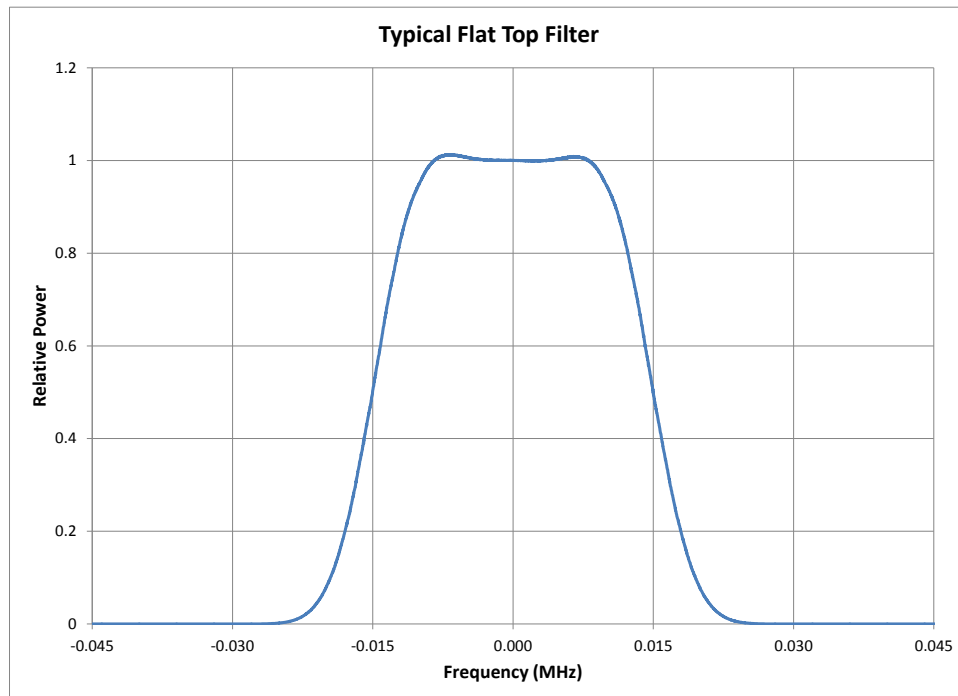Figure 9.5.1-2 Comparison of a Gaussian Shaped RBW Filter to a Rectangular NBW with the Same Frequency Bandwidth

Figure 9.5.1-1 Example of a Flat Top Filter with 30 KHz RBW

The following procedure may be used to determine the $CF_{RBW/NBW}$ value for use in Equation 9.5.1-2.

1. Connect the output of a stable CW signal generator to the input of the spectrum analyzer to be evaluated. A 10 MHz reference connection is recommended to ensure that the two instruments are phase and frequency locked.
2. Set the center frequency for both units to 1 GHz (the choice of center frequency is somewhat arbitrary but should be in the range of normal operation of the spectrum analyzer for the target tests.)
3. Set the signal generator level to be approximately 10 dB below the reference level (top of the display window) of the spectrum analyzer.
4. Set the RBW to 30 kHz (or whatever RBW is to be evaluated).
5. Set the VBW to maximum.
6. Set the frequency span to 200 kHz (at least six times the RBW setting)
7. Select the RMS detector.
8. Set the number of sweep points to at least 1001, or the maximum allowed by the spectrum analyzer, but no more than 10,001.
9. Set the sweep time to one second.
10. Take one sweep and record the resulting trace. The shape of the RBW filter should be clearly visible centered in the trace.
11. Convert the trace from dBm to linear power units:

Equation 9.5.1-2

$$P_{Linear} = 10^{P_{dB}/10}$$

12. Normalize the trace by dividing all points by the value at the center frequency. Note: If a 10 MHz reference clock is not used, the center of the RBW filter may not appear in the exact center of the trace. For a Gaussian filter, using the maximum point in the trace is usually sufficient. However, for a rectangular/flat top filter where the filter can actually increase to either side of the center frequency, determination of the actual center of the filter is critical.

13. Sum up the normalized linear trace values. Note: This sum is impacted by the noise floor of the analyzer. This calculation assumes the peak is at least 40 dB above the noise floor and the span is not significantly larger than the visible bandwidth, such that the residual terms from the noise floor are negligible in the sum. To determine if there is a detectable impact from the noise, points near the noise floor may be set to zero and the resulting sum compared to the original.

14. Determine the frequency step size of the trace by dividing the frequency span by the number of trace points minus one.

15. The correction factor is then given by:

<div align="right">Equation 9.5.1-3</div>

$$CF_{\frac{RBW}{NBW}} = \frac{RBW}{f_{StepSize}} \times \frac{1}{Sum}$$

$$= \frac{RBW}{F_{Span}} \times \frac{N-1}{\sum_{i=1}^{N} P_{Norm_i}}$$

where *RBW* is the selected resolution bandwidth, $f_{StepSize}$ is the frequency step size of the trace, Sum is the sum of the normalized linear trace values, F_{Span} is the frequency span of the trace, N is the number of points in the trace, and P_{Norm_i} are the individual normalized linear power trace points.

16. The correction factor may be converted to dB to allow it to be added directly to a resulting ICP result in dBm, where the *RBW* is used in place of *NBW*.

<div align="right">Equation 9.5.1-4</div>

$$CF_{dB} = 10 \log_{10} \left(CF_{\frac{RBW}{NBW}} \right)$$

9.6   Time Dependent Signals

Time dependent communication signals like the TDMA signals for GSM, TDD signals for LTE/NR, and pulsed signals for 802.11 introduce additional challenges for accurately measuring the power of the transmitted signal. The power must be measured only over the valid period(s) of the transmitted pulse and often multiple pulses must be averaged together to obtain enough dwell time and sample averaging for a stable power measurement. In many cases, either the total channel power or integrated channel power methods may be used, but appropriate trigger signals and hardware or software gating is required to only measure the desired signal. In many cases, this makes the total channel power approach easier since video triggering can be used to synchronize to start of a pulse. This is easy for frequency division duplex (FDD) signals like GSM, where the desired signal is isolated in frequency (Figure 9.6-1). However, for time division duplex (TDD) technologies including TD-LTE (Figure 9.6-2) and 802.11, where both uplink and downlink share the same frequency spectrum, additional mechanisms may be necessary

to isolate the uplink from the downlink. In some cases, the communication tester may provide a frame trigger that can be used in conjunction with trigger offsets on the analyzer to synchronize measurements to a portion of a trace. Even then, the integrated channel power method requires additional considerations since the required frequency sweep time at the typical narrow resolution bandwidths used is often considerably longer than the pulse length of a single subframe or packet. This results in a frequency dependence of the desired measured signal (Figure 9.6-3) that must be filled in to obtain the necessary channel frequency response for integration. This is possible given the availability of a repetitive signal and a mechanism to adjust the time dependence of the signal (Figure 9.6-4) to gate out the desired portion of the time dependent trace (Figure 9.6-5). This gating can be done either as a post processing step using multiple frequency sweeps, or some analyzers include an internal gating function that can pause the sweep and only measure during a specified time interval after each trigger signal. Alternately a signal/IQ analysis mode may be used to capture the raw IQ samples and filter out the desired time and frequency information desired as shown in Figure 9.6-6.

For time dependent/pulsed communication, it's important that the sampling rate and data point resolution both be high enough to obtain good resolution of the pulse in question. Since a single data point acquired using an RMS detector is actually the average of many samples over some time period, points near the edge of the rise and fall of a pulse or the edge of a time slot will contain samples taken outside the desired measurement window. In addition, pulsed signals may require a short period to stabilize. For these reasons, it's important that only valid samples in the middle of the pulse be used to determine the average power. In most cases, the center 85% of a pulse is a safe range, although in cases where the behavior of the signal and the analyzer sampling are well known, this may be pushed up to around 95%.

For video or burst triggered mechanisms, spurious triggering may result as the pulse level approaches the trigger level. Likewise, the trigger level must be far enough above the noise floor that the noise doesn't cause random triggering. Due to this, the minimum dynamic range requirement is referenced from the trigger level rather than the noise floor. This is in order to reduce the number of spurious triggers caused by the nulls reaching the trigger level. Provided this requirement is met, pulses unable to meet the specified width criteria after several retries may use the maximum signal level measured during the sweep rather than the average of the entire pulse window. Similarly, the value of the trigger level may be substituted for signal levels below the trigger level that are unable to cause the analyzer to trigger. These allowances are made since these values will be in deep nulls of the pattern and have an insignificant effect on the TRP.

For the purposes of characterizing antenna performance, the minimum required power measurement is given by the linear average of at least $N_{samples}$ samples across the central P_{center}% of at least N_{bursts} valid burst(s). This is typically accomplished using the RMS detector of a spectrum analyzer with a sample resolution of $t_{burst} * P_{center}/100/N_{samples}$ or better. Alternatively, the average of more than one burst may be used to reach the required sample count using either the RMS or sample detectors. In no case shall the sample rate be less than the symbol rate. The linear average of multiple bursts may also be used to reduce the random component of the uncertainty due to any variation in pulse magnitude. For multi-slot signals, the linear average of the center P_{center}% of all active timeslots in one cycle should be used. A valid burst is defined as one having a width of t_{burst} ±P_{burst}%. The spectrum analyzer must be set for zero-span using video or burst triggering with a resolution bandwidth of f_{RBW} and video bandwidth of f_{VBW}. The trigger level should be set as close to the noise floor as possible without generating spurious triggers (typically 5-10 dB above the noise). For single timeslot measurements of a single pulse, the sweep time should be set such that the pulse takes up the majority of the available analyzer window. For multi-slot measurements, the span can be set to just larger than the total number of timeslots to be measured. Ideally there should be at least 100 points per timeslot to ensure that the center P_{center}% of each timeslot can be easily determined.

If a power meter is used, it must be capable of triggering from and measuring burst modulated signals with complex modulation formats. It must also have the capability to exclude segments of the beginning and ending of the burst so that the average power level of a defined central region can be measured. The power meter sensor must have a minimum video bandwidth of at least 300 kHz. The sample rate of the power meter must be sufficiently high that a minimum of 300 samples a taken across the central 85% of

the pulse Power meters using diode detectors are sampling detectors. The meter should be configured to respond as an RMS detector.
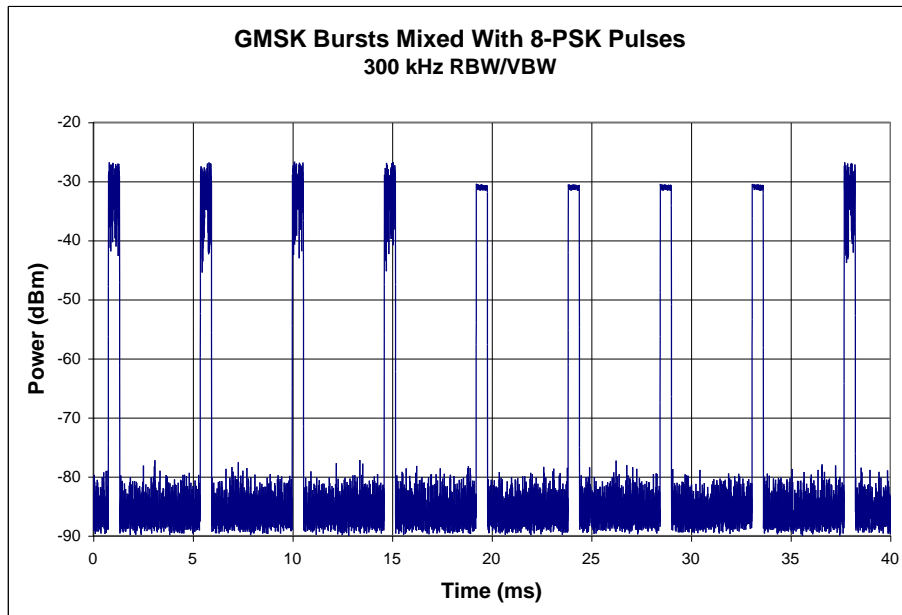
GMSK Bursts Mixed With 8-PSK Pulses
300 kHz RBW/VBW

Figure 9.6-1 Example of a Time Dependent FDD Signal

TD-LTE Single Frame (Ten Subframe) Time Dependence
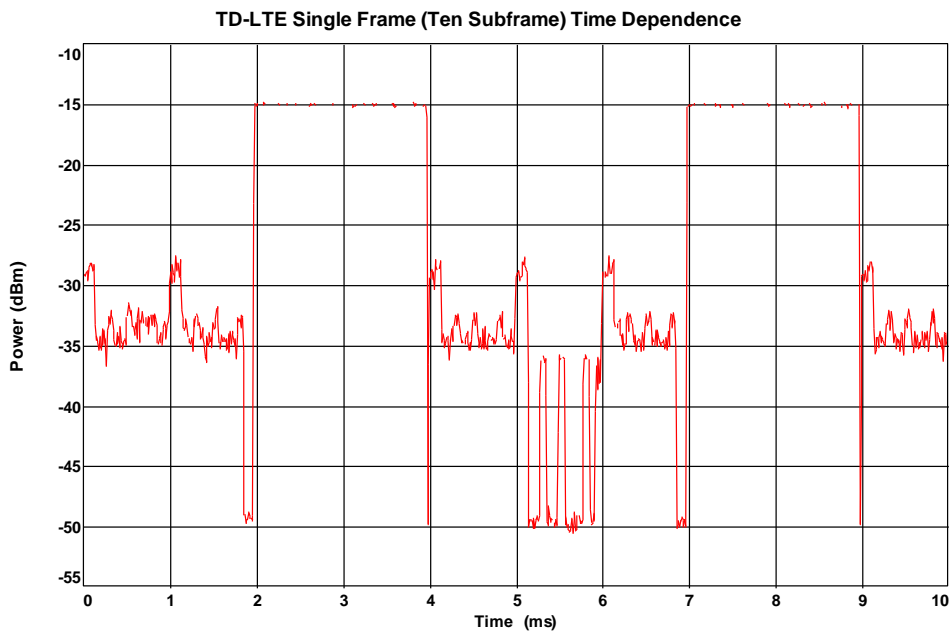
Figure 9.6-2 Example of a TDD Signal With Interspersed Uplink and Downlink Time Slots

TD-LTE Frequency Response Curve
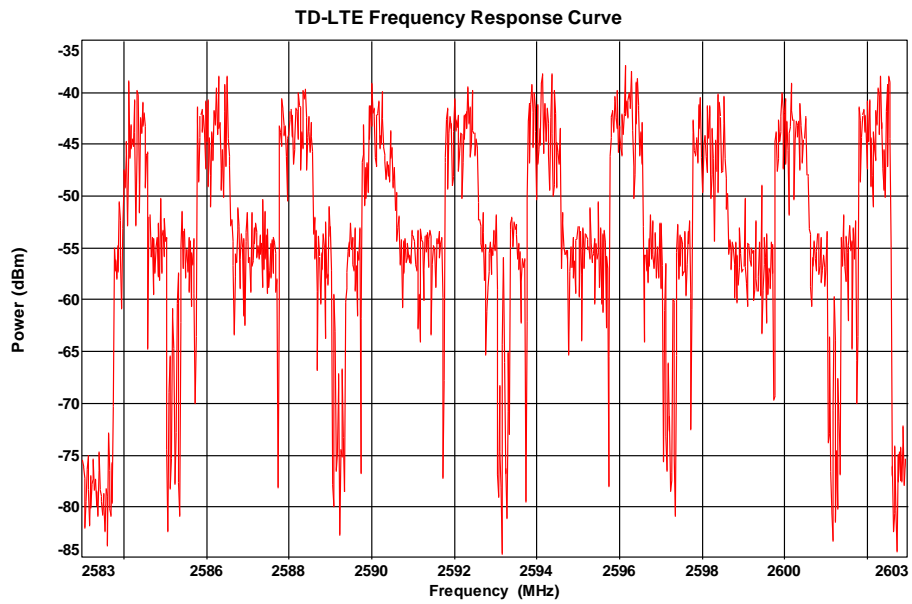
Figure 9.6-3 Example Frequency Sweep of a TDD Signal Showing Interspersed Uplink and Downlink Time Slots as a Function of Frequency Due to Sweep Time
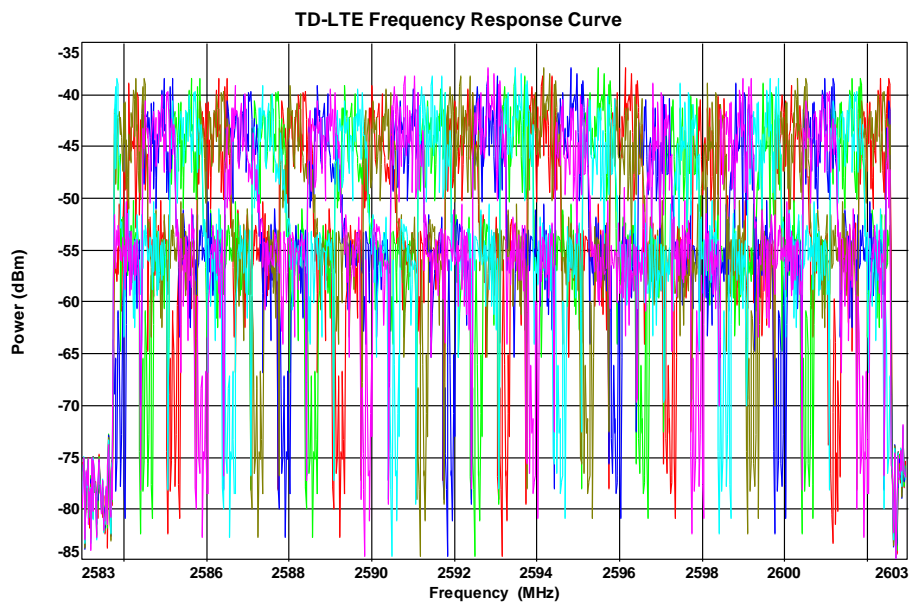
TD-LTE Frequency Response Curve

Figure 9.6-4 Using a Frame Trigger and a Sweep Trigger Delay to Offset the Frequency Dependence of a Repetitive Signal
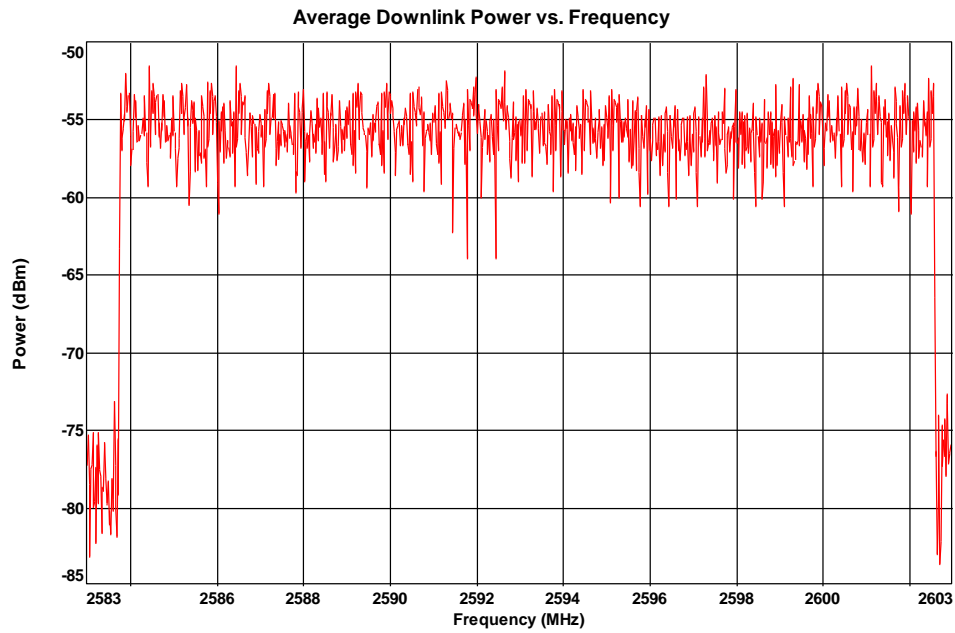
Average Downlink Power vs. Frequency

Figure 9.6-5 Extracted Signal Produced by Gating Multiple Trigger Offset Frequency Sweeps
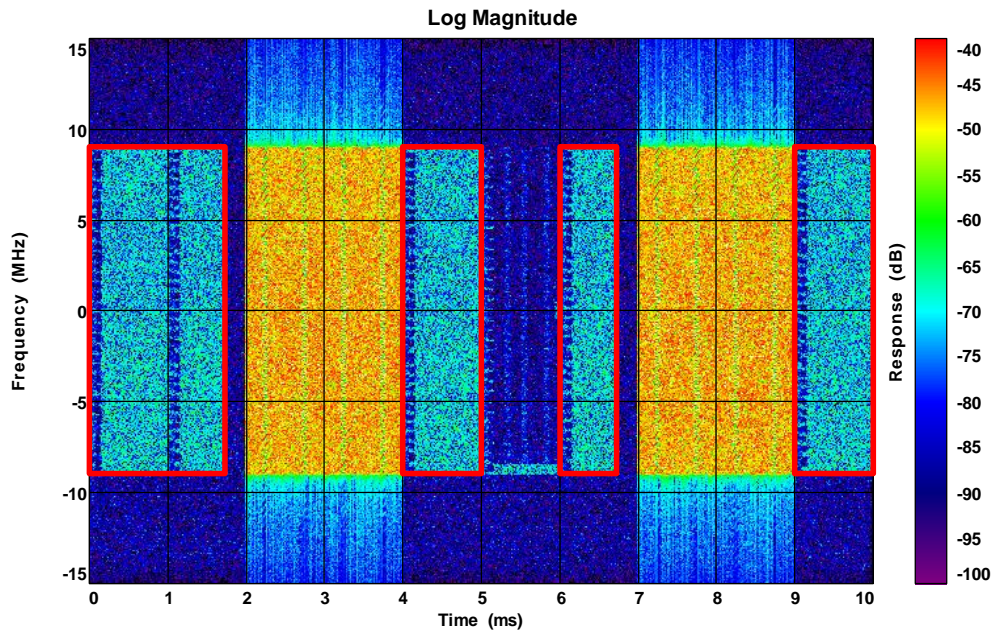
Log Magnitude

Figure 9.6-6 Using a Broadband Signal Analyzer to Extract a Desired Time Dependent Signal

9.7 GSM/GPRS (GMSK Modulation)

GSM Circuit Switched and GPRS Packet Switched modes use a constant envelope modulation known as Gaussian Minimum Shift Keying (GMSK) that encodes one bit per symbol. The signal is slotted into 8 timeslots of approximately 0.577 ms with 148 symbols per slot.

For the purposes of characterizing antenna performance, the process defined in Section 9.6 shall be used to measure valid GMSK pulses using the following settings.

Table 9.7-1 GMSK Modulation

Parameter	Value
$N_{samples}$	1100
P_{center}	85%
N_{bursts}	1
t_{burst}	0.577 ms
P_{burst}	10%
f_{RBW}	300 kHz
f_{VBW}	300 kHz

Refer to the following figures for examples of acceptable and unacceptable GSM pulses, as well as typical behavior as the signal approaches the trigger level. Note that as expected, the noise level increases as the signal approaches the noise floor. However, it should also be noted that the use of average pulse power as opposed to peak power reduces the uncertainty of the result due to the noise by approximately the square root of the number of points averaged. This is because the noise is a random error effect and the averaging process reduces the uncertainty, effectively lowering the noise floor.
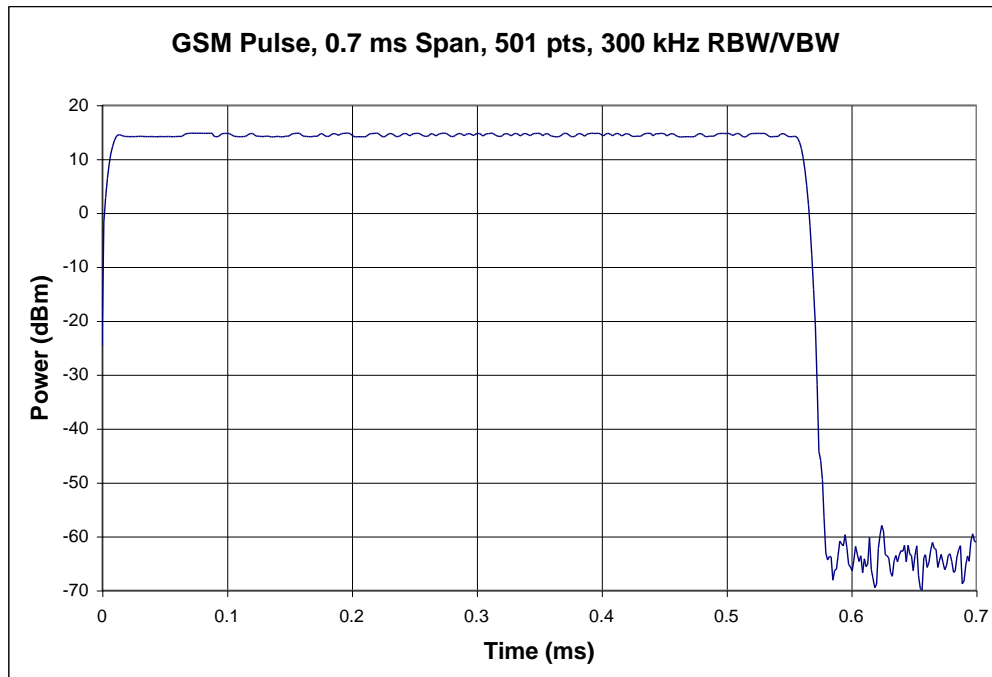
GSM Pulse, 0.7 ms Span, 501 pts, 300 kHz RBW/VBW

Figure 9.7-1 Sample GSM Power Envelope with Acceptable Resolution
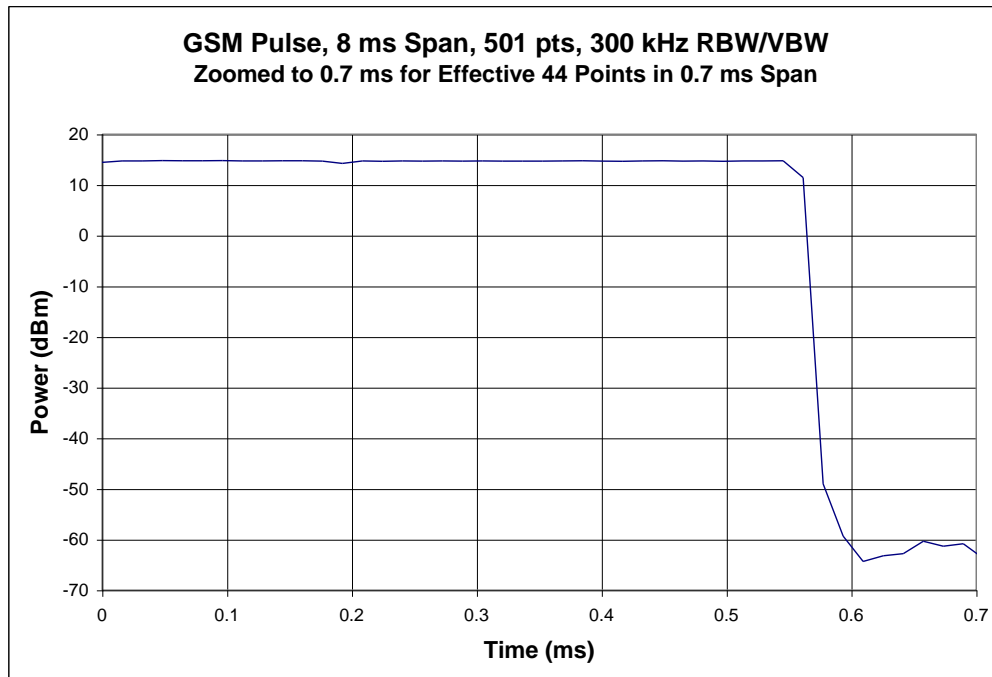
Figure 9.7-2 Sample GSM Power Envelope with Insufficient Resolution

GSM Pulses, 0.7 ms Span, 501 pts, 300 kHz RBW/VBW
Signal approaching noise floor still triggers cleanly, but ~3-4 dB of noise.
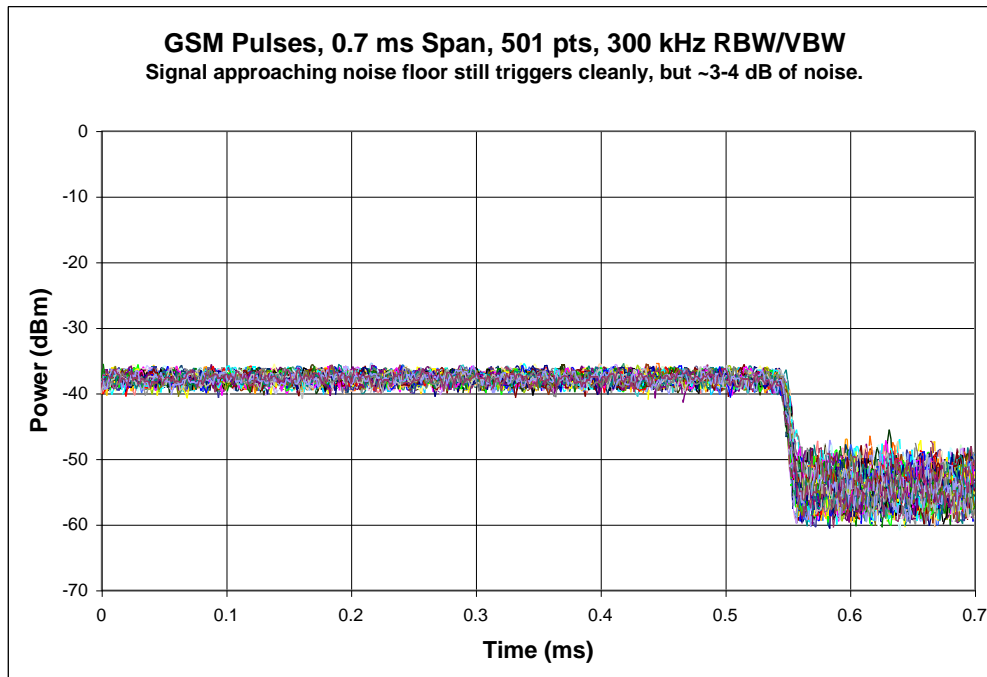
Figure 9.7-3 Sample GSM Pulses Showing Increase in Noise as Signal Approaches Trigger Level

9.8   EGPRS/EDGE (8PSK Modulation)

EGPRS (EDGE) Packet Switched modes use a non-constant envelope modulation (8-PSK) modulation known as 8-Phase Shift Keying (8-PSK) that encodes three bits per symbol. The signal is slotted into 8 timeslots of approximately 0.577 ms with 148 symbols per slot. The non-constant modulation envelope of the 8-PSK pulse has almost 20 dB variation peak-to-null, and causes the average power of each frame to vary significantly based on the content of the frame, necessitating the average of multiple frames in order to obtain a stable average power reading. Some GMSK pulses are randomly interspersed between the 8-PSK pulses and must be detected separately and removed from the measurement. The treatment of the 8-PSK pulses is similar to that for GSM.

For the purposes of characterizing antenna performance, process defined in Section 9.6 shall be used to measure valid GMSK pulses using the following settings.

Table 9.8-1 8PSK Modulation

Parameter	Value
$N_{samples}$	1100
P_{center}	85%
N_{bursts}	20
t_{burst}	0.577 ms
P_{burst}	10%

Parameter	Value
f_{RBW}	300 kHz
f_{VBW}	300 kHz

Due to the depth of nulls seen in 8-PSK pulses, the minimum dynamic range requirement is increased by 20 dB and referenced from the trigger level rather than the noise floor.

Refer to the following figures for examples of acceptable and unacceptable 8-PSK pulses, as well as typical behavior as the signal approaches the trigger level. Note that as expected, the noise level increases as the signal approaches the noise floor. However, it should also be noted that the use of average pulse power as opposed to peak power reduces the uncertainty of the result due to the noise by approximately the square root of the number of points averaged. This is because the noise is a random error effect and the averaging process reduces the uncertainty, effectively lowering the noise floor.
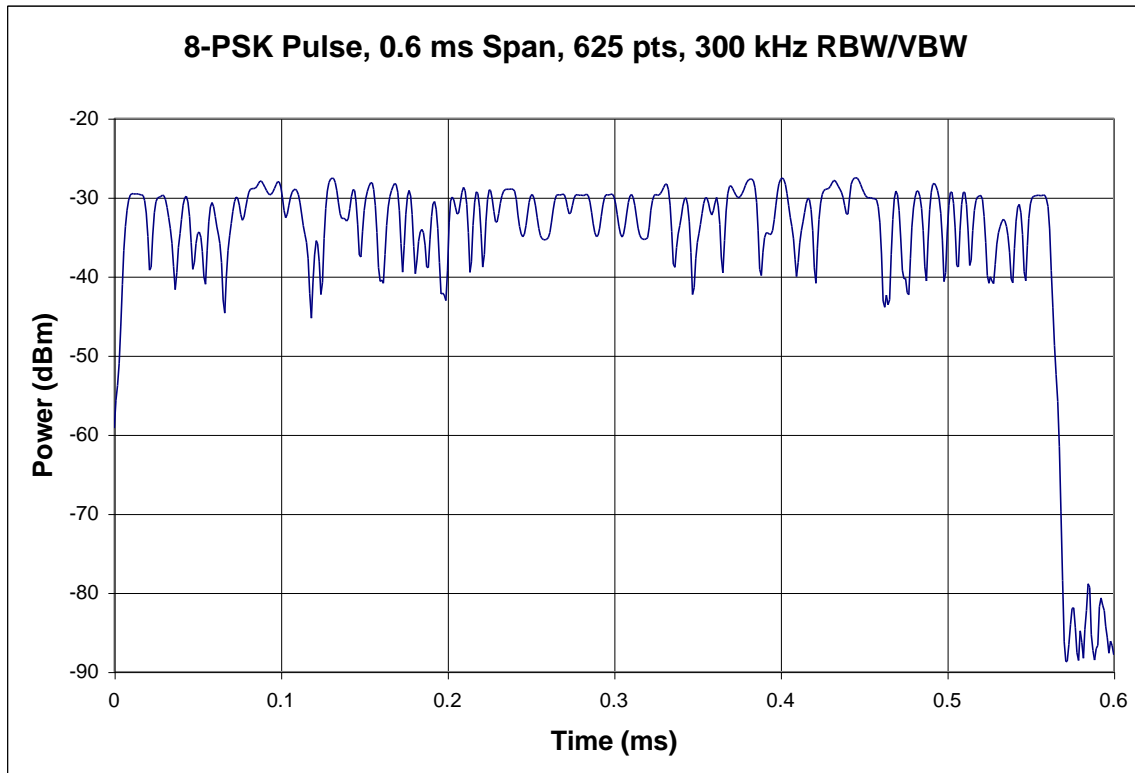
8-PSK Pulse, 0.6 ms Span, 625 pts, 300 kHz RBW/VBW

Figure 9.8-1 Sample 8-PSK Power Envelope with Acceptable Resolution

Ten 8-PSK Pulses, 0.6 ms Span, 625 pts, 300 kHz RBW/VBW
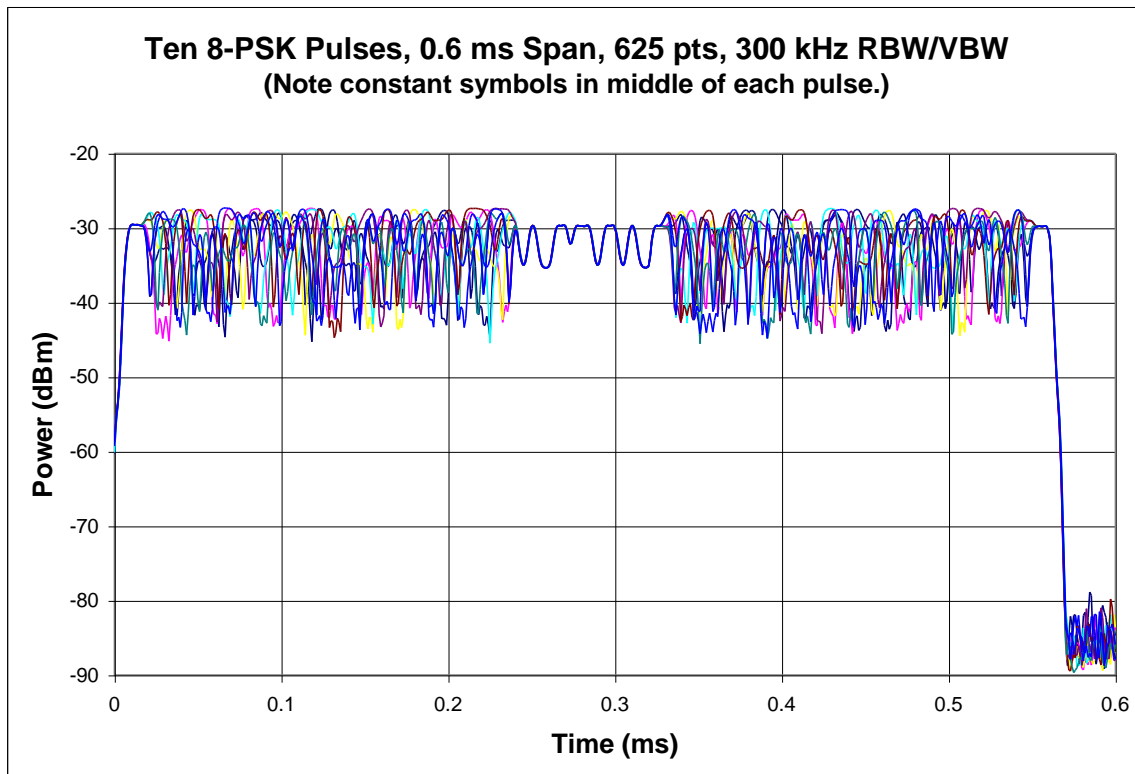**(Note constant symbols in middle of each pulse.)**

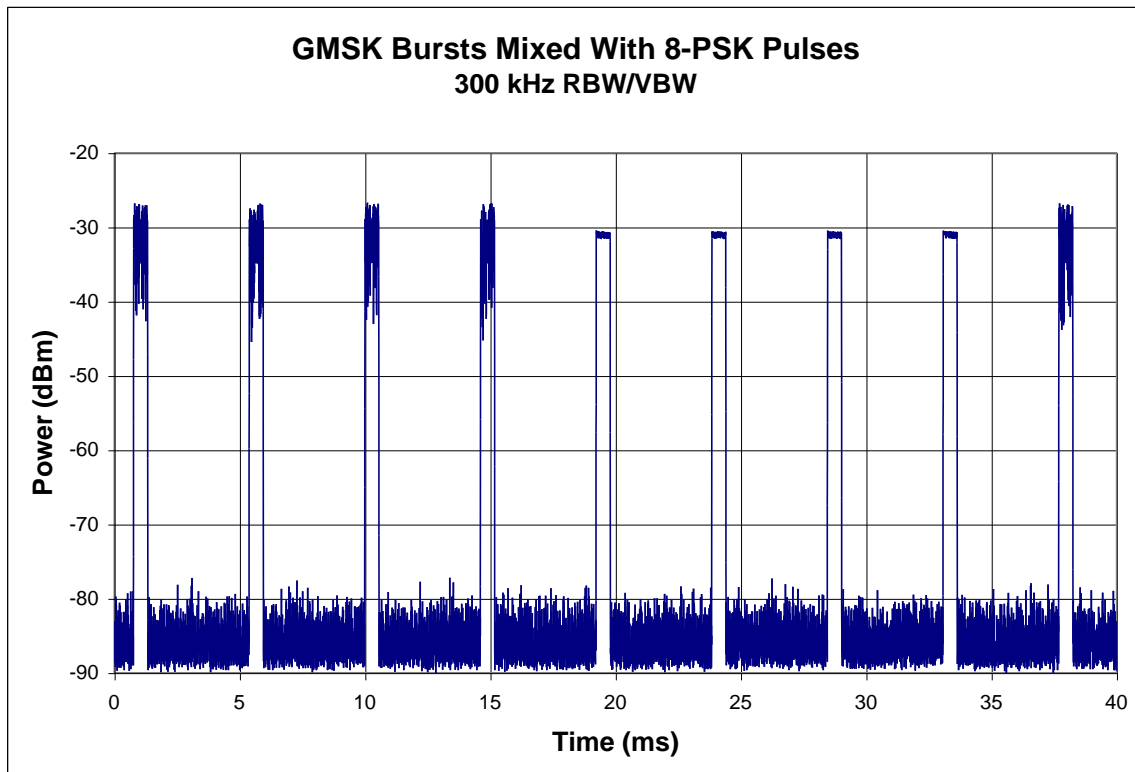Figure 9.8-2 Multiple 8-PSK Pulses with Random Data Content

Figure 9.8-3 Example of GMSK Bursts Mixed in with 8-PSK Data

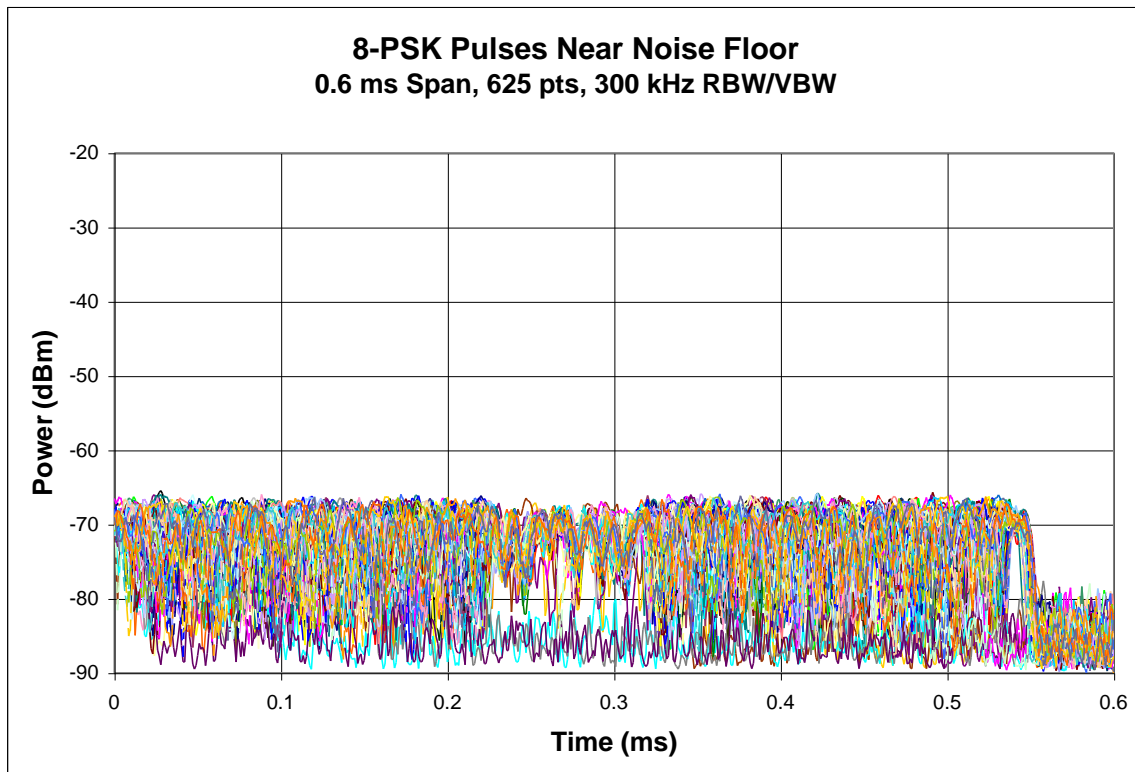Figure 9.8-4 Sample 8-PSK Pulses Showing Mis-Triggering and Increase in Noise at Low Levels

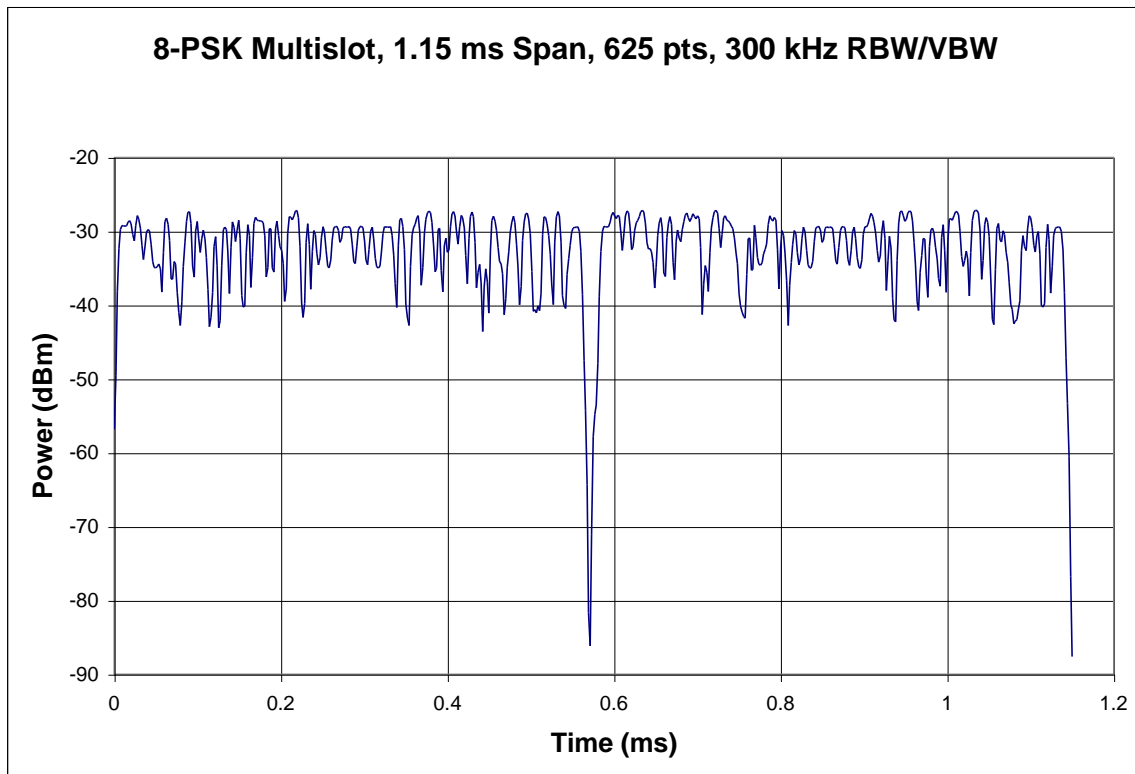**8-PSK Multislot, 1.15 ms Span, 625 pts, 300 kHz RBW/VBW**

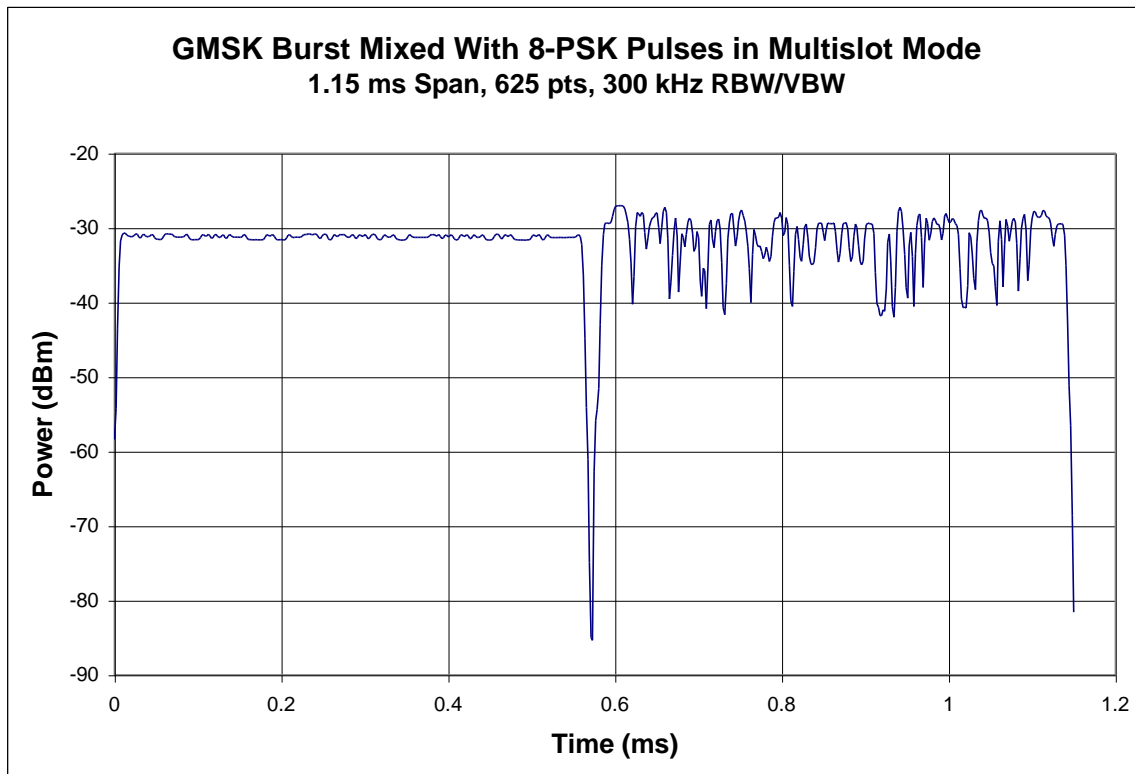Figure 9.8-5 Sample Multislot 8-PSK Pulses

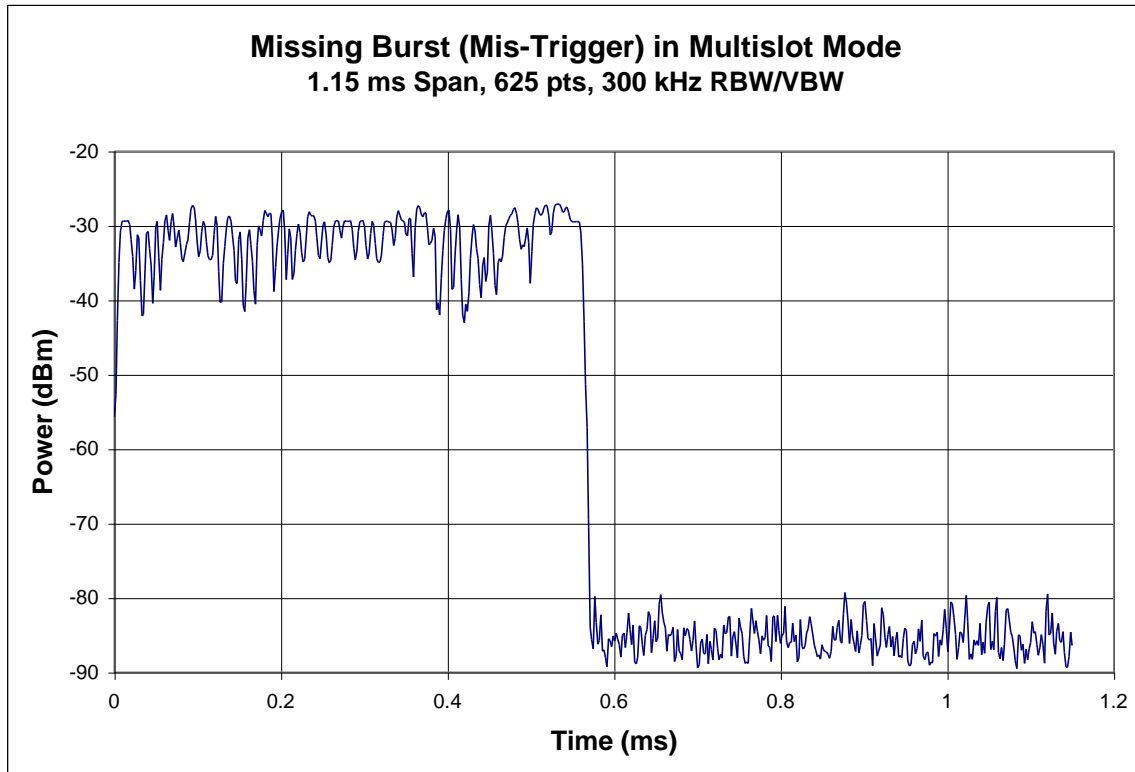Figure 9.8-6 Bad 8-PSK Multislot Trace Resulting from GMSK Burst

Figure 9.8-7 Bad 8-PSK Multislot Trace Resulting from Mis-Triggering

9.9   WCDMA (UMTS)

Wideband CDMA uses a digital spread spectrum technology for communication. The communication channel is similar to CDMA, but with a wider bandwidth. As with CDMA, the base station can manage power control dynamically by sending binary "up" or "down" signals to maintain the received power at a desired range. Maximum output power is set by sending the "up" bit signal constantly. After a few milliseconds, the device will be at maximum power. The resulting power may be measured with either the total power (Section 9.4) or integrated channel power (Section 9.5) methods using the parameters in Table 9.9-1.

Table 9.9-1 WCDMA Power Measurement Parameters

Parameter	Value
f_{span}	5 MHz
f_{RBW}	30 kHz
$f_{Gaussian}$	20 MHz
$f_{flat\ top}$	8 MHz
$T_{dwell}\ or\ T_{sweep}$	100 ms

CTIA
Certification

Parameter	Value
$T_{short\ dwell}$ or $T_{short\ sweep}$	20 ms
P_{flat}	60%

Refer to the following figures for examples of WCDMA frequency response traces using RMS and sample detectors and the corresponding running average, as well as an example of a bad sweep.
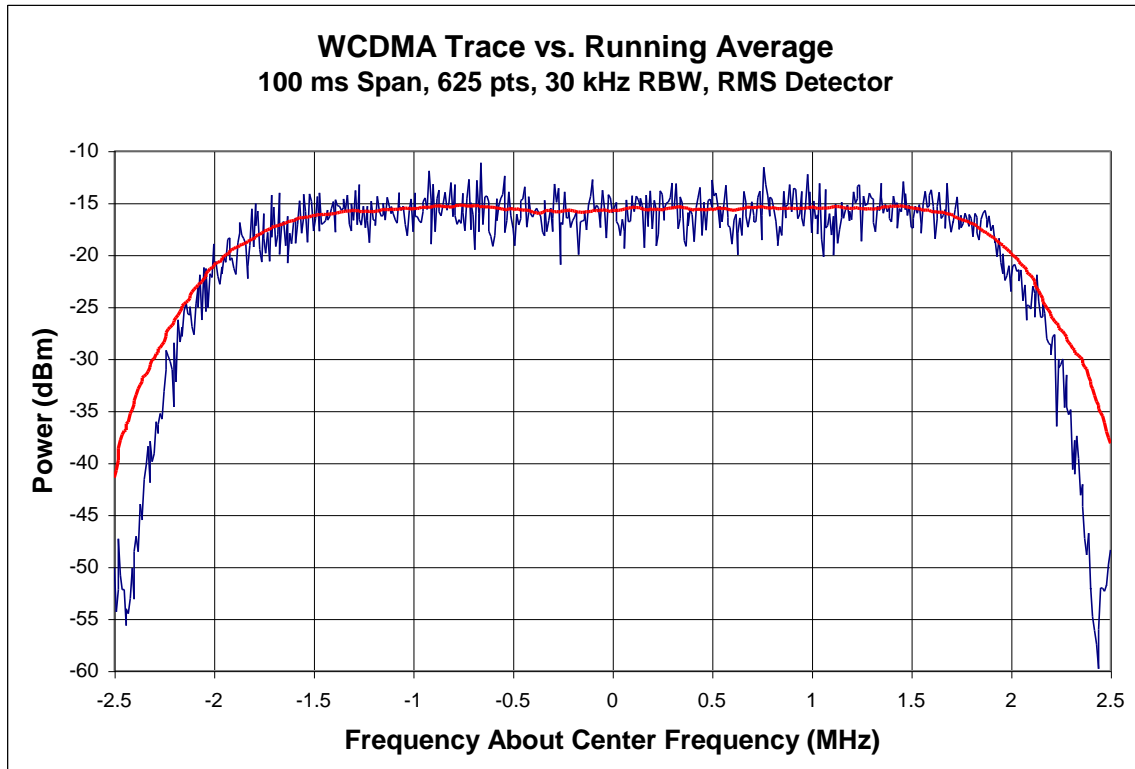

Figure 9.9-1 Example of Valid Frequency Response Trace Using RMS Detector
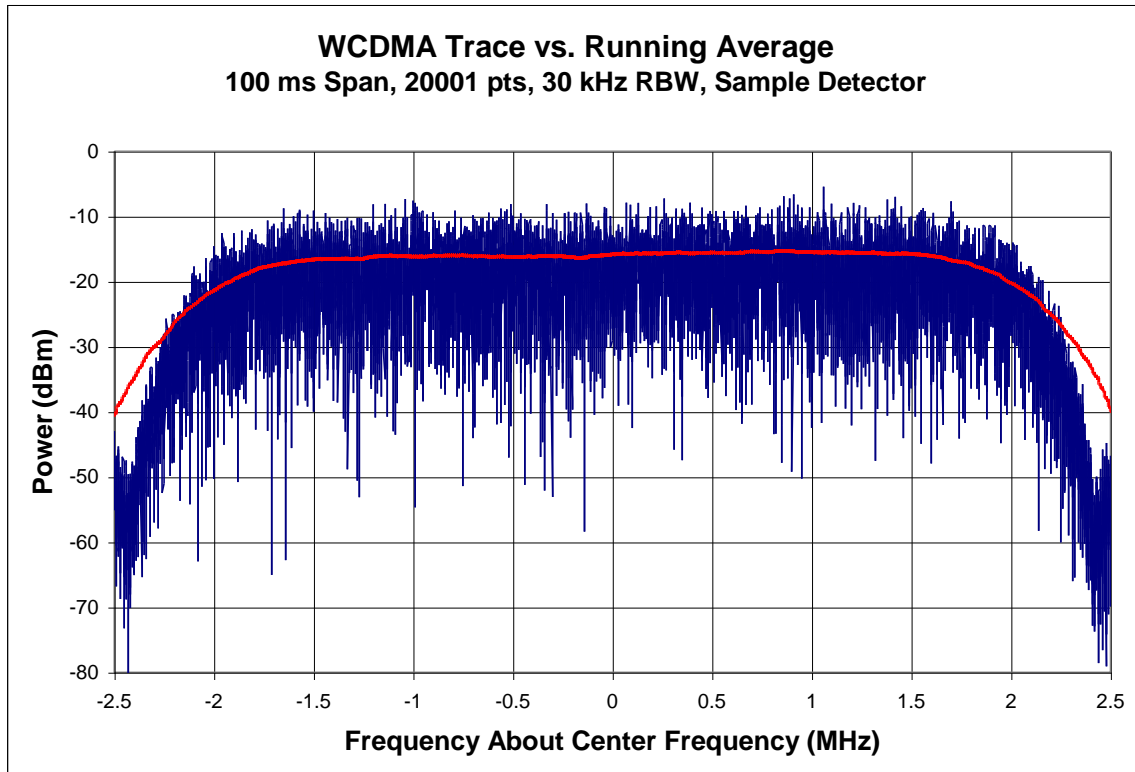
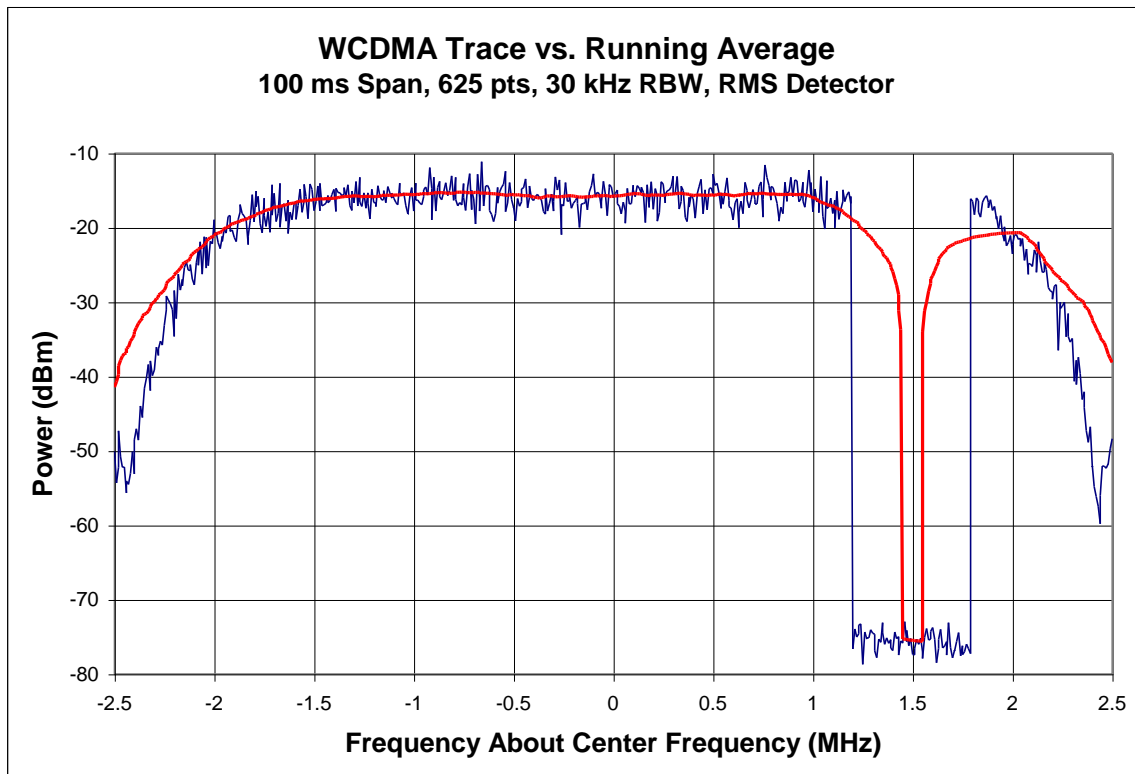Figure 9.9-2 Example of Valid Frequency Response Trace Using Sample

Figure 9.9-3 Example of a Signal Drop-Out During an RMS Sweep

9.10   LTE

LTE uses SC-FDMA to produce a digital spread spectrum where specific sub-channels may be used or unused depending on the configuration information provided by the eNodeB base station. Thus, the occupied bandwidth is configurable by the number of specified resource blocks (RBs) independent of the actual channel bandwidth, allowing multiple UEs to share one channel. Each resource block is 180 kHz wide (200 kHz including guard intervals). The current TRP requirements specify sub-channel bandwidths of 12 RBs or 2.4 MHz for 10 MHz channels, 8 RBs or 1.6 MHz for 5 MHz channels, including a suitable guard band. While there are a number of different power control options for LTE, the test plan expects maximum power to be produced by sending the "up" command constantly. After a few hundred milliseconds, the device will be at maximum power.

LTE supports two frame structure types to enable both FDD and TDD modes of operation. Both types of frame are 10 ms in duration and consist of 10 subframes of 1 ms duration (see *3GPP TS 36.211* [9]). In TDD mode, the frame can be divided into two half frames, with one special subframe per frame or half frame to facilitate downlink to uplink switching. A number of subframe and special subframe configurations are supported. The uplink period of the special subframe cannot be used for user plane data (PUSCH). Thus, under the default subframe configuration specified in *3GPP TS 36.508* [10], the UE will be transmitting 2 ms bursts every 5 ms to transport user plane data in PUSCH.

For the purposes of characterizing antenna performance, the resulting power may be measured with either the total power (Section 9.4) or integrated channel power (Section 9.5) methods using the parameters in Table 9 10-1, centered on the occupied bandwidth defined by the resource block allocation. A stable trace is defined as all points within ±0.5 dB of the midpoint value. In either case, the required frequency offsets specified in Table 9 10-1 may be determined generally as $RBStart + RBAllocation - Total RBs/2 * 0.18$ MHz.

Table 9 10-1 Broadband Power Mode Measurement Requirements

Channel BW (MHz)	RB Allocation	RB Start	Frequency Offset (MHz)	f_{span}	$f_{Gaussian}$	$f_{flat\,top}$
5	8	0	-1.53	1.6	4	2
		8	-0.09			
		17	+1.53			
10	12	0	-3.42	2.4	8	3
		19	0.0			
		38	+3.42			
20	18	0	-7.38	3.6	12	4.5
		41	0.0			
		82	+7.38			
f_{RBW}		30 kHz				
T_{dwell} or T_{sweep}		100 ms				
$T_{short\,dwell}$ or $T_{short\,sweep}$		20 ms				
P_{flat}		70%				
Note 1: The Subchannel BW, including guard band, may be reconsidered in future versions as scaling guard band requirements with number of RBs may not be appropriate.						

In addition, for the case of measurements with the TDD frame structure, the broadband power measurement is the linear average of the center 95% of the 2ms burst and the measurement shall be triggered in order to synchronize the measurement with the burst. If a power meter is used, it must be capable of triggering from and measuring the average power of multiple bursts of modulated signals with complex modulation formats.

Refer to the following figures for examples of LTE frequency response traces for various configurations.
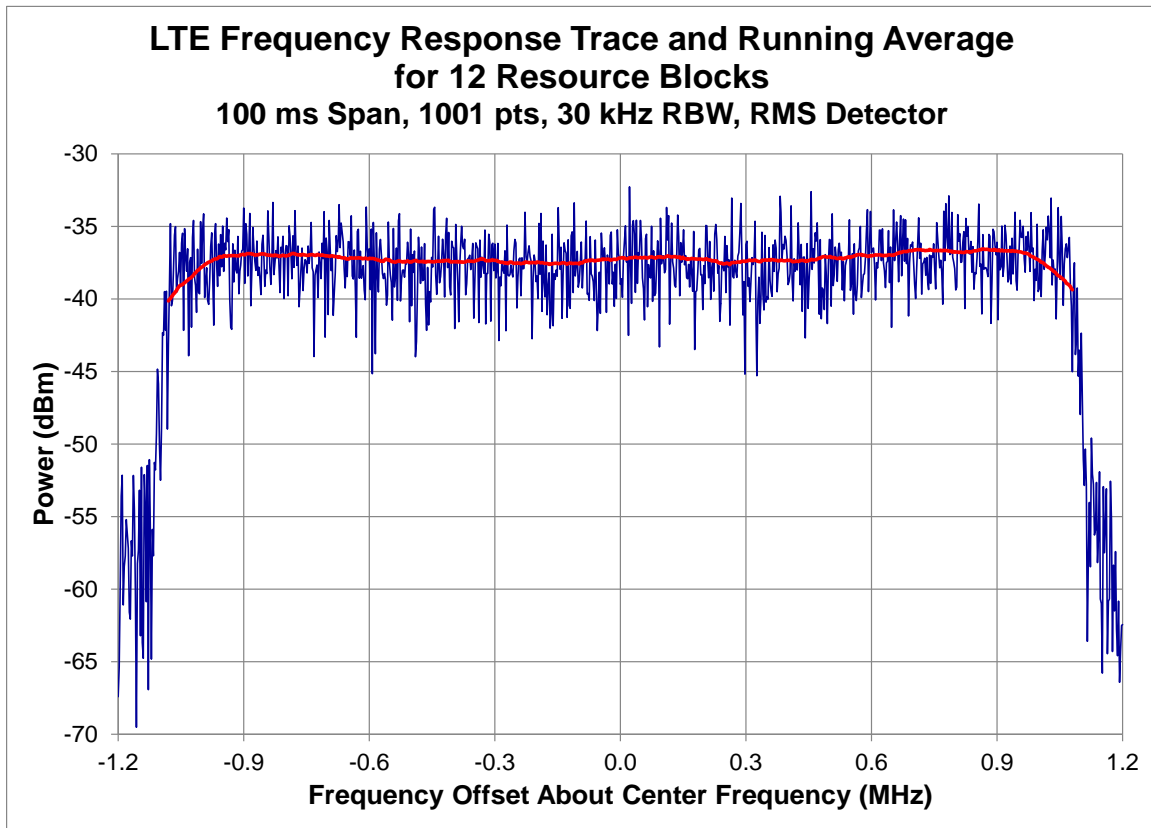
Figure 9.10-1 Example of Valid LTE Frequency Response Trace Using RMS Detector
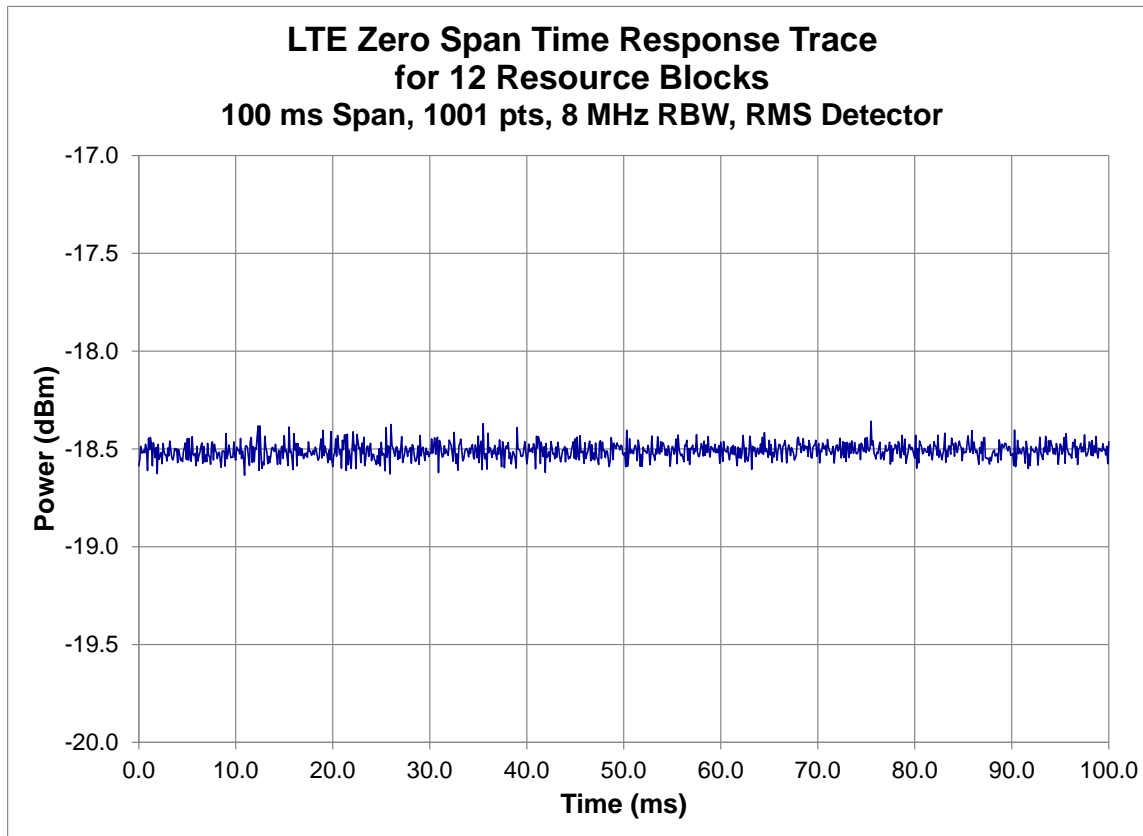
Figure 9.10-2 Example of Valid LTE Wideband Time Response Trace Using RMS Detector

9.11   LTE Category M1

LTE Category M1 supports FDD, half-duplex FDD (HD-FDD), and TDD modes of operation. Devices that operate in FDD or TDD mode shall be tested using the spectrum analyzer broadband power mode or the power meter guidelines outlined in Section 9.10. The spectrum analyzer settings specified in Table 9 10-1 shall be replaced with the settings in Table 9.11-1 below.

Table 9.11-1 LTE Category M1 Broadband Power Mode Measurement Requirements

Channel BW (MHz)	Power Class	RB Allocation	f_{span}[1]	$f_{Gaussian}$ (MHz)	RB Start	Frequency Offset (MHz)
5	3	1	0.2	3	0	-2.16
					13	0.18
					24	2.16
	5	3	0.6	3	0	-1.98
					13	0.36
					22	1.98
10	3	4	0.8	3	1	-3.96
					25	0.36
					45	3.96
	5	5	1.0	3	1	-3.87
					25	0.45
					44	3.87
20	3	6	1.2	4	2	-8.10
					50	0.54
					92	8.10
	5	6	1.2	4	2	-8.10
					50	0.54
					92	8.10

Note 1: The Subchannel BW, including guard band, may be reconsidered in future versions as scaling guard band requirements with number of RBs may not be appropriate.

In addition, for the case of measurements with HD-FDD, the broadband power measurement shall be the linear average of the center 95% of the 3 ms burst and the measurement shall be triggered in order to synchronize the measurement with the burst. If a spectrum analyzer is used, the settings in Table 9.11-1 shall be used. If a power meter is used, it must be capable of triggering from and measuring the average power of multiple bursts of modulated signals with complex modulation formats.

9.12   LTE Category NB1 (NB-IoT)

LTE Category NB1 supports half-duplex FDD (HD-FDD) mode of operation with a maximum channel bandwidth of 180kHz (200kHz including guard intervals). The occupied bandwidth is configurable by the transmission bandwidth configuration (Ntone), allowing multiple UEs to share one channel.

The current TRP requirements specify a transmission bandwidth configuration Ntone = 1 with a 15kHz sub-carrier spacing (i.e. sub-channel bandwidth is 15kHz) allocated at the lower or higher edge of the channel bandwidth, so there is a very small difference (<100kHz) between the test channel (i.e., FUL) and the actual center frequency for the subcarrier allocation. Therefore, power measurements shall be done on FUL.

For the purposes of characterizing antenna performance, the broadband power mode described in Section 9.4 may be used, with the following modifications. The spectrum analyzer shall be set to a RBW of 300kHz and VBW of 1MHz. The broadband power measurement shall be the linear average of the center 95% of the 8ms burst and the measurement shall be triggered in order to synchronize the measurement with the NPUSCH burst.

If a power meter is used, it must be capable of triggering from and measuring the average power of multiple bursts of modulated signals with complex modulation formats.

9.13   NR FR1

NR uses CP-OFDM in the Uplink and Downlink as well as DFT-s-OFDM in the Uplink. The occupied bandwidth is configurable by the number of specified resource blocks (RBs) independent of the actual channel bandwidth, allowing multiple UEs to share one channel. NR FR1 supports scalable sub-carrier spacing (SCS) of 15 kHz, 30 kHz, and 60 kHz as well as wider channel bandwidths (CBWs) compared to LTE. The relationship between SCS, CBW, and maximum transmission bandwidth configuration NRB is outlined in *3GPP TS 38.101-1* [11], specifically Section 5.3.2. While there are a number of different power control options for NR, the test plan expects maximum power to be produced by sending the "up" command constantly. After a few hundred milliseconds, the device will be at maximum power.

NR supports two frame structure types to enable both FDD and TDD modes of operation. Both types of frame are 10 ms in duration and consist of 10 subframes of 1 ms duration.

For the purposes of characterizing antenna performance, the resulting power may be measured with either the total power (Section 9.4) or integrated channel power (Section 9.5) methods using the parameters in Table 9.13-1 centered on the occupied bandwidth defined by the resource block allocation.. The required frequency offsets specified in Table 9.13-1 may be determined generally as $(\text{RBStart}) + (\text{RBAllocation} - \text{Total RBs})/2) * 12 * \text{SCS}$.

Table 9.13-1 Broadband Power Mode Measurement Requirements for NR FR1

CBW [MHz]	SCS [KHZ]	N_{RB}	RB Allocation	f_{span} (MHz)	$f_{Gaussian}$ (MHz)	RB Start	Frequency Offset [MHz]
5	15	25	12	2.645	6	6	-0.09
10	15	52	25	5.125	11	12	-0.27
15	15	79	36	7.245	15	18	-0.63
20	15	106	50	9.905	20	25	-0.54
40	15	216	108	20.545	42	54	0
60	30	162	81	30.810	62	40	-0.18
100	30	273	135	50.290	101	67	-0.72

f_{RBW}	30 kHz
T_{dwell} or T_{sweep}	100 ms
$T_{short\ dwell}$ or $T_{short\ sweep}$	20 ms
P_{flat}	70%

Power meters using diode detectors are sampling detectors. The comments pertinent to sampling detectors in the preceding paragraphs apply to these detectors, e.g., a total of at least 20,000 samples should be averaged across the band.

In addition, for the case of measurements with the TDD frame structure, the broadband power measurement is the linear average of the center 95% of the 1 ms burst and the measurement shall be triggered to synchronize the measurement with the burst. If a power meter is used, it must be capable of triggering from and measuring the average power of multiple bursts of modulated signals with complex modulation formats.

Revision History

Date	Version	Description
February 2022 **Appendix A**	4.0.0	Initial release. **Section 2:** • Consolidated range lengths from SISO OTA test plan (Section 3.1) • Minimum range length calculation taking effective radiating aperture and dimension of quiet zone into account • Addition of bands: GPS L5, GALILEO E1, n78 **Section 3:** • Consolidated test frequencies from SISO, mm-wave, and Large-Form-Factor OTA test plans • Addition of bands: n258, GPS L5, GALILEO E1, n78 • Removal of A-GLONASS • Updated Table 3-5 to reflect that a minimum of 21 points per channel shall be used for precharacterization tests **Section 4:** moved from SISO OTA test plan (Section 4) **Section 5:** moved from SISO OTA test plan (Section 3) **Section 6:** moved from Test Plan for Wireless Large-Form-Factor with the following updates: • Updated Section 6.2.2 step 3 to allow labs to test for the Proximity Effect in a single 10 MHz band located at the center frequency in the lowest technology band • Updated Section 6.2.3 to allow labs to do the spatial uniformity precharacterization only at the highest loading condition if they wish. **Section 7:** • Moved from mm-wave OTA test plan (Section 3) • Amplitude QoQZ verification clarification **Section 8:** • Moved from mm-wave OTA test plan (Appendix F) • Fixture misalignment correction for phase QoQZ measurements **Section 9:** Moved from SISO OTA test plan (Appendix D)
May 2022	4.0.1	**Section 6:** Miscellaneous editorial fixes.
November 2022	4.0.2	**Section 3:** Added clarifications related to determining VNA frequency step size for precharacterization of reverberation-chamber setups.
July 2023	4.0.3	**Section 3:** Added n78 in Table 3 1 **Section 5:** Corrected references (editorial fixes) in Section 5.1 **Section 9:** Clarification on the use of communication testers in Section 9.2.2.
November 2023	4.0.4	**Section 1:** Corrected References in Section 1.4